

**DAVID W. TAYLOR NAVAL SHIP  
RESEARCH AND DEVELOPMENT CENTER**

Bethesda, Md. 20084



**AD A 041189**

**HIGHLY SKEWED PROPELLER DESIGN FOR A  
NAVAL AUXILIARY OILER (AO 177)**

by

D. T. Valentine  
and  
A. Chase

APPROVED FOR PUBLIC RELEASE. DISTRIBUTION UNLIMITED

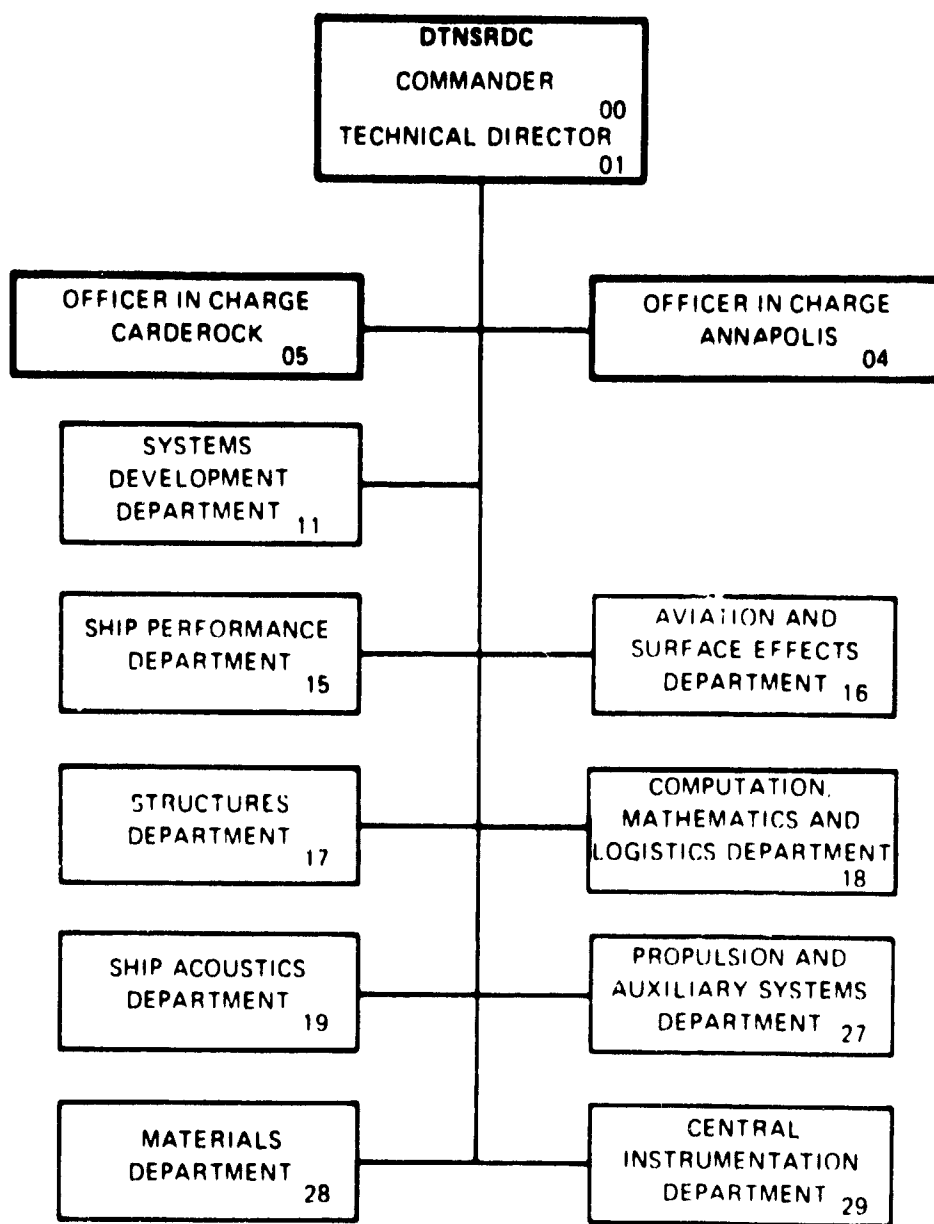
**SHIP PERFORMANCE DEPARTMENT  
DEPARTMENTAL REPORT**

**AD NO. \_\_\_\_\_  
DDC FILE COPY**

September 1976

Report SPD-544-12

## MAJOR DTNSRDC ORGANIZATIONAL COMPONENTS



## UNCLASSIFIED

SECURITY CLASSIFICATION OF THIS PAGE (When Data Entered)

REPORT DOCUMENTATION PAGE		READ INSTRUCTIONS BEFORE COMPLETING FORM
14 REPORT NUMBER SPD-544-12	2. GOVT ACCESSION NO.	3. RECIPIENT'S CATALOG NUMBER 9
4. TITLE (or Item Summary) Highly Skewed Propeller Design for a Naval Auxiliary Oiler (AO 177)		5. SPAN OF REPORT & PERIOD COVERED Final / kept
6. AUTHOR(S) D. T. Valentine A. Chase		7. PERFORMING ORG. REPORT NUMBER 7
8. CONTRACT OR GRANT NUMBER(S)		
9. PERFORMING ORGANIZATION NAME AND ADDRESS David W. Taylor Naval Ship Research and Development Center Bethesda, Maryland 20084		10. PROGRAM ELEMENT PROJECT, TASK AREA & WORK UNIT NUMBERS Work Request N65197-76-WR 65139; 1524-501 & 1524-002
11. CONTROLLING OFFICE NAME AND ADDRESS Naval Ship Engineering Center Center Building, Prince Georges Plaza Hyattsville, Maryland 20782		11. REPORT DATE September 1978
12. MONITORING AGENCY NAME & ADDRESS (if different from Controlling Office) 108p.		13. NUMBER OF PAGES 107
14. DISTRIBUTION STATEMENT (of this Report) Approved for public release; distribution unlimited		15. SECURITY CLASS (of this report) UNCLASSIFIED
16. DISTRIBUTION STATEMENT (of the abstract entered in Block 20, if different from Report)		15a. DECLASSIFICATION/DOWNGRADING SCHEDULE
17. SUPPLEMENTARY NOTES		
18. KEY WORDS (Continue on reverse side if necessary and identify by block number) cavitation vibration highly-skewed propeller		
19. ABSTRACT (Continue on reverse side if necessary and identify by block number) The design of a skewed propeller for the AO-177 Class Fleet Oiler is presented and the design procedure used is described in detail. The design objective of the skewed propeller was to minimize propeller vibration without adversely affecting efficiency. Calculations predict that, at full power design conditions, the final 7-bladed, 21-foot (6.4 meters) diameter design will reduce unsteady thrust to about 0.28 percent of steady thrust and unsteady torque to about 0.35 percent of steady torque. Endurance speed is predicted to be met at 11 percent less than design endurance power. Speed at full power is		

**UNCLASSIFIED**

CONT

SECURITY CLASSIFICATION OF THIS PAGE(When Data Entered)

→ predicted to be 21.25 knots (10.9 m/s) at 100 propeller rpm (10.5 rad/s). The criteria of 10 percent margin on back bubble cavitation at full power, full load displacement is calculated to be met. In addition no back bubble cavitation is predicted at ballast conditions. At full-power design-conditions, stresses throughout the blades are calculated to be well below the allowable limit of 12,500 psi (86.2 MPa).

ACCESSION NO.	
NTIS	White Section <input checked="" type="checkbox"/>
DOC	Self Section <input type="checkbox"/>
UNANNOUNCED	<input type="checkbox"/>
JUSTIFICATION .....	
.....	
DITION/AVAILABILITY CODES	
.....	
SPECIAL	
.....	

D D  
REF ID: A65117  
R JUN 8 1977  
RECEIVED  
D

**UNCLASSIFIED**

SECURITY CLASSIFICATION OF THIS PAGE(When Data Entered)

## TABLE OF CONTENTS

	Page
ABSTRACT.....	1
ADMINISTRATIVE INFORMATION.....	1
INTRODUCTION.....	1
PROPELLER DESIGN CONDITIONS.....	3
PROPELLER DESIGN.....	6
DESIGN PROCEDURE.....	6
PRELIMINARY DESIGN ANALYSIS.....	9
LIFTING LINE DESIGN.....	12
PROPELLER GEOMETRY.....	13
SKEW ANGLE DISTRIBUTION.....	18
LIFTING SURFACE DESIGN.....	22
FINAL DESIGN CHECK.....	25
OFF DESIGN CALCULATIONS.....	27
DISCUSSION OF EXPERIMENTAL EVALUATION.....	30
SUMMARY.....	34
REFERENCES.....	37
APPENDIX.....	82

LIST OF FIGURES

	Page
1 - Measured Values of the Axial, Tangential and Radial Velocity Components in the Wake of the AO-177 Class Fleet Oiler (Model 5326); See Reference 4.....	40
2 - Schematic of the Design Procedure.....	45
3 - Hydrodynamic Pitch Distributions Investigated for the AO-177 Class Fleet Oiler Propeller Design.....	46
4 - Influence of Blade Area and Wake Variations on Cavitation Erosion on Merchant Ship Propellers; See Reference 15.....	47
5 - Radial Distribution of Thickness-To-Chord Ratio Based on Strength and Cavitation Criteria for the Final AO Propeller Design.....	48
6 - Radial Distribution of the Mean Advance Angle, the Maximum Variations of the Advance Angle, and the Pressure Factor.....	49
7 - Cavitation Inception Diagram for the 0.6 Radius of the AO Propeller.....	50
8 - Cavitation Inception Diagram for the 0.7 Radius of the AO Propeller.....	51
9 - Cavitation Inception Diagram for the 0.8 Radius of the AO Propeller.....	52
10 - Cavitation Inception Diagram for the 0.9 Radius of the AO Propeller.....	53
11 - Several Examples of Geometry Changes Evaluated in the AO Design from the Viewpoint of Minimizing Unsteady Forces.....	54
12 - Comparison of Predictions of Unsteady Thrust, and of Blade Shape for the Preliminary and Final Designs for AO.....	55
13 - Comparison of Alternating Forces with Mil-Standards.....	56
14 - Drawing of Propeller 4677 (Final AO Propeller Design).....	57
15 - Modified Goodman Working Stress Diagram.....	58
16 - Blade Deflections Calculated Using a Finite Element Method.....	59
17 - Maximum Principal Stresses Calculated on the Suction Side of the AO Propeller Blade Using a Finite Element Method.....	60
18 - Maximum Principal Stresses Calculated on the Pressure Side of the AO Propeller Blade Using a Finite Element Method.....	61

	Page
19 - Open-Water Characteristics for the Final AO Propeller.....	62
20 - Towing Tank and Trial Powering Predictions for AO, $C_A = 0.0005$ .....	63
21 - Powering Predictions with Power Margin For AO, $C_A = 0.0005$ .....	64
A1 - Trailing Edge Geometry for Propellers.....	93
A2 - Hub Configuration.....	95

## LIST OF TABLES

	Page
1 - Design Conditions.....	65
2a - Resistance and Propulsion Data for AO-177 Class Fleet Oiler for Full-Load, Clean Hull, Calm Seas, and Zero True Wind.....	66
2b - Design Point.....	66
3 - Model 5326(AO) Radial Distribution of Harmonic Longitudinal and Tangential Velocity Components.....	67
4 - Circumferential Average Axial Velocity Distribution of Wake....	70
5 - Lifting Line Design of AO-177 Class Fleet Oiler Propeller.....	71
6 - Geometric Characteristics of Final AO-177 Class Fleet Oiler Highly Skewed Propeller Design.....	77
7 - Summary of AO-177 Class Fleet Oiler Design Point Analytical Predictions.....	78
8 - Lifting Surface Corrections Factors for AO-177 Class Fleet Oiler Highly Skewed Propeller.....	79
9 - Performance Values at Endurance Condition.....	80
10 - Performance Values at Full Power Ballast Condition.....	81
A1 - Definition of Terms Used in Tables A2, A3, and Figures A1 and A2.....	84
A2 - Propeller Geometry.....	86
A3 - Propeller Offsets.....	88

## NOTATION

$a$	Mean-line designation. Fraction of the chord from leading edge over which loading is uniform at the ideal angle of attack.
$A$	Area of blade section
$A_e$	Expanded area, $z/r_h^R$ cdr
$A_0$	Disc area of propeller, $\pi R^2$
$A_e/A_0$	Expanded Area Ratio
$\overline{BM}, \hat{BM}$	Mean and alternating bending moments, respectively.
BTF	Blade thickness fraction
$C_A$	Incremental resistance coefficient for model to ship correlation
$C_D$	Drag coefficient of section
$C_L$	Lift coefficient of section at ideal angle of attack, $L/( (1/2) \rho V_r^2 c )$
$C_{L_D}$	Lift coefficient at design conditions
$C_{L_{OD}}$	Lift coefficient at off design conditions
$C_N$	Section modulus coefficient
$C_{P_{MIN}}$	The negative of the minimum pressure coefficient
$C_p$	Local pressure coefficient, $(p-p_\infty)/( (1/2) \rho V_r^2 )$
$C_{PS}$	Power coefficient based on ship speed
$C_{PSI}$	Inviscid power coefficient based on ship speed
$C_{PT}$	Thrust power coefficient
$C_{PTI}$	Inviscid thrust power coefficient
$C_S$	Section area coefficient, $A/ct$
$C_{Th}$	Thrust loading coefficient, $T/( (1/2) \rho V_A^2 A_0 )$
$C_{ThS}$	Thrust loading coefficient based on ship speed, $T/( (1/2) \rho V^2 A_0 )$

NOTATION CONTINUED

$C_{ThSI}$	Inviscid thrust loading coefficient based on ship speed
$c$	Section chord length
$c_{LE}$	Expanded distance from generator axis to leading edge
$c_{TE}$	Expanded distance from generator axis to trailing edge
$D$	Propeller diameter
$D$	Drag of section
$F$	Factor for estimating local angles of attack, $1/(1+2\pi\tan(\beta_I-\beta)/C_L)$
$\tilde{F}_H$	Amplitude of blade frequency harmonic of transverse horizontal force
$\tilde{F}_V$	Amplitude of blade frequency harmonic of transverse vertical force
$f_M$	Camber of section
$f_{M2D}$	Camber required to produce specified lift coefficient at ideal angle of attack in two-dimensional flow
$G$	Nondimensional circulation, $\Gamma/(2\pi RV)$
$g$	Acceleration due to gravity
$H$	Head. Distance from propeller center line to water surface.
$H_L$	Local head. Distance from specific point on propeller to water surface.
$J_V$	Advance coefficient, $J = \frac{V}{nD}$
$J$	Advance coefficient, $J = \frac{V(1-w_t)}{nD} = \frac{V_A}{nD}$
$k_c$	Camber correction
$k_t$	Angle of attack correction for thickness
$k_a$	Ideal angle of attack correction
LER	Leading edge radius

NOTATION CONTINUED

L	Local effective lift per unit area, $(1/2)\rho v_r^2 c_L$
$\tilde{M}_H$	Amplitude of blade frequency harmonic of bending moment about the transverse horizontal axis
$\tilde{M}_V$	Amplitude of blade frequency harmonic of bending moment about the vertical axis
n	Propeller revolutions per unit time
$(P/D)_I$	Propeller section hydrodynamic pitch ratio, $\pi x \tan^2 I$
P	Propeller section pitch
$P_D$	Delivered power at propeller, $2\pi n Q$
$P_E$	Effective power
$P_S$	Power delivered to shaft aft of gearing and thrust block
p	Local pressure
$p_\infty$	Pressure at infinity
$\bar{Q}, \tilde{Q}$	Mean and alternating torque, respectively
R	Radius of propeller
r	Radial distance from propeller center
RL-LE	Propeller centerline (skew line) to leading edge distance
RL-TE	Propeller centerline (skew line) to trailing edge distance
T	Thrust
$\bar{T}, \tilde{T}$	Mean and alternating thrust, respectively

NOTATION CONTINUED

t	Thickness or thrust deduction fraction
$\tan\beta_I$	Tangent of hydrodynamic pitch angle
t/c	Thickness to chord ratio
TER	Trailing edge radius
TEFR	Trailing edge fairing radius
$u_A$	Axial induced velocity at propeller section
$u_T$	Circumferential induced velocity at propeller section
v	Ship speed
$v_A$	Axial wake velocity or speed of advance
$v_L/v$	Local velocity ratio (at sections being investigated)
$v_N/v$	Normal velocity ratio
$v_T$	Tangential wake velocity
$v_T/v$	Tangential velocity ratio
$v_X/v$	Longitudinal velocity ratio
$w_t$	Taylor wake fraction
$w_v$	Volumetric-mean wake fraction
x	Nondimensional radial distance from propeller center = r/R
$y_L$	Added thickness to lower offset
$y_U$	Added thickness to upper offset
z	Number of blades

NOTATION CONTINUED

$z_R$	Rake
$\alpha$	Section equivalent angle of attack in two-dimensional flow
$\alpha_I$	Ideal angle of attack required to produce specified lift coefficient in two-dimensional flow
$\beta$	Circumferential mean advance angle, $\tan^{-1} V(1-w_x)/\pi x n D$
$\beta_I$	Hydrodynamic flow angle
$\Gamma$	Circulation about blade section
$\Delta\alpha$	Local angle of attack minus circumferential mean angle of attack
$\Delta\beta$	Local advance angle minus circumferential mean advance angle
$\lambda_e$	Effective aspect ratio of propeller blade
$\eta$	Estimated propeller efficiency, $C_{PT}/C_{PS}$
$\eta_B$	Propeller behind efficiency, $TV_A/P_D$
$\eta_D$	Propulsive efficiency, $P_E/P_D$
$\eta_I$	Estimated inviscid propeller efficiency, $C_{PTI}/C_{PSI}$
$\theta$	Position angle about propeller axis in propeller plane, measured from vertical upward counterclockwise looking forward
$\theta_R$	Effective local rake angle, $\tan^{-1}(z_R/r)$
$\theta_s$	Skew angle in the projected plane measured from a radial line through the midchord of the section at the hub to the radial line through the midchord of the section at the local radius, positive in direction opposite to ahead rotation
$\rho$	Mass density of water
$\rho_o$	Mass density of propeller
$\sigma_L$	Local cavitation number, $2gH_L/V_r^2$
$\sigma$	Cavitation number at shaft centerline, based on speed of advance, $2gH/V_A^2$

**NOTATION CONTINUED**

$\bar{\sigma}$

**Time average stress**

$\tilde{\sigma}$

**Fluctuating stress**

## ABSTRACT

The design of a skewed propeller for the AO-177 Class Fleet Oiler is presented and the design procedure used is described in detail. The design objective of the skewed propeller was to minimize propeller vibration without adversely affecting efficiency. Calculations predict that, at full power design conditions, the final 7-bladed, 21-foot (6.4 meters) diameter design will reduce unsteady thrust to about 0.28 percent of steady thrust and unsteady torque to about 0.35 percent of steady torque. Endurance speed is predicted to be met at 11 percent less than design endurance power. Speed at full power is predicted to be 21.25 knots (10.9 m/s) at 100 propeller rpm (10.5 rad/s). The criteria of 10 percent margin on back bubble cavitation at full power, full load displacement is calculated to be met. In addition, no back bubble cavitation is predicted at ballast conditions. At full-power design-conditions, stresses throughout the blades are calculated to be well below the allowable limit of 12,500 psi (86.2 MPa).

## ADMINISTRATIVE INFORMATION

This project was carried out for the Naval Ship Engineering Center (NAVSEC) under Work Request N65197-76-WR 65139. Work was performed at the David W. Taylor Naval Ship Research and Development Center (DTNSRDC) under Work Unit Numbers 1524-501 and 1524-002.

## INTRODUCTION

The Naval Ship Engineering Center (NAVSEC) requested the David W. Taylor Naval Ship Research and Development Center (DTNSRDC) to design a propeller for a naval auxiliary oiler (AO-177). The objective was to design a propeller with minimum unsteady propeller forces resulting from the propeller operating in the spatially non-uniform inflow velocity distribution in the ship's wake. In so doing, propulsive efficiency and possible cavitation suppression were not to be sacrificed.

to any significant extent. Typically, based on a number of years experience developed at DTNSRDC, such a design calls for the application of skew. A judicious selection of skew will usually result in significantly reducing propeller-induced vibration and in improving cavitation performance as compared to propellers of conventional configuration<sup>1</sup>.

The application of highly skewed propellers to propel ships<sup>2</sup> is relatively new; therefore, definitions of skew and highly skewed may be helpful. The definition of skew, or skew-back is the displacement of any blade section along the pitch helix measured from the generator line to the reference point of the blade section. It is positive in the opposite direction of ahead motion. Typically, skewed propellers are described by expressing the tip skew angle as a percentage of the blade spacing angle, i.e., the projected skew angle,  $\theta_s(r)$ , at the tip radius,  $r=R$ , divided by the angular spacing between the blades,  $2\pi/Z$ , where  $Z$  is the number of blades. If the skew angle of any blade section exceeds 50 percent of the blade spacing angle, the propeller would be categorized as highly skewed. In the case of the AO-177 Class oiler propeller, the propeller is highly skewed because it has a tip skew of 87.5 percent.

The objective of this report is to present the design procedure and decisions which led to the final geometric configuration of a 21 foot diameter (6.4 meters), 7 blades, 45 degrees non-linear skew for

<sup>1</sup>Cumming, R.A., Morgan, W.B., and Boswell, R.J., "Highly Skewed Propellers," The Transactions of the Society of Naval Architects and Marine Engineers, Vol. 80, 1972

<sup>2</sup>Valentine, D.T. and Dashnaw, F.J., "Highly Skewed Propeller for San Clemente Class Ore/Bulk/Oil Carrier Design Considerations, Model and Full-Scale Evaluation," First Ship Technology and Research (STAR) Symposium, August 1975

the AO-177 ship. The propeller design problem is that of choosing the geometric configuration which minimizes vibratory forces and cavitation, maximizes efficiency, and has adequate strength characteristics. The following sections describe the specified design conditions, the pertinent ship data required as input into the design problem (wake survey, resistance, and propulsion interaction coefficients), the design procedure and decisions, and summary of the final design and its predicted performance characteristics.

#### PROPELLER DESIGN CONDITIONS

The design conditions specified for the AO-177 propeller were a combination of machinery and performance constraints imposed by NAVSEC and summarized in Table 1. The design was based on resistance data (effective power) and propulsion data (interaction coefficients based on stock propeller powering experiments) obtained in experiments performed in the David Taylor Model Basin<sup>3</sup>. These data are presented in Table 2. The propeller was designed for the full-power speed based on the estimated trial condition resistance data, viz., data for calm seas, clean hull, zero true wind and design displacement, draft and trim. The full-power speed was not specified, but would be the speed at which 24,000 shaft horsepower (17,897 kw) was absorbed at the full-power shaft speed.

---

<sup>3</sup> Remmers, K. and Hecker, R., "Powering Predictions of a Naval-Auxiliary Oiler (AO) (Model 5326 with stock propellers 4272A and 4510A)," David Taylor Naval Ship Research and Development Center Report SPD-544-03, May 1974

Although the endurance speed of 20 knots (10.3 m/s) is required to be attained at 80 percent of the available power, the 6 percent power margin modifies this somewhat. The margin of 6 percent was imposed by NAVSEC on shaft power to ensure that the endurance conditions would be met. This means that the ship would have to achieve 20 knots (10.3 m/s) with 6 percent less than the specified endurance power, or  $19,200 - 0.06(19,200) = 18,048$  SHP (13,458 kw). Therefore, the requirement states that the predicted, endurance power according to model experiments should be 18,048 SHP (13,458 kw) or less in order to meet the design condition within the specified margin.

It would be desirable to eliminate all forms of cavitation throughout the operating range of the ship. Unfortunately, this is impossible due to large circumferential changes in the inflow to the propeller. Therefore, the propeller must be designed to minimize certain types of cavitation at the expense of other, hopefully less detrimental, forms. For the AO it was decided to eliminate back bubble cavitation, since this form of cavitation is closely associated with cavitation erosion and thrust breakdown. In order to ensure that back bubble cavitation was eliminated at all operating conditions, a 10 percent margin was placed on back-bubble cavitation-inception speed. That is, the predicted inception of this form of cavitation could not occur below full power speed (at the design point) plus 10 percent.

It has been shown<sup>1,2</sup> that the proper choice of blade skew usually reduces vibration excitation forces imparted to the hull and main propulsion system. It was, therefore, decided that skew should be used in the AO propeller if calculation of the unsteady bearing forces indicated

that these forces were significantly reduced. In order to predict the unsteady forces generated by the propeller, a wake survey was run and a harmonic analysis performed on the circumferential variations of the longitudinal and tangential components of the wake<sup>4</sup>. The wake survey was conducted at an operating condition corresponding to the design displacement of 27,380 tons (273 MN), a mean draft of 32.5 feet (9.9 m), a trim of 1.5 feet (0.46 m) at the stern, and a ship speed of 20 knots (10.3 m/s) at 100 rpm (10.5 rad/s). The measured values of the circumferential variations in the axial, tangential and radial velocity components are presented in Figure 1. From these data, similar results are obtained for other radii by interpolation. Subsequently, the harmonic components of the circumferential variations are computed by Fourier analysis the results of which are presented in Table 3. The circumferential averages of the axial components of the wake velocities, or the nominal wake data are presented in Table 4.

When a propeller operates behind a ship, the flow is changed around the stern and the effective inflow is different into the propeller from that if the propeller were not there. The difference is a function of the wake and propeller loading. At the present time there is no rational method available for correcting the radial distribution of nominal wake obtained from a wake survey for the effects of the propeller. However, an average correction can be applied which has proven reasonably successful in the past for obtaining the desired ship speed and shaft speed at design power. This method uses the ratio of the volumetric mean wake velocity from the wake survey and the effective wake velocity (one minus the Taylor wake fraction) from the stock propulsion experiment, i.e.,

<sup>4</sup>Remmers, K.D. and Hendrican, A.L., "Analysis of Wake Survey of a Naval Auxiliary Oiler (AO 177 Class) Represented by Model 5326," David Taylor Naval Ship Research and Development Center Report SPD-544-05, May 1975.

$$(V_x/V)_{\text{corrected}} = \frac{(1-w_t)}{(1-w_v)} (V_x/V)_{\text{nominal}}$$

where  $(1-w_t)$  equal effective wake from stock propulsion experiments;  $(1-w_v)$  equal volumetric mean wake from wake survey; and  $V_x/V$  equal nominal, circumferential-mean, longitudinal-velocity ratio from the survey. Values  $(V_x/V)$  corrected are given in Table 4.

## PROPELLER DESIGN

### Design Procedure

The propeller design was based on the design specifications and ship data presented in the previous section. The objective, as stated before, was to minimize vibration without adversely affecting efficiency and cavitation resistance. Figure 2 is a schematic representation of the design procedure. The propeller design procedure consists of, essentially, six phases, namely:

(i) Preliminary Design: In this phase preliminary estimates are made of diameter, aperture clearance, blade area ratio to avoid thrust breakdown, propeller rotation speed, blade outline, design conditions such that the propeller is compatible with the ship and the propulsion machinery from the standpoint of efficiency and vibration, as well as NAVSEC prescribed constraints and military specifications.

(ii) Lifting Line Design: In this phase the radial load distribution and the radial hydrodynamic pitch angle are computed using the Lerbs<sup>5</sup> induction factor method.

<sup>5</sup>Lerbs, H.W., "Moderately Loaded Propellers with a Finite Number of Blades and an Arbitrary Distribution of Circulation," Transactions of the Society of Naval Architects and Marine Engineers, Vol. 60, p 73-117, 1952

(iii) Propeller Geometry: In this phase the blade chord lengths, the thickness distribution, and the skew angle distribution are determined from the viewpoint of minimizing vibratory forces in order to be compatible with military specifications, to minimize cavitation to prevent erosion and vibration, and to insure adequate strength.

(iv) Lifting Surface Design: In this phase the final geometric pitch distribution and camber distribution are determined using the lifting surface procedure of Cheng<sup>6</sup> together with the thickness corrections of Kerwin and Leopold<sup>7</sup>. In addition, the final propeller offsets are determined including fillets, trailing and leading edge details, additional thickness added to the trailing edge where required, tip geometry, rake (to insure proper location of blade with respect to definition of skew, and proper aperture location), hub details, and location of the propeller on the hub.

(v) Final Design Check: In this phase the propeller is reviewed to verify that it has adequate strength from the viewpoint of fatigue, to check the off-design performance in fouled and ballast conditions, and to summarize the final design predictions in terms of required speed margins, military specifications, and other NAVSEC specified constraints. This phase includes the accomplishment of a finite element stress analysis computation of the propeller for the steady ahead loading.

---

<sup>6</sup>Cheng, H.M., "Hydrodynamic Aspects of Propeller Design Based on Lifting Surface Theory, Part II - Arbitrary Chordwise Load distribution," David Taylor Naval Ship Research and Development Center Report 1803, June 1965

<sup>7</sup>Kerwin, J. and Leopold, R., "A Design Theory for Subcavitating Propellers," Transactions of the Society of Naval Architects and Marine Engineers, Vol. 72, p 294-335, 1964

(vi) Experimental Evaluation: In this phase, experiments are conducted as an independent check of the propeller design. Open-water characteristics, self-propulsion performance, cavitation inception, and cavitation erosion potential are determined experimentally and compared with the design predictions and the design requirements.

The analytical design procedure currently used at DTNSRDC and basically used in this design has been described previously in general terms by Cox and Morgan<sup>8</sup>. It should be noted that the procedure is iterative in nature and that the first five phases are overlapping and interrelated. After the experimental evaluation of the initial design selection is completed, the possibility of doing a more refined iteration always exists. In the majority of the design problems handled by this procedure the initial design selection is usually the final design. However, where unusual problems arise it may be necessary to redesign the propeller. A reanalysis of the trailing edge shape was requested by the sponsor. Because this iteration was accomplished in the design, the description of the design will concentrate on presenting the results of the final design, for which the only difference is a change in the trailing edge outline as compared with the initial design selection. Additional information on the iteration and resulting change will be discussed in subsequent sections when differences between the initial and final designs appear throughout the design procedure.

---

<sup>8</sup>Cox, G.G. and Morgan, W.B., "Application of Theory to Propeller Design," Marine Technology, Vol. 9, No. 4, p 419-429, October 1974

### Preliminary Design Analysis

Preliminary design calculations were performed by NAVSEC prior to the detailed propeller design. The calculations were performed by computer methods using lifting line theory based on Lerbs' induction factors<sup>5</sup> in order to check propeller efficiency as a function of diameter, D, expanded area ratio,  $A_E/A_0$ , propeller rotational speed, N, and number of blades, Z. Diameters of 21 through 24 feet (6.4 through 7.3 meters) were tried. Expanded area ratios of 0.65 to 0.85 were used and the blade outline for each ratio was calculated using the formula recommended by Morgan, Silovic, and Denny<sup>9</sup>, since experience has shown this outline to be satisfactory for preliminary analysis. Values of shaft speed from 90 to 110 rpm (9.4 to 11.5 rad/s) and values of Z of 5, 6, and 7 were evaluated. For this investigation NAVSEC elected to apply a 2 percent speed margin\* on the effective power,

---

<sup>9</sup> Morgan, W.B., Silovic, V., and Denny, S.B., "Propeller Lifting-Surface Corrections," Transactions of the Society of Naval Architects and Marine Engineers, Vol. 76, p 309-347, 1968

\*A speed margin is derived by replotting the  $P_E$  curve. In this case, the values of speed desired are increased by 2 percent and values of  $P_E$  read from the  $P_E$  curve at this new speed. These new  $P_E$  values become the  $P_E$  with margin at the originally desired speed. To illustrate, if 20 knots is the desired speed, the original  $P_E$  curve is read at 20 knots plus 2 percent of 20 knots or 20.4 knots. The value of  $P_E$  at 20.4 knots is read and re-plotted at 20 knots. This is repeated throughout the speed range until a new  $P_E$  curve is generated. The  $P_E$  curve with margin may be substantially higher than the curve without margin, especially if the slope of the original curve is steep.

and use a Lerbs' optimum load distribution to evaluate various propeller parameters at the full load and full power operating condition. Values of  $V_x/V$ ,  $l-w_T$ , and  $l-t$  were corrected for diameter variations using data presented in References 3 and 4. The conclusions of the NAVSEC performed, preliminary design analysis are reflected in the design conditions already presented in Table 1. Their calculations indicated that efficiency increased as  $N$  decreased in the range of  $N$  considered. Since 100 rpm (10.5 rad/s) was the minimum allowable because of constraints imposed by the size of the reduction gear, 100 rpm (10.5 rad/s) was selected as the design rotational speed. The selection of diameter, number of blades, and expanded area ratio were left open since unsteady forces and cavitation performance are sensitive to their variation. From the viewpoint of propulsive efficiency the NAVSEC calculations indicated that 5, 6, or 7 blades, any diameter between 21 and 24 feet (6.4 and 7.3 meters), and any area ratio between 0.65 and 0.85 are acceptable.

The blade area ratio selected for the AO-177 propeller is 0.77. This selection was based on the fact that the operating point as plotted on the Burrill and Emerson<sup>10</sup> cavitation diagram is just above the suggested merchant ship limit, and is well below the thrust breakdown point insuring avoidance of thrust breakdown in this design.

The primary consideration in this design was to minimize the unsteady propeller forces without adversely affecting efficiency,

---

<sup>10</sup> Burrill, L.C. and Emerson, A., "Propeller Cavitation: Further Tests on 16-Inch Model Propellers in the Kings College Cavitation Tunnel," Northeast Coast Institute of Engineers and Shipbuilders, Vol. 79, p 295-320, 1962-63

cavitation characteristics, and strength. Therefore, the selection of blade number and diameter was in part based on the production of propeller vibratory forces, which meant in this case the application of the Tsakonas, et al<sup>11</sup>, unsteady propeller program with additional refinements since the publication of Reference 11. This program is based on linearized, unsteady, lifting-surface theory. Within the linearized assumptions the propeller responds to each harmonic of the circumferential variation of the wake, independent of the other harmonics. Due to the symmetry of the propeller, only multiples of the blade frequency forces and moments are transmitted through the shafting, and usually (as in the present case) the blade frequency is of primary concern. The blade rate (or blade frequency) harmonics corresponding to 5, 6, and 7 blades are the 5th, 6th, and 7th harmonic, respectively. From the radial distribution of the normal velocity\* component amplitudes and angular location of maximum amplitudes, calculations can be performed for various propeller geometries using the Tsakonas, et al, program. Using this program calculations of the unsteady forces were performed for 5 and 7 blades and diameters from 21 to 24 feet (6.4 to 7.3 meters). Prior to evaluating changes in geometry in terms of unsteady load production, vibration calculations based on the propeller weight and center of gravity estimates were made. The calculations indicated that the 6-bladed design would be a poor

<sup>11</sup>Tsakonas, S., Breslin, J., and Miller, M., "Correlation and Application of Unsteady Flow Theory for Propeller Forces," Transactions of the Society of Naval Architects and Marine Engineers, Vol. 75, p 158-193, 1967

\*The normal velocity, normal to the nose-tail line of the blade section, is related to the longitudinal and tangential wake velocities as follows (Refer to References 1 and 11).

$$V_N/V = (V_x/V)\cos \phi - (V_t/V)\sin \phi$$

choice since a shaft resonance was predicted at approximately the full-power shaft speed. Therefore, 6-blades were eliminated from consideration. The unsteady force calculations indicated that a 7-bladed 21-foot (6.4 meters) diameter propeller would yield the lowest unsteady forces in terms of blade number and diameter variations.

#### Lifting Line Design

The radial load distribution on the blades affects the propeller efficiency, cavitation characteristics, stress in the blades, and unsteady pressure forces induced on the hull. The load distribution is directly related to the radial variation of hydrodynamic pitch along the blade. Several hydrodynamic pitch distributions were investigated with regard to propulsive efficiency and blade stress to determine the effect of changes in the radial load distribution. The AO design, hydrodynamic pitch distribution is compared with the corresponding Lerbs' optimum hydrodynamic pitch distribution in Figure 3. Lifting-line theory based on Lerbs' induction factors<sup>5,12</sup> was used for predicting the propeller performance. The result of reducing the pitch as shown in Figure 3 corresponds to a predicted decrease in ship speed of less than 0.1 knot as compared with the Lerbs' optimum design.

The effect of the radial-load distribution on the cavitation characteristics and the unsteady pressure forces induced on the hull cannot be determined quantitatively, but can only be inferred. Unloading the blade tip reduces the unsteady pressure field fluctuations in the vicinity of the hull near the blade tip, helps alleviate the tendency

---

<sup>12</sup> Morgan, W.B. and Wrench, J.W., "Some Computational Aspects of Propeller Design," Methods of Computational Physics, Vol. 4, Academic Press, Inc., New York, p 301-331, 1965

toward cavitation in this area, delays tip-vortex cavitation inception and tends to reduce the blade stresses. The principal disadvantage of unloading the tip is that there is a decrease in efficiency. The magnitude of this decrease depends on the amount of unloading.

As pointed out above, the hydrodynamic pitch distribution selected for the AO design resulted in a very small change in predicted ship speed. The tip unloading will help suppress tip vortex cavitation inception and generally improve the cavitation characteristics near the tip, and give a satisfactory stress distribution. No unloading was applied near the hub. Unloading in this area, to reduce hub vortex cavitation, is not considered necessary for ships of this type, and is therefore not generally done.

Table 5 presents the lifting line design for the AO-177, final propeller design. The analytically predicted speed for this propeller at the full-load design condition absorbing the full, 24,000 SHP (17,897 kw) at 100 rpm (10.5 rad/s) is 21.4 knots (11.0 m/s).

#### Propeller Geometry

The selection of the final propeller geometry consists of determining the radial distribution of chord length, thickness, skew pitch, and camber. The latter two are determined from lifting-surface corrections, given the rest of the geometry, and the circulation distribution and hydrodynamic pitch distribution at the design point as calculated by lifting-line theory. These results are presented in a subsequent section. The first three geometrical parameters are determined by constraints set on the design

by the sponsor and the designers. These constraints were discussed previously.

The blade outline suggested by Cox<sup>13</sup>, also given in Morgan, Silovic and Denny<sup>9</sup> was selected initially. It is slightly wider towards the tip than the Troost series outline<sup>14</sup>. Several alterations in the blade outline were considered in terms of contributing to the reduction of the alternating forces produced by the propeller while maintaining good cavitation characteristics and no loss in propeller efficiency. Again, using the Tsakonas, et al<sup>11</sup>, program to compute the effect of changes in geometry on the propeller produced vibratory forces, the designers found that a somewhat narrower blade outline as compared with the Cox<sup>13</sup> and Morgan, et al<sup>9</sup>, outline resulted in predictably lower alternating forces. Therefore, the final design blade outline with the comparatively narrower width towards the tip (also including an increase in chord length at approximately the 0.5 radius which was a result of the iteration on the design discussed in a subsequent section) is presented in Table 6. The modifications of the initially selected blade outline were due to the resulting reduction in alternating forces, and the requested changes by the sponsor. Cavitation performance, strength integrity, and powering performance were not altered significantly as a result of the blade outline change.

---

<sup>13</sup>Cox, G.G., "Corrections to the Camber of Constant Pitch Propellers," Royal Institute of Naval Architects, Vol. 103, p 227-243, 1961

<sup>14</sup>Troost, L., "The Pitch Distribution of Wake-Adapted Marine Propellers," Transactions of the Society of Naval Architects and Marine Engineers, Vol. 64, p 357-374, 1956

In order to evaluate this propeller for possible cavitation erosion, the correlation of erosion experimental data presented by Lindgren and Bjarne<sup>15</sup> was applied. They presented a correlation of model data indicating under what conditions a merchant ship propeller can be expected to erode. The influence of wake variations and blade area ratio on cavitation erosion of merchant ship propellers is shown in Figure 4. Included on the figure is the design point for the final AO propeller. Using this correlation as a design criterion for the elimination of cavitation erosion, the expanded area ratio of 0.77 and the blade-outline selected for this design were considered acceptable.

The thickness distribution was selected based on strength and cavitation considerations. Stresses were calculated by a simple, cantilever beam analysis with a correction to account for the stresses due to skew. The mean values of the stresses for the steady ahead, full-power design condition are all less than 6,500 psi (44.8 MPa). NAVSEC required that the stresses calculated by the above method not to exceed 12,500 psi (86.2 MPa) anywhere on the blade. The actual design limit decided upon by the designers of 6,500 psi (44.8 MPa) instead of 12,500 psi (86.2 MPa) was dictated by fatigue considerations to be described later. Also, if the stress level of 12,500 psi (86.2 MPa) were reached at the hub, the thickness to chord ratio ( $t/c$ ) would be less than 0.2. Since, in addition to fatigue considerations the weight was acceptable and no advantage in either cavitation or viscous drag would be realized at  $t/c$  values less than 0.2, this  $t/c$  was selected at the hub. Figure 5 presents the final  $t/c$  distribution along with the maximum principal stresses computed by beam theory and the cavitation criteria described next.

<sup>15</sup> Lindgren, H. and Bjarne, E., "Studies of Propeller Cavitation Erosion," Conference on Cavitation, Edinburgh, arr. by Institute of Mechanical Engineers, Preprints, p. 241-251, 1974.

Cavitation inception was estimated by calculating the angle of attack variation using the variation in advance angle experienced by each blade section in one revolution, such that

$$\alpha = \alpha_i - \frac{\Delta\beta}{k_c + \frac{2}{\lambda_e}}$$

where:

$k_c$  is the ratio of camber required in three dimensional flow to camber required in two dimensional flow to produce the same lift at the ideal angle of attack.  $k_c = 1.0$  was used for this calculation only (experience at DTNSRDC indicates that this is adequate for this calculation).

$\lambda_e$  is the effective aspect ratio:

$$\lambda_e = \frac{c_L}{\pi \tan(\beta_i - \beta)}$$

Local cavitation numbers ( $\sigma_L$ ) were then calculated using the axial and tangential induced velocities and the longitudinal and tangential wake velocities<sup>4</sup> such that

$$\sigma_L = \frac{2gH_L}{(v_x + u_a)^2 + (2\pi nr - u_t - v_t)^2}$$

where:

$H_L$  is the static head in feet which is equal to the distance from point on the propeller where the local cavitation number is being calculated to the water surface. This includes effects of trim or change in free surface height due to wave making at the stern.  $v_x$  and  $v_t$  are axial and tangential wake velocities, respectively.  $u_a$  and  $u_t$  are axial and tangential induced velocities, respectively. With the advance angle data in Figure 6 in addition to the local advance variation

based on data in Figure 1, the inception of cavitation was then predicted by plotting the angle of attack variation with cavitation number on the cavitation inception curves for the NACA 66 (TMB modified) thickness form with the NACA  $a=0.8$  camberline<sup>16</sup>. These hydrofoils were used because of their low drag, good cavitation characteristics, and because the NACA  $a=0.8$  meanline achieves experimentally its theoretically predicted performance.

In this design the calculations were done by computer at each 10 percent radial station for each 15 degree angular position around the propeller disc, and for angular positions corresponding to maximum and minimum values of angle of attack. This method gave a fairly complete picture of predicted cavitation inception. Figures 7 through 10 are cavitation inception curves for the 60 through 90 percent radii for the final AO design. The cavitation free region is the area located inside of the curves, while the top portion of the curve indicates predicted back sheet cavitation, the lower portion indicates probable face cavitation, and the left side indicates back-bubble cavitation inception. Figures showing cavitation performance inside the 60 percent radius were not shown since all points fell inside the curves. Thickness to chord values were varied such that the inception of back-bubble cavitation was delayed until full power speed plus the 10 percent margin at design conditions and face cavitation as predicted analytically had to be tolerated beyond the 80 percent radius since increasing the thickness would reduce the back bubble margin. Back sheet cavitation was unavoidable beyond the 60 percent radius.

<sup>16</sup> Brockett, T., "Minimum Pressure Envelopes for Modified NACA 66 Sections with NACA  $a=0.8$  Camber and BUSHIPS Type I and II Sections," David Taylor Naval Ship Research and Development Center Report 1780, February 1966

The variation of thickness to chord ratio to obtain the desired cavitation characteristics was accomplished by varying thickness only, since it was desired to keep the blade outline constant in order to minimize unsteady forces, i.e., the criterion used to choose blade outline was the reduction of unsteady forces. Concurrently, cavitation characteristics were checked to ensure adequate margin against thrust breakdown.

Thickness values at the 30, 40, and 50 percent radii were chosen such that a smooth transition in t/c was maintained between the hub and the 60 percent radius. The resulting thickness distributions, which were chosen for the final designs, gave adequate cavitation and strength characteristics, and a smooth distribution of stresses and t/c. The final thicknesses are plotted in Figure 5 indicating conformance with the design criteria.

#### Skew Angle Distribution

Once the number of blades is selected, the next step in minimizing the propeller unsteady forces is to pick the magnitude and distribution of skew angle. The objective is to select a skew distribution which results in a combination of values of unsteady thrust, torque, side force and bending moments such that these vibration excitation forces are below the levels specified by Mil-Std-167 and Mil-Std-1472A. The present state of the art does not allow an optimum skew to be calculated, i.e., it is not possible to start with desired values of unsteady thrust, torque, side forces, and bending moments and calculate the skew distribution and blade outline necessary to achieve these values. Picking skew is therefore a cut and try operation based on certain qualitative and quantitative methods which will be described below.

A large amount of data is available at DTNSRDC which indicates that a judicious selection of the radial skew angle distribution reduces the magnitude of propeller-induced vibration-excitation forces transmitted through the shafting to the bearings and through the water to the hull plating and rudder<sup>1</sup>. Also, a substantial amount of skew angle tends to increase the tolerance to cavitation inception caused by the operation of the propeller in a circumferentially varying inflow<sup>17</sup>. Although the data show that highly skewed propellers are generally desirable, the data provide little guidance for selecting the appropriate radial distribution of skew angle for a given application.

The selection of the skew angle distribution in a typical propeller design problem is the predominant geometrical parameter controlling the propeller unsteady loading. This is a direct result of the mechanism of cancellation, from root to tip, of the unsteady loading on the blades by which skew angle reduces the unsteady bearing forces. The effect of skew angle distribution on the bearing forces can be evaluated by the use of unsteady lifting surface theory. Tsakonas, et al<sup>11</sup>, have compared a limited number of experimental results obtained by Boswell and Miller<sup>18</sup> for a series of propellers operating in simplified wake patterns. Cumming, et al<sup>1</sup>, point out that these experiments substantiate the calculation procedure. Consequently, the Tsakonas, et al, computer program was used to assist in selecting the final skew distribution for the

<sup>17</sup> Boswell, R.J., "Design, Cavitation Performance, and Open-Water Performance of a Series of Research Skewed Propellers," David Taylor Naval Ship Research and Development Center Report 3339, March 1971

<sup>18</sup> Boswell, R.J. and Miller, M.L., "Unsteady Propeller Loading - Measurement, Correlation with Theory, and Parametric Study," David Taylor Naval Ship Research and Development Center Report 2625, October 1968

AO propeller. In addition, the magnitudes of the unsteady loads predicted by this program were compared with the military standards for vibration excitation forces.

For helpful hints on selecting skew angle by evaluating the shape of the wake, i.e., how the blade frequency and side force harmonics differ radially, the reader is referred to a paper by Cumming, et al<sup>1</sup>. Following their suggestion, the circumferential blade frequency components of the normal-to-the-blade velocity for the 7-bladed AO designs are plotted in Figures 11 and 12. Skew angle distributions which are intended to satisfy the minimization of unsteady thrust and torque criteria, were selected with the idea of having large skew angle changes where the crest does not vary significantly from the radial coordinate and less skew angle change where the crest shifts to a position such that along the original radial coordinate the crest changes sign, i.e., it changes to a trough. If there is no change in sign, skew tends to reduce the unsteady thrust and torque. In this case, increasing the amount of skew will reduce the unsteady thrust and torque. For the 7-bladed AO designs the blade frequency harmonic amplitude does change sign radially near the t.p. This sign change can make substantial reductions in unsteady forces difficult to attain. However, the judicious selection of a non-linear skew distribution in the AO design reduced the thrust and torque dramatically.

Side forces are sensitive to the  $Z \pm 1$  harmonics. Sign changes in the harmonics will tend to increase side forces when skew is applied. Side forces will be reduced by increasing skew if the  $Z \pm 1$  harmonics have maximum amplitude locations which do not vary radially. The problem then is to reduce unsteady thrust, torque, and side forces; the unsteady

thrust and torque being considered of principal importance, the side forces of lesser, although significant, importance. At this stage of the design the hull is fixed, and nothing can be done to change the wake harmonics. Further, since the unsteady thrust and torque are of primary importance, it was decided to tailor skew, by changing its radial distribution, to reduce  $\widetilde{T}$  and  $\widetilde{Q}$ , making the final choice that with the best combination of reduction of unsteady thrust, torque and side forces. In addition, the location of the maximum amplitude of the normal velocity components for the 6th and 8th harmonics did not change radially; consequently, the side forces were expected to be reduced substantially with high skew.

Concurrent with changes in skew angle distribution, changes in number of blades, blade outline and diameter were also evaluated in terms of their effects on the propeller produced unsteady loading. Blade numbers of 5, 6, and 7, diameters from 17 feet to 23 feet (5.18 to 7.01 meters) and blade outlines with narrower tips were considered and evaluated using the Tsakonas, et al, program and the appropriate blade frequency wake harmonics. Several skew angle distributions were selected based on an evaluation of the circumferential variations in the wake velocity and, subsequently, the corresponding unsteady forces were computed. The results of this cut and try procedure indicated that the most appropriate design in terms of meeting the military standards for vibration excitation is a 7 bladed propeller, 21 feet (6.4 meters) in diameter, with a slightly narrower blade outline in comparison with the initially selected shape (discussed before in this paper) and with a 45 degree (0.8 rad) tip skew with a nonlinear radial distribution

of skew angle; see Table 6. Several examples of some of the geometry changes and skew distributions evaluated are given in Figure 11. These blade shapes were considered as additional changes in the iteration of the preliminary (or original) design as requested by the sponsor. The preliminary and final designs are presented in Figure 12. In essence, the sponsor's request was to evaluate the feasibility of eliminating or reducing the skew without sacrificing propulsive efficiency (i.e., ship speed) or predicted vibration excitation (i.e., meet military specifications on ship vibration). The results indicated that a revision of the highly curved trailing edge of the original design was possible and still be able to meet the vibration requirements of Mil-Std-167 and Mil-Std-1472A; see Figure 13.

The predicted unsteady forces for the final AO propeller design are summarized in Table 7. The design meets the military standards and the shape requirements of the sponsor. Also, even though the present state-of-the-art prohibits the precise determination of the vibration excited by the vector sum of the hull pressure forces plus the bearing forces, the skew angle distribution is expected to reduce the amplitude of both the pressure force (as demonstrated by Teel and Denny<sup>19</sup>) and the bearing-force components (as computed in this investigation).

#### Lifting-Surface Design

The final camber and pitch distributions were determined from lifting-surface correction factors computed by a method of Cheng<sup>6</sup> and

<sup>19</sup> Teel, S.S. and Denny, S.B., "Field Point Pressures in the Vicinity of a Series of Skewed Marine Propellers," David Taylor Naval Ship Research and Development Center Report 3278, August 1970.

together with the thickness corrections of Kerwin and Leopold<sup>7</sup>. It is emphasized that the pitch correction due to skew is very substantial, and a skewed propeller with a desired load distribution can only be designed by lifting surface techniques. Table 8 presents the lifting surface correction factors calculated for the final AO-177 propeller. The final design is summarized in Table 6 and Figure 14.

The final geometric properties necessary for manufacture, namely, pitch, chord length, skew, maximum camber, maximum thickness, rake, trailing edge epsilon (added trailing edge thickness), and blade section offsets, were faired by computer at each 2-1/2 percent of propeller radius from hub to the 95 percent radius, and at each 1 percent of propeller radius from the 96 to 99 percent radii. The values derived were then plotted to ensure the fairing had been done correctly. These values are listed in the appendix.

As previously stated, the hydrofoil used was the NACA 66 series sections with NACA  $a=0.8$  meanline. Thickness was added at the trailing edge in order to ensure adequate strength. The additional thickness is added to the trailing edge in such a manner as to maintain the original, maximum thickness-to-chord ratio, i.e., from the maximum thickness location to the trailing edge, the hydrofoil shape is modified using the following equations

$$Y_u = ((t/2) - \epsilon)^2 Y_t + \epsilon + f_M \cdot Y_c$$

$$Y_L = ((t/2) - \epsilon)^2 Y_t + \epsilon - f_M \cdot Y_c$$

where:

$Y_u$  = upper offset in inches

$Y_L$  = lower offset in inches

$t$  = maximum blade section thickness in inches

$\epsilon$  = additional trailing edge thickness specified as a function of radius in inches

$f_M$  = camber in inches

$y_t/t$  = half-thickness, hydrofoil thickness form offset divided by maximum thickness

$y_c/f_M$  = camber line offset divided by maximum camber

$\epsilon$  was added to the full scale design where needed based on the following criteria: from  $x=0.2$  to  $0.85$ ,  $\epsilon=0$  is trailing edge thickness is greater than 0.4 inches\* full-scale,  $\epsilon=(1/2)$ . ( $0.4$  = trailing edge thickness) if trailing edge thickness is less than 0.4 inches full-scale; from  $x=0.85$  to tip  $\epsilon=(1/2)$  ( $0.15 t_{max}$ ). The final results are tabulated in the Appendix.

The trailing edge detail, Figure A1 of the Appendix, is an anti-singing design currently used at DTNSRDC. The hub geometry (see Figure A2 of the Appendix) is a truncated cone designed to properly fair with the stern tube housing and fairwater cap. The blades are located on the hub such that the mid-chord of the 70 percent radius will coincide with the location shown on the lines drawing. The hub is of sufficient length to overhang the blades at their greatest forward and aft dimensions, by at least seven inches, in order to protect them from damage during handling and storage. The fillets at the juncture of the blades and hub will be applied according to Navy standard practice.

---

\* 0.4 inches was chosen as the trailing edge thickness criteria based on several recent propellers designed at DTNSRDC.

Rake\*\* was added to the propeller in order to maintain the blade centerline (skew line) at the proper position. During the design phase, calculations were made assuming the pitch to be equal to the hydrodynamic pitch ( $\beta_1$ ) of the propeller. When lifting surface corrections were applied to obtain the geometric pitch ( $\phi$ ), a substantial difference was caused in the position of the blade sections with respect to the blade reference line. Rake was added to bring the blade centerline back to the longitudinal position it occupied during the design phase, where skew was applied along the hydrodynamic pitch helix.

The details of the final design propeller geometry are given in Table 6 and in the Appendix.

#### FINAL DESIGN CHECK

##### Fatigue Life

In order to calculate the fatigue life, the unsteady propeller blade loading was calculated using the unsteady lifting surface theory of Tsakonas, et al.<sup>11</sup>. Full power design conditions were assumed. The program was set up to calculate the

---

\*\* Rake as used in this report is defined as the longitudinal displacement forward or aft of the blade sections successively from the radial reference line. This rake does not include warp induced rake (warp being the projected skew angle and skew being linear dimension along the pitch helix). Rake aft is considered positive. It should be noted that this is a broader definition of rake than normally used, since rake is commonly defined as an angle, giving the inclination of the radial reference line forward or aft.

unsteady loading and bending moments due to the first eight harmonics of the wake. It was observed that contributions to the unsteady loading due to harmonics greater than the eighth were negligibly small. The steady bending moments were predicted from the loading generated using lifting-line theory based on Lerbs' induction factors<sup>5</sup>. Steady stress was predicted from beam theory as previously described. Since the steady bending stress is proportional to the steady bending moment, it follows that unsteady bending stress is proportional to the unsteady bending moment. Therefore, the product of the steady stress and the ratio of the steady and unsteady bending moments is equal to the unsteady stress:

$$\bar{\sigma} = \frac{\overline{BM}}{\overline{BM}} \bar{\sigma}$$

where:

$\overline{BM}$  is the steady bending moment,  $\widetilde{BM}$  is the unsteady bending moment,  $\bar{\sigma}$  is the steady stress, and  $\widetilde{\sigma}$  is the unsteady stress.

Figure 15 shows the maximum stress point (the 0.2 radius) on a modified-Goodman, working stress diagram. The properties for the propeller material are those specified by NAVSEC and given in the "Propeller Design Condition" section. The diagram shows that the final design has adequate fatigue strength characteristics.

A finite element method<sup>20</sup> was used to check the strength integrity as determined using the modified, simple beam approximation. The stresses were calculated for the steady ahead full-power loading and are presented

---

<sup>20</sup>Genalis, P., "Elastic Strength of Propellers - An Analysis by Matrix Methods (Including a Programmer's Manual and a User's Manual)," David Taylor Naval Ship Research and Development Center Report 3397, July 1970

in Figures 16, 17, and 18, respectively. The deflections of the blade at full power indicate that the pitch distribution is not altered significantly and therefore, should not affect the predicted shaft speed at full-power. The maximum principal stresses computed on the back and face of the propeller are consistent with beam theory estimates. Also, no areas on the blade surface contains high stress concentrations. The conclusion from these calculations is that for the AO-177 propeller has adequate strength.

The performance predictions based on the analytical design procedure described up to this point for the full-power design point are summarized in Table 7. In the next section the off-design performance and, in particular, the endurance speed power requirements are determined.

#### OFF DESIGN CALCULATIONS

Since the design conditions state that 20 knots must be maintained at 80 percent power (full load, clean hull, calm seas) and that there be no back bubble cavitation at full power, it was important to check performance and cavitation characteristics at off design conditions. An inverse propeller computer program<sup>7</sup> developed at the Massachusetts Institute of Technology (MIT) was used in the evaluation.

Calculations were run at design conditions as a check on the accuracy of the program. Thrust and power values were within 0.15 percent of the lifting line design values. In order to predict endurance power and rpm, thrust was calculated using the relation  $T = 326P_E/V_s(1-t)$ ; where  $P_E$  is in units of horsepower and  $V_s$  is ship speed in knots. Speed-power information was obtained from Reference 3. The Inverse

Program was then run at 20 knots (10.3 m/s) ship speed with a range of possible shaft speeds. The thrust values predicted by the program at each shaft speed were checked against the calculated thrust. When the values coincided, endurance conditions were considered to be predicted. Shaft power, speed, etc. are calculated as part of the program output and listed in Table 9.

The worst case from a cavitation standpoint was considered to be full power at the ballast condition. Inflow velocity was greatest, making angle of attack the most negative. Submergence was least, and, when combined with the increased inflow velocity, made the cavitation index a minimum.

To find the conditions necessary to calculate cavitation at ballast the Inverse Program was again used. Since neither ship speed nor propeller shaft speed was known, the program was run at a range of shaft speeds for given estimated ship speeds. Desired thrust was calculated as before at each estimated speed. The thrust calculated by the program was compared with the desired thrust at each speed. For a given speed, thrust and also  $P_g$ , varied with shaft speed. When the thrusts matched at full power, the correct conditions have been found. Performance values for the ballast condition at full power are given in Table 10.

From the values of lift coefficient due to angle of attack calculated by the Inverse Program, the changes in angle of attack were estimated as follows:

1. At each radius the change in lift coefficient was calculated.  
 $\Delta C_L = C_{LaOD} - C_{LxD}$ , where  $C_{LxD}$  is the lift coefficient at design conditions,  $C_{LaOD}$  is the lift coefficient at the off design condition to be investigated, and  $\Delta C_L$  is the change in lift coefficient due to the change in angle of attack.

2. For each  $\Delta C_L$ ,  $\Delta\alpha$  is calculated using the relation  $\Delta\alpha = \Delta C_L (2\pi(1-0.83 t/c))$  from the report of Brockett<sup>16</sup>, where  $t/c$  is the thickness to chord ratio of the section and  $\Delta\alpha$  is the estimated change in angle of attack.

In all cases,  $\Delta\alpha$  was of negative sign and less than 0.005 degrees in magnitude, and was therefore ignored. Had it been significant, however, it would have been added to the value of  $\alpha$  calculated for the design conditions.

To calculate the change in local cavitation number,  $\sigma_L$ , the relation  $\sigma_L = 2gH_L / (V_L/V)^2 V^2$  was used. Since only the conditions of most severe cavitation were of interest, the points corresponding to the maximum and minimum  $\alpha$ , and the minimum  $\sigma_L$ , as calculated for the design conditions, were investigated at the 0.7, 0.9 and 0.9 radii. The values of  $(V_L/V)^2$  were found from:

$$(V_L/V)^2 = (V_x/V)^2 + (\pi x/J_A)^2$$

where  $V_L$  is the local velocity at the section being investigated,  $V$  is ship speed,  $V_x$  is longitudinal velocity of the flow at the radius and angular position being considered ( $V_x/V$  is given in the wake survey),  $x$  is the nondimensional propeller radius and  $J_A$  is the advance coefficient,  $J_A = V(l-w_t)/nD$ ,  $D$  is propeller diameter,  $(l-w_t)$  is the effective wake fraction,  $n$  is rotation speed and  $H_L$  is the local head, due to submergence at the point being investigated.  $H_L = H - r \cos \theta$  where  $H$  is the vertical distance from the centerline of the shaft to the surface of the water; including any contribution from trim or wave making, plus atmospheric pressure (equal to 34 feet or 10.4 meters of water) minus vapor pressure (approximately equal to 1 foot or 0.305 meter of water), and  $\theta$  is the angle between the vertical and the point being investigated. The predictions

indicated that no back bubble cavitation is expected throughout the operating range of the ship. The other forms of cavitation are minimized to the extent possible.

#### DISCUSSION OF EXPERIMENTAL EVALUATION

Model experiments were conducted to evaluate the powering and cavitation performances for the AO-177 Class Naval fleet oiler<sup>21</sup>. The experiments are conducted for two reasons. One is to provide an independent check on the design calculations; and, two, the experimental results provide data which can be used to facilitate the prediction of off-design performance under a variety of conditions. Model propeller 4677 corresponds to the final AO propeller and was tested on hull model 5326, representing the AO-177 Class ship. Open-water, powering, and cavitation experiments were conducted in order to evaluate the propeller design. The open-water experiment was performed to provide predictions of propeller performance for use in the propulsion experiments and to calibrate tunnel velocity for the cavitation experiments. The powering experiment was performed to determine propulsion performance. The cavitation experiments were performed to predict the effect of cavitation on ship powering and to evaluate the possibility of blade erosion. The details of the experimental procedures and conditions are described in Reference 21. In addition, experimental results

---

<sup>21</sup>Hendrican, A. and Remmers, K., "Powering and Cavitation Performance for a Naval Fleet Oiler, AO-177 Class (Model 5326 with Propeller 4677)," David Taylor Naval Ship Research and Development Center Report SPD-544-14, January 1976

for the preliminary design<sup>22,23</sup> are compared with the final design in this reference. Only the results pertaining to the design requirements are presented and compared with the design predictions in this section.

The open-water characteristics for the AO-177 Class fleet oiler, highly skewed propeller is presented in Figure 19. The minimum Reynolds number based on the 0.7 radius chord length and inflow speed of the experiment as reported in Reference 21 was  $5 \times 10^5$ .

The results of towing tank resistance and self-propulsion experiments for  $C_A = 0.0005$  are presented in Figure 20. The difference in the tank and trial predictions of effective horsepower is that the latter is corrected for zero true wind. With the assumption that the propulsive coefficient and thrust deduction are the same for both the trial and tank data, the corresponding trial shaft power was computed. Based on a statistical correlation of the shaft speed of conventional (not highly skewed) propellers propelling surface ships presented in 1962<sup>24</sup>, and considered still applicable for conventional propellers as of January 1976<sup>21</sup>, a reduction in shaft speed of 2 percent for a  $C_A = 0.0005$  was found\*. The effect of high skew on this correlation has not been

---

<sup>22</sup> Murray, L. and Hecker, R., "Powering Predictions of a Naval Auxiliary Oiler (AO) (Model 5326 with Design Propeller 4645)," David Taylor Naval Ship Research and Development Center Report SPD-544-10, September 1974

<sup>23</sup> Remmers, et al, "Cavitation Performance of a Propeller Design for a Naval Auxiliary Oiler (AO-177 Class) (Model 5326 with Design Propeller 4645)," David Taylor Naval Ship Research and Development Center Report SPD-544-11, September 1974

<sup>24</sup> Hadler, J.B., Wilson, C.J., and Beal, A., "Ship Standardization Trial Performance and Correlation with Model Predictions," Transactions of the Society of Naval Architects and Marine Engineers, Vol. 70, 1962

\*This rpm correction is presently being reevaluated.

evaluated as yet. Many more full scale applications are required in order to accomplish this evaluation. Therefore, this correlation, correction factor must be viewed cautiously. However, since, in this case, it is only 2 percent, the differences in the tank and trial predictions of shaft speed are well within any reasonable variation in its predictability. As shown in the figure, the propeller should absorb 24,000 shaft horsepower (17,897 kw) at 98 or 99 rpm (10.3 or 10.4 rad/s) and propel the ship 21.5 knots (11.1 m/s). The thrust deduction ( $l-t$ ) and Taylor wake ( $l-w_T$ ) determined for this condition are 0.87 and 0.77, respectively. The predicted speed based on lifting line theory is 21.4 knots (11 m/s), which assumed a thrust deduction and wake fraction of 0.86 and 0.78, respectively. Figure 21 presents the powering predictions in accordance with NAVSEC policy. i.e., the only change to the tank data is the inclusion of air drag and a 3 percent power margin. The full-power prediction from these data is a ship speed of 21.4 knots (11.0 m/s) and a shaft speed of 100 rpm (10.5 rad/s). All the predictions are within two percent of the desired shaft speed for the full-power. Therefore, these results lead to the conclusion that the propeller does meet the full-power design requirement of absorbing the full-power of 24,000 SHP (17,897 kw) at 100 rpm (10.5 rad/s).

The speed requirement specified by the sponsor was 20 knots (10.3 m/s) to be attained with no more than 18,048 hp (13,458 kw) as determined from the model tests. This requirement was met, and is graphically illustrated in Figures 20 and 21. At 20 knots (10.3 m/s) the AO is expected to absorb 16,300 hp (12,155 kw) at 89 rpm (9.3 rad/s) based on the NAVSEC powering predictions, which is well within the requirement of the sponsor.

The cavitation experiments performed with the final design (model 4677) were conducted in a new wake screen developed during the iteration part of the design. The main reason for constructing a new screen was that a reevaluation of the available, originally selected screen indicated that it did not model the AO wake as well as originally anticipated.<sup>21</sup> The preliminary (or original) AO propeller design (model 4645) showed tendencies to erode when it was tested in the first wake screen, which led to an investigation into finding out why this occurred. The result was that the wake screen was not close enough to the AO. Both propellers were tested in the new wake. Both cavitation inception and erosion experiments were conducted. The major results for the final design are given below.

The inception of back cavitation was predicted to occur at 20.9 knots (10.75 m/s) at about the 0.9 radius. At a speed slightly greater than the full-power speed, namely 21.9 knots (11.27 m/s) the back sheet extends to at most the 0.8 radius. No face cavitation or back bubble is predicted for any operating condition of this ship. These results, although similar to the design predictions, show much less cavitation than calculated. This is not unusual since it is known that the blade surface cavitation inception characteristics computed by two-dimensional hydrofoil theory are conservative.<sup>25</sup> Tip vortex cavitation inception (corrected for Reynolds number) is 10.4 knots (5.35 m/s). Hub vortex cavitation inception could not be determined because the propeller was mounted on the downstream shaft in the 24-inch water tunnel. Also, this experiment indicated that thrust breakdown would most assuredly not be a problem.

---

<sup>25</sup> Brocket, T., "Steady Two-Dimensional Pressure Distribution on Arbitrary Profiles," David Taylor Naval Ship Research and Development Center Report 1821, October 1965.

A nominal 40-hour erosion experiment was conducted with propeller 4677 and the new AO-177 wake screen in the 24-inch water tunnel. Inspection of the propeller after 40 hours of operation showed no evidence of black anodization erosion. It was, therefore, concluded that for propellers of this type if the anodizing does not erode there should not be erosion problems full scale. This experiment verified the predicted results based on the experiments of Lindgren and Bjarne<sup>15</sup>.

For completeness, the experimental results of the preliminary design as compared with the final design are as follows. The preliminary design (model 4645) showed nearly the same cavitation characteristics as the final design. In addition, no erosion was observed on the preliminary design after a 40-hour erosion test in the new wake; consequently, no erosion problems are expected full-scale for this propeller, too. A comparison of the powering predictions at full power for the two designs indicated that the full power speed for the new design is 0.1 knot less than the original design. Therefore, both designs met the performance requirements satisfactorily. The final design and the preliminary design are acceptable alternatives, as expected. However, the final design also satisfies the requirement of a more structurally conservative trailing edge contour, and as a result is the recommended propeller design for the AO-177 Class fleet oiler.

#### SUMMARY

A 21-foot (6.4 meters) diameter, 7-bladed propeller with a 45 degree (0.8 rad) tip-skew angle and a nonlinear distribution of skew specifically selected to reduce the alternating forces produced by

the propeller was designed for the final AO-177 Class fleet oiler propeller. The design procedure, the predicted design performance, and the results of the experimental evaluation were discussed in this report. The main objective was to design a propeller with minimum, propeller-excited vibratory forces as calculated using the available unsteady lifting surface theory, computer program. In particular, the unsteady thrust, and the horizontal and vertical bearing forces were to be reduced to values below the upper limits specified by Mil-Std-167 and Mil-Std-1472A, respectively. These requirements were met, i.e., the predicted unsteady thrust for the final design is 2,600 pounds (11.6 KN) which is less than the 3,000 pounds (13.3 KN) upper limit and the predicted vertical and horizontal side forces are 960 pounds and 230 pounds (4.3 KN and 1.0 KN), respectively, which are well below the 2,000 pound (8.9 KN) upper limit. These results are achieved without sacrificing strength, propulsion performance, or cavitation performance.

Propulsion experiments verified that the propeller met the performance requirements, i.e., the propeller is expected to absorb the 24,000 shaft horsepower (17,897 kw) at 99 rpm (10.4 rad/s) which is one percent lower than the design value of 100 rpm (10.5 rad/s). The maximum speed is predicted to be 21.5 knots (11.1 m/s). The endurance speed of 20 knots (10.3 m/s) is attained at a shaft power of approximately 16,000 SHP (11,930 kw) which is well below the specified upper limit of 18,048 hp (13,458 kw). Cavitation experiments show that the propeller met the design cavitation performance, i.e., no face cavitation, no midchord back bubble cavitation, only leading edge back sheet from the 0.8 radius to the tip is expected along with hub and tip vortex cavitation. The

blade surface, back cavitation, according to the model predictions, is expected to occur at a speed in excess of 20 knots (10.3 m/s). The erosion experiment verified that erosion should not be a problem full-scale. In conclusion, the propeller as designed met all the design requirements and it is recommended as the propeller for the AO-177 Class fleet oiler (propeller model 4677).

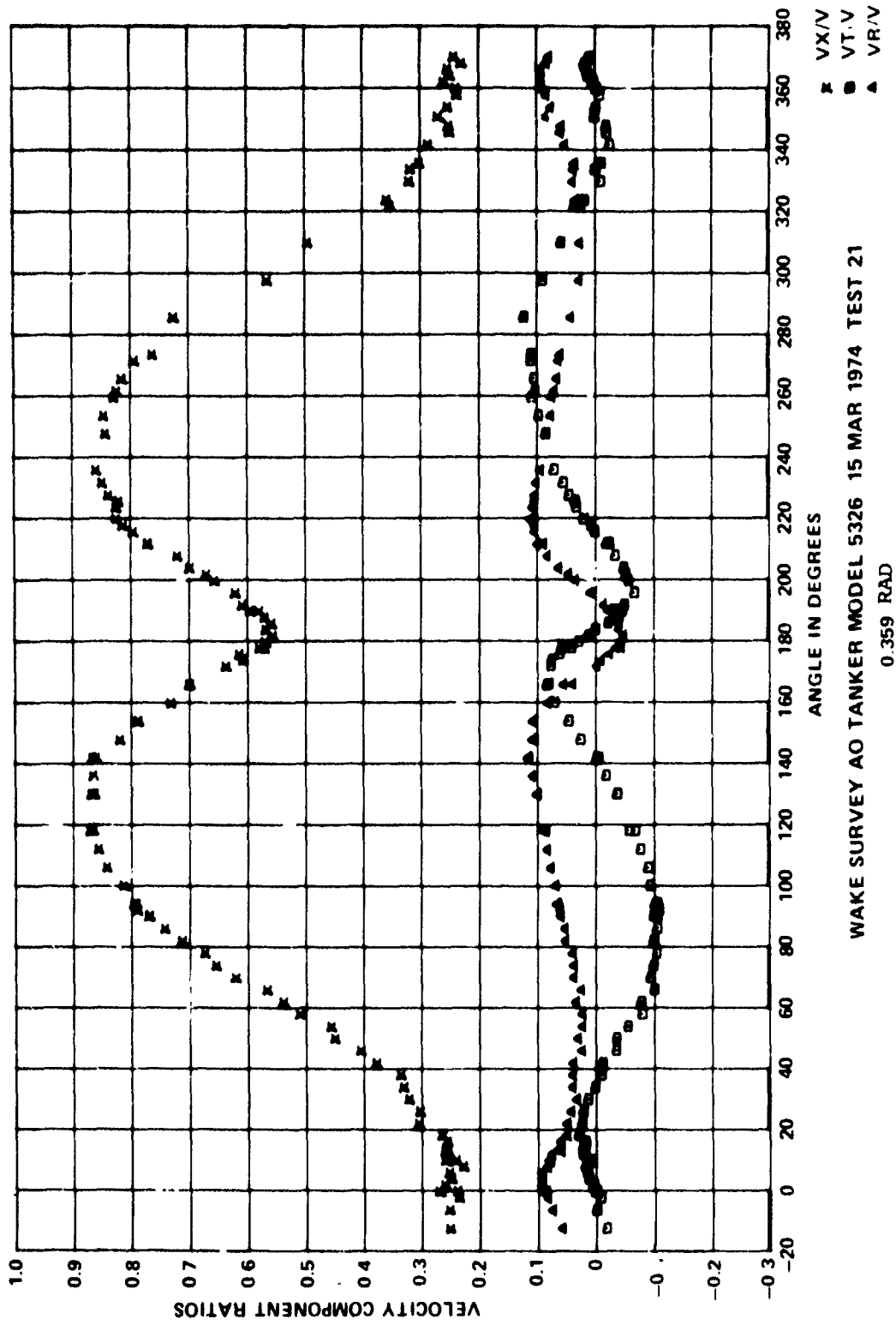
## REFERENCES

1. Cumming, R.A., Morgan, W.B., and Boswell, R.J., "Highly Skewed Propellers," Transactions of the Society of Naval Architects and Marine Engineers, Vol. 80, 1972
2. Valentine, D.T. and Dashnow, F.J., "Highly Skewed Propeller for San Clemente Class Ore/Bulk/Oil Carrier Design Considerations, Model and Full-Scale Evaluation," First Ship Technology and Research (STAR) Symposium, August 1975
3. Remmers, K. and Hecker, R., "Powering Predictions of a Naval-Auxiliary Oiler (AO) (Model 5326 with Stock Propellers 4327A and 4510A)," David Taylor Naval Ship Research and Development Center Report SPD-544-03, May 1974
4. Remmers, K.D. and Hendrican, A.L., "Analysis of Wake Survey of a Naval Auxiliary Oiler (AO-177 Class) Represented by Model 5326," David Taylor Naval Ship Research and Development Center Report SPD-544-05, May 1975
5. Lerbs, H.W., "Moderately Loaded Propellers with a Finite Number of Blades and an Arbitrary Distribution of Circulation," Transaction of the Society of Naval Architects and Marine Engineers, Vol. 60, p 73-117, 1952
6. Cheng, H.M., "Hydrodynamic Aspects of Propeller Design Based on Lifting Surface Theory, Part II - Arbitrary Chordwise Load Distribution," David Taylor Naval Ship Research and Development Center Report 1803, June 1965
7. Kerwin, J. and Leopold, R., "A Design Theory for Subcavitating Propellers," Transactions of the Society of Naval Architects and Marine Engineers, Vol. 72, p 294-335, 1964
8. Cox, G.G. and Morgan, W.B., "Application of Theory to Propeller Design," Marine Technology, Vol. 9, No. 4, p 419-429, 1974
9. Morgan, W.B., Silovic, V., and Denny, S.B., "Propeller Lifting-Surface Corrections," Transactions of the Society of Naval Architects and Marine Engineers, Vol. 76, p 309-347, 1968
10. Burhill, L.C. and Emerson, A., "Propeller Cavitation: Further Tests on 16-Inch Model Propellers in the Kings College Cavitation Tunnel," Northeast Coast Institute of Engineers and Shipbuilders, Vol. 79, p 295-320, 1962-63
11. Tsakonas, S., Breslin, J., and Miller, M., "Correlation and Application of Unsteady Flow Theory for Propeller Forces," Transactions of the Society of Naval Architects and Marine Engineers, Vol. 75, p 158-193, 1967

12. Morgan, W.B. and Wrench, J.W., "Some Computational Aspects of Propeller Design," Methods of Computational Physics, Vol. 4, Academic Press, Inc., New York, p 301-331, 1965
13. Cox, G.G., "Corrections to the Camber of Constant Pitch Propellers," Royal Institute of Naval Architects, Vol. 103, p 227-243, 1961
14. Troost, L., "The Pitch Distribution of Wake-Adapted Marine Propellers," Transactions of the Society of Naval Architects and Marine Engineers, Vol. 64, p 357-374, 1956
15. Lindgren, H. and Bjarne, E., "Studies of Propeller Cavitation Erosion," Conference on Cavitation, Edinburgh, arr. by Institute of Mechanical Engineers, Preprints, P 241-251, September 1974
16. Brockett, T., "Minimum Pressure Envelopes for Modified NACA 66 Sections with NACA  $a=0.8$  Camber and BUSHIPS Type I and II Sections," David Taylor Naval Ship Research and Development Center Report 1780, February 1966
17. Boswell, R.J., "Design, Cavitation Performance, and Open-Water Performance of a Series of Research Skewed Propellers," David Taylor Naval Ship Research and Development Center Report 3339, March 1971
18. Boswell, R.J. and Miller, M.L., "Unsteady Propeller Loading-Measurement, Correlation with Theory, and Parametric Study," David Taylor Naval Ship Research and Development Center Report 2625, October 1968
19. Teel, S.S. and Denny, S.B., "Field Point Pressures in the Vicinity of a Series of Skewed Marine Propellers," David Taylor Naval Ship Research and Development Center Report 3278, August 1970
20. Genalis, P., "Elastic Strength of Propellers - An Analysis by Matrix Methods (Including a Programmer's Manual and a User's Manual)," David Taylor Naval Ship Research and Development Center Report 3397, July 1970
21. Hendrican, A. and Remmers, K., "Powering and Cavitation Performance for a Naval Fleet Oiler, AO-177 Class (Model 5326 with Propeller 4677)," David Taylor Naval Ship Research and Development Center Report SPD-544-14, January 1976
22. Murray, L. and Hecker, R., "Powering Predictions of a Naval Auxiliary Oiler (AO) (Model 5326 with Design Propeller 4645)," David Taylor Naval Ship Research and Development Center Report SPD-544-10, September 1974
23. Remmers, et al, "Cavitation Performance of a Propeller Design for a Naval Auxiliary Oiler (AO-177 Class) (Model 5326 with Design Propeller 4645)," David Taylor Naval Ship Research and Development Center Report SPD-544-11, September 1974

24. Hadler, J.B., Wilson, C.J., and Beal, A., "Ship Standardization Trial Performance and Correlation with Model Predictions," Transactions of the Society of Naval Architects and Marine Engineers, Vol. 70, 1962
25. Brockett, T., "Steady Two-Dimensional Pressure Distribution on Arbitrary Profiles," David Taylor Naval Ship Research and Development Center Report 1821, October 1965

Figure 1 Measured Values of the Axial, Tangential and Radial Velocity Components  
in the Wake of the AO 177-Class Fleet Oiler (Model 5326)  
(See Reference 4)



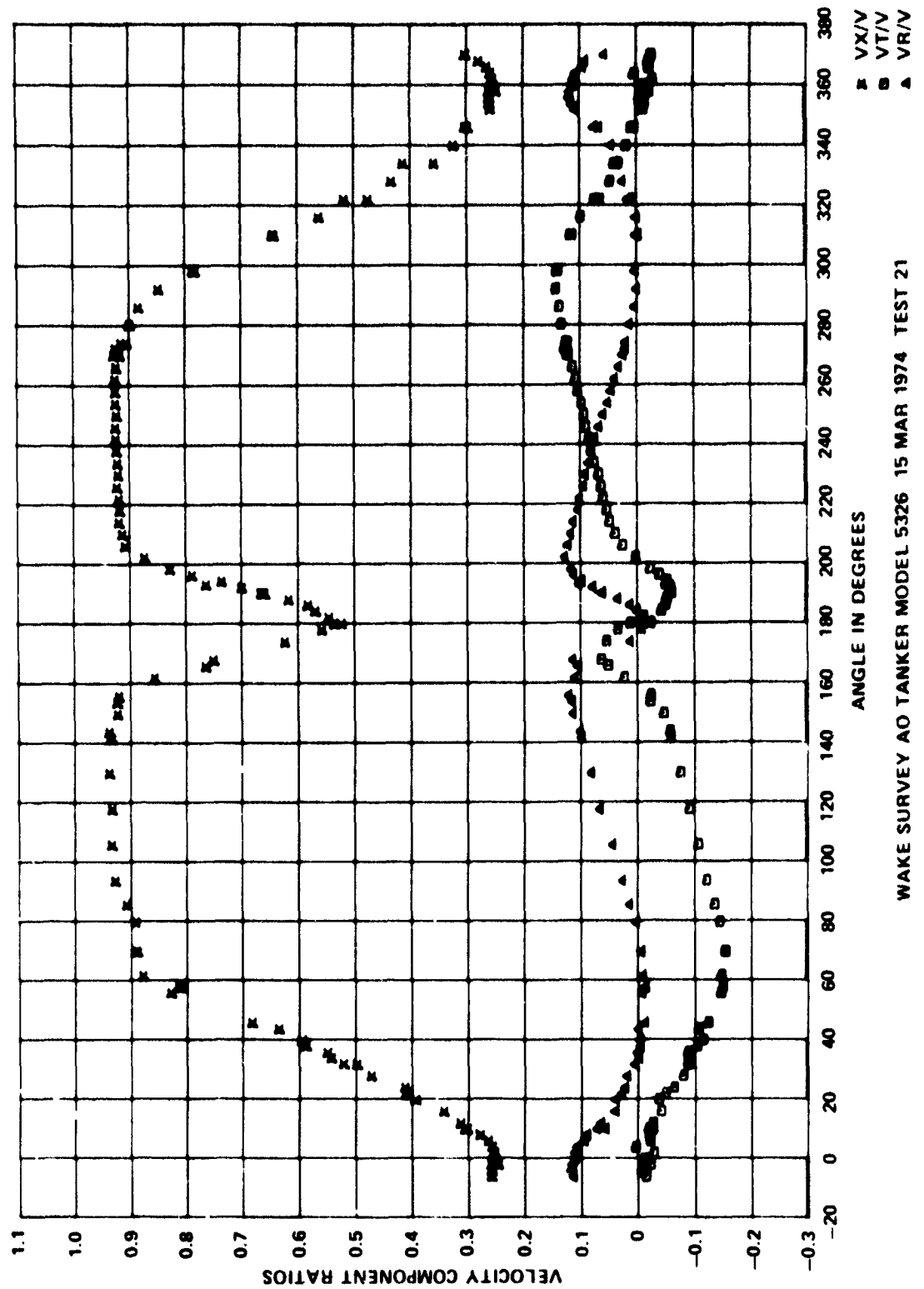


Figure 1 (Continued)

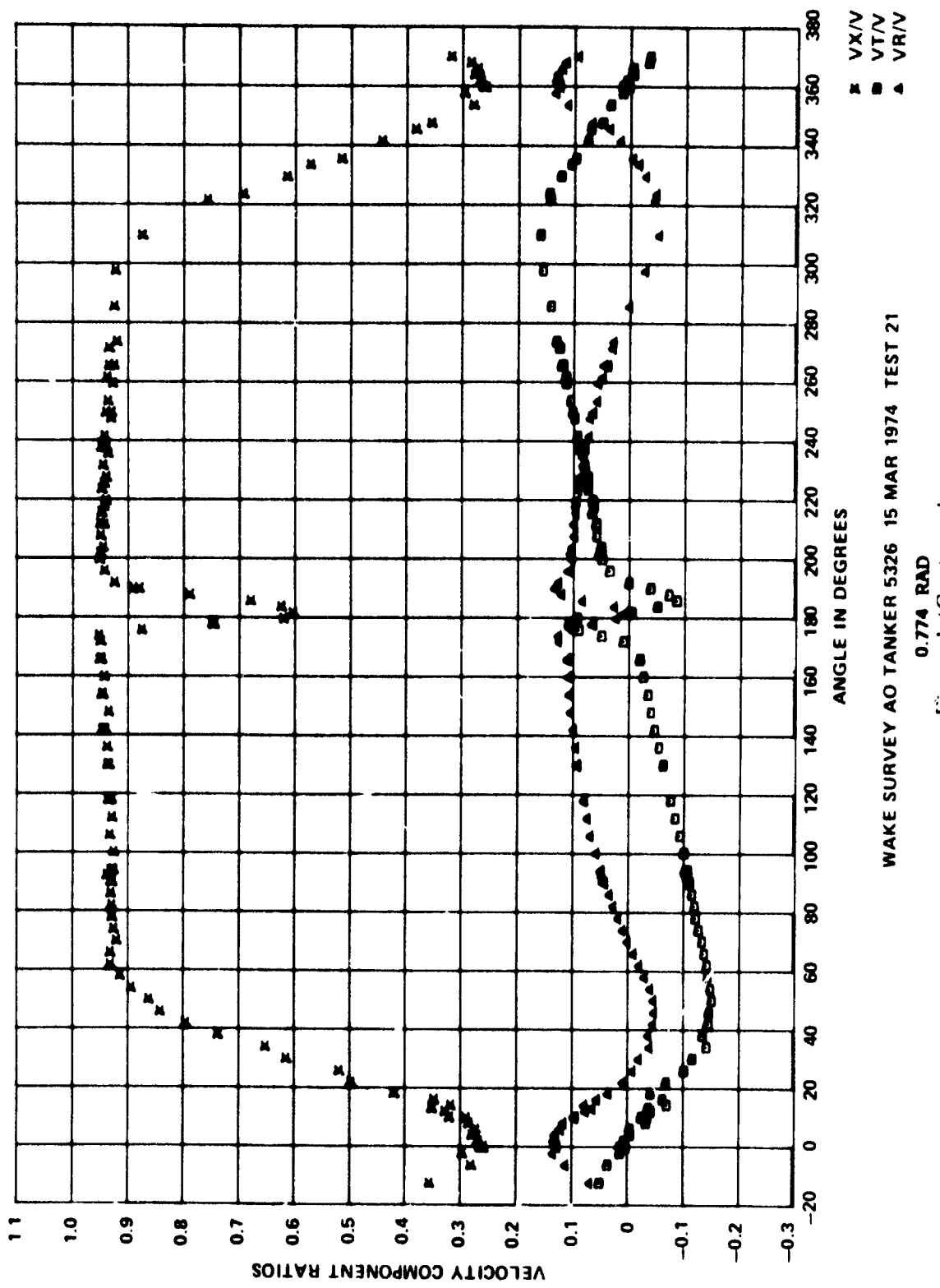


Figure 1 (Continued)

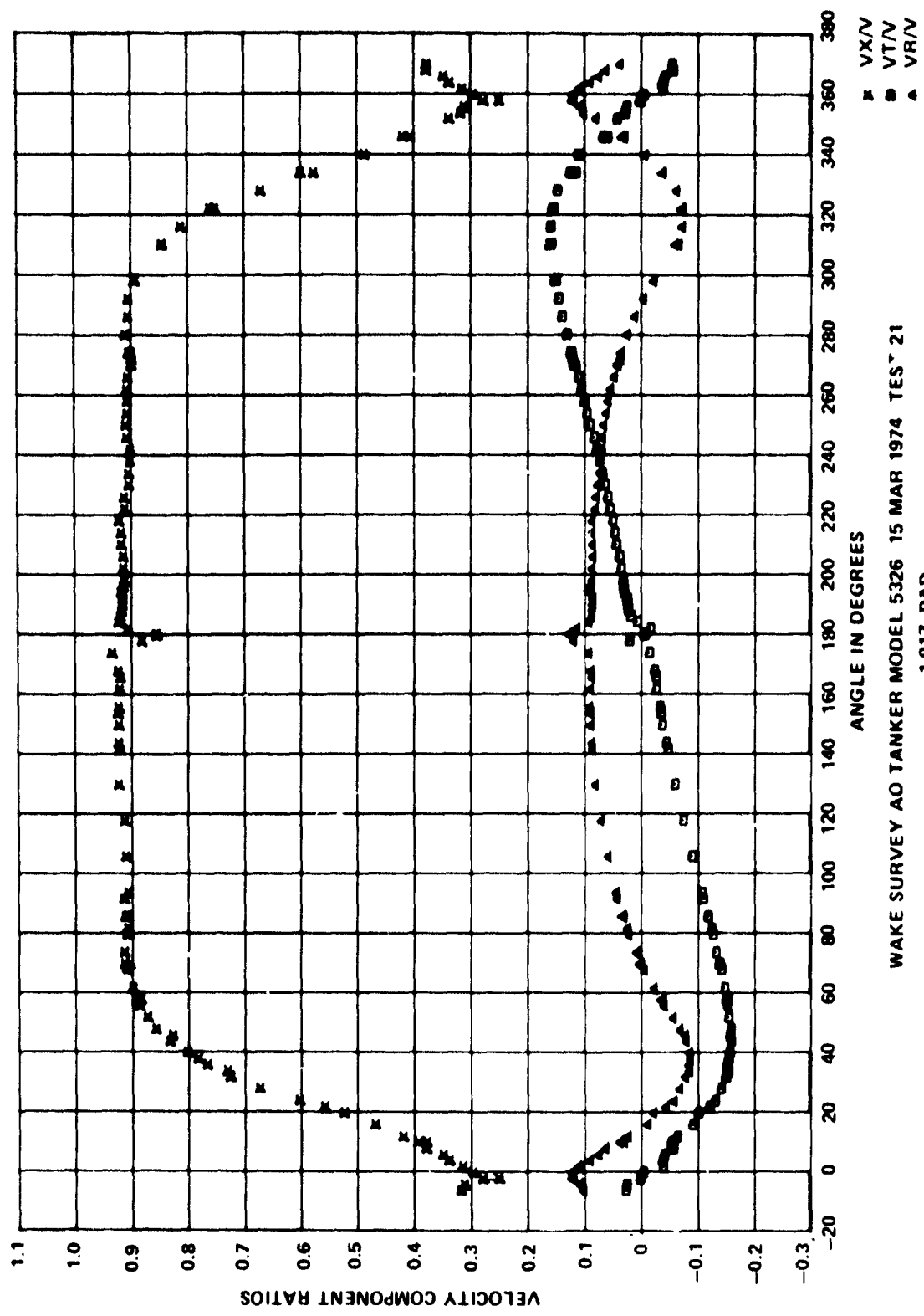


Figure 1 (Continued)

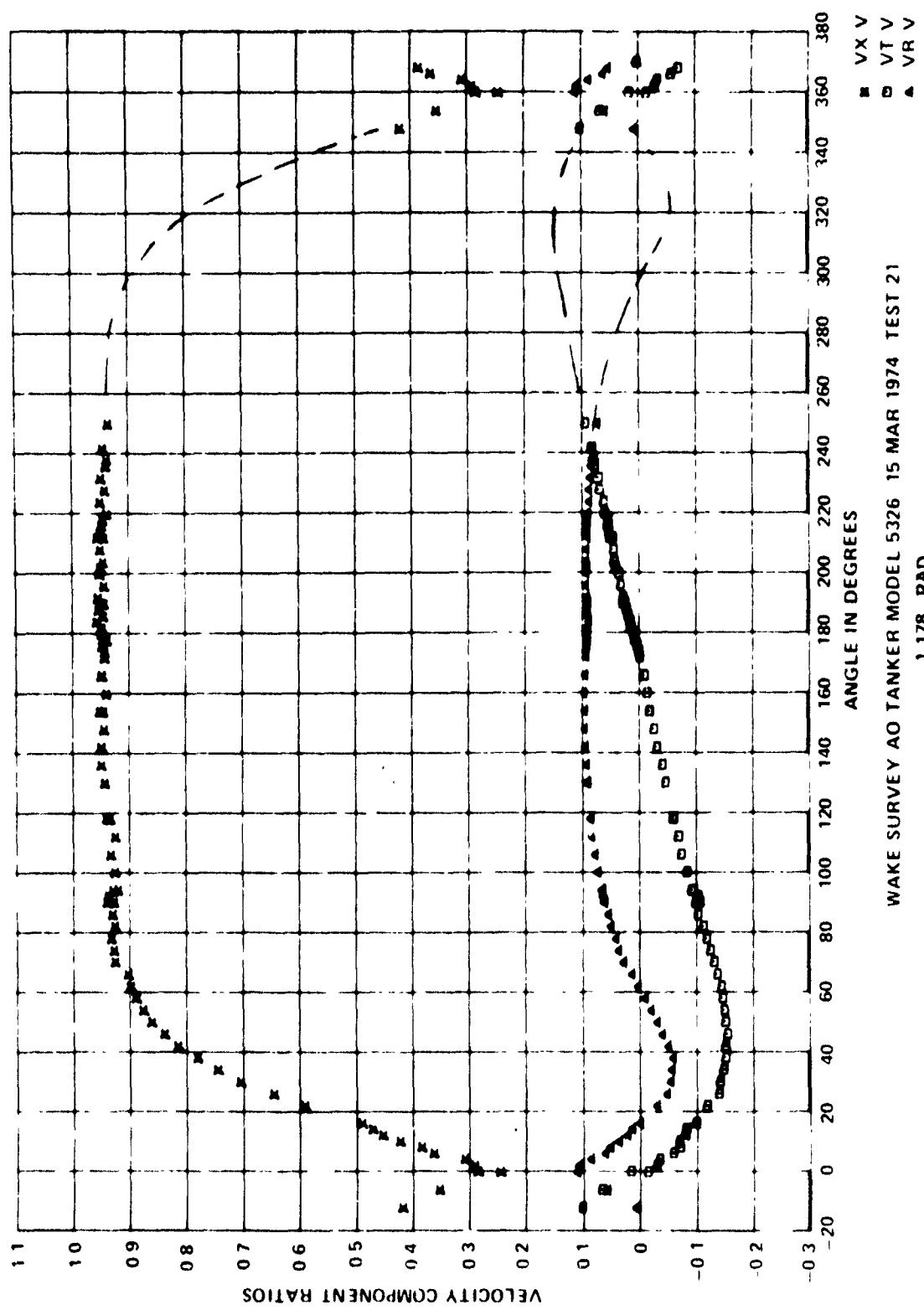


Figure 1 (Continued)

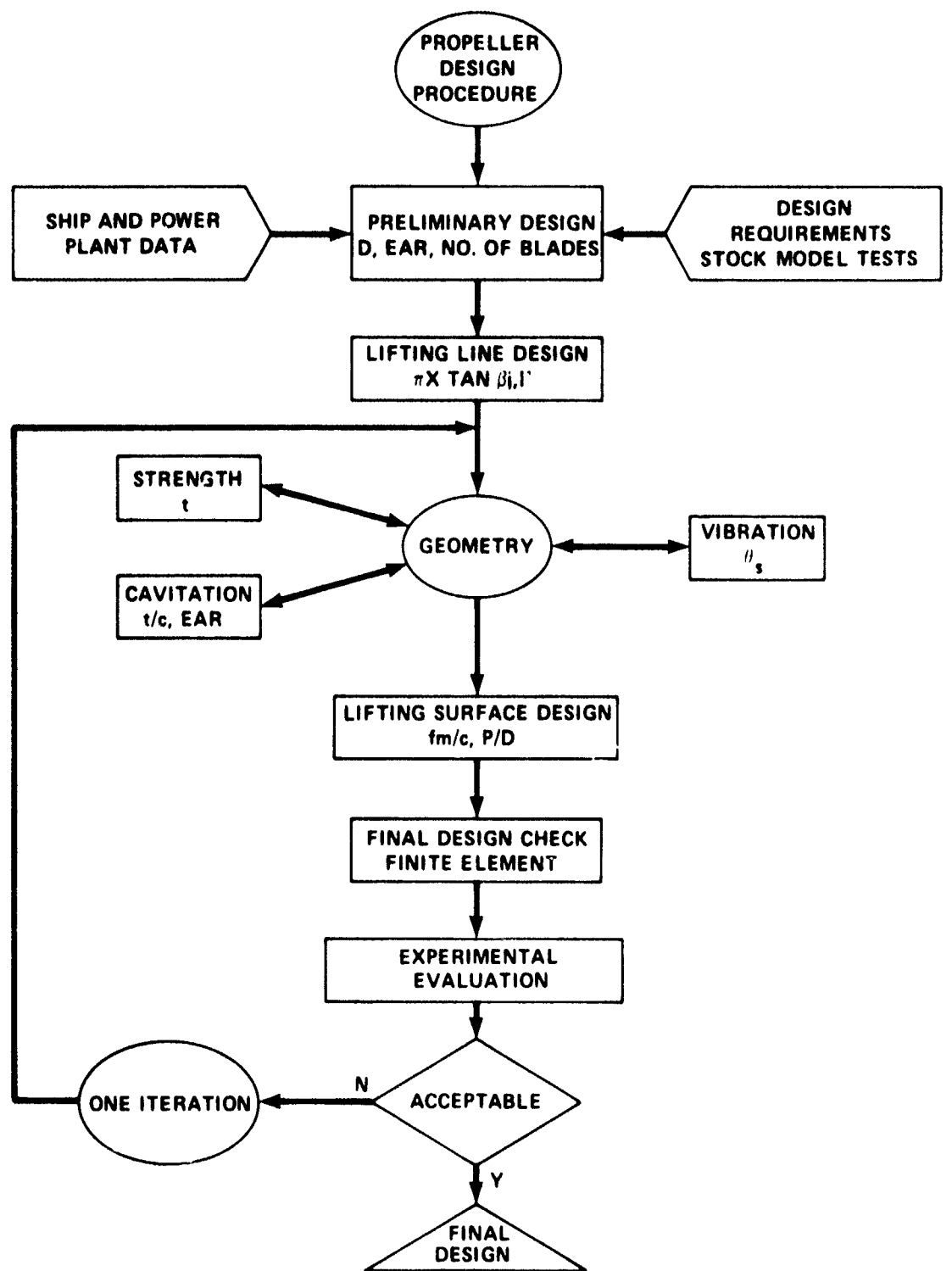


Figure 2 – Schematic of the Design Procedure

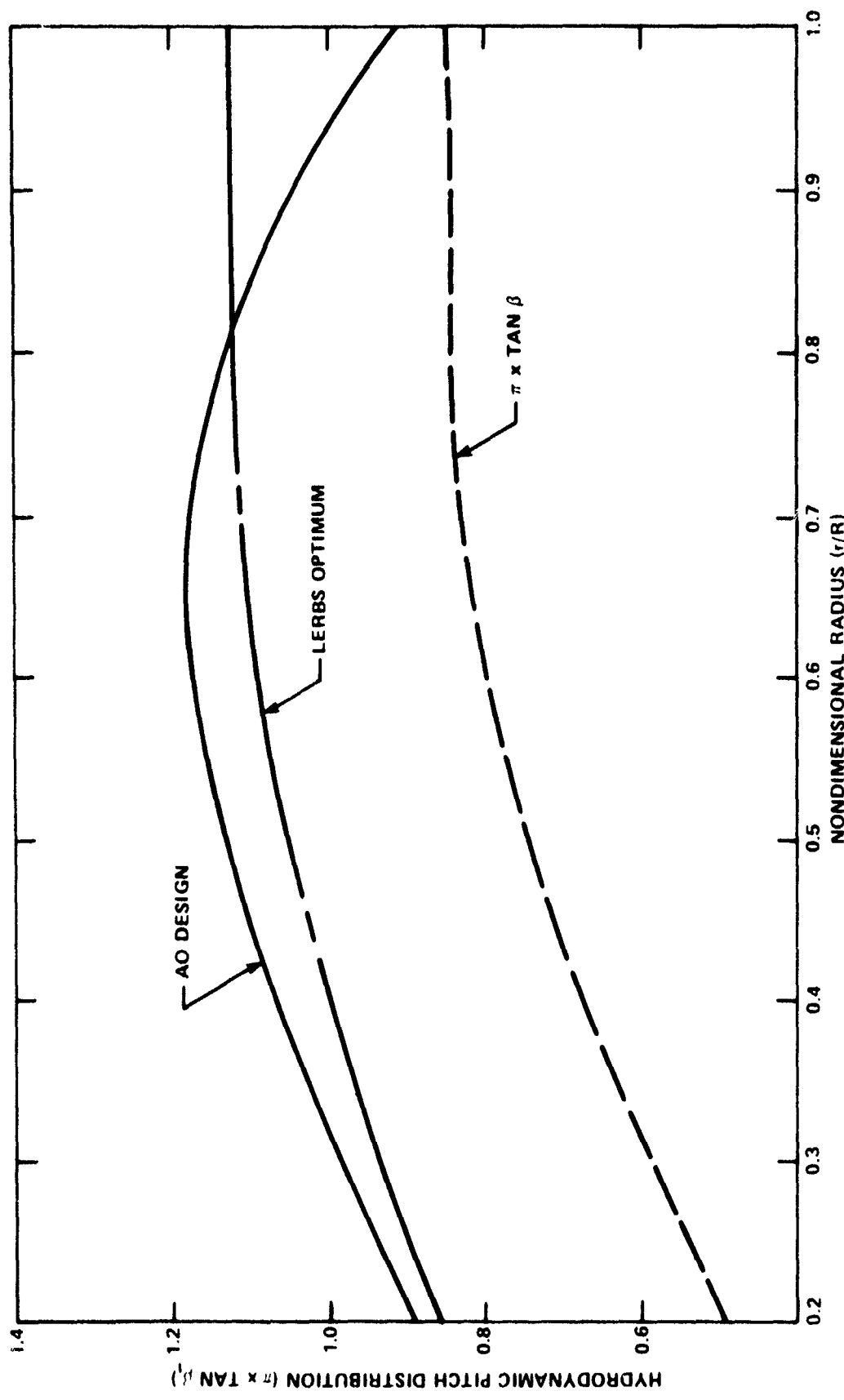


Figure 3 Hydrodynamic Pitch Distributions Investigated for the AO-177-Class Fleet Oiler Propeller Design

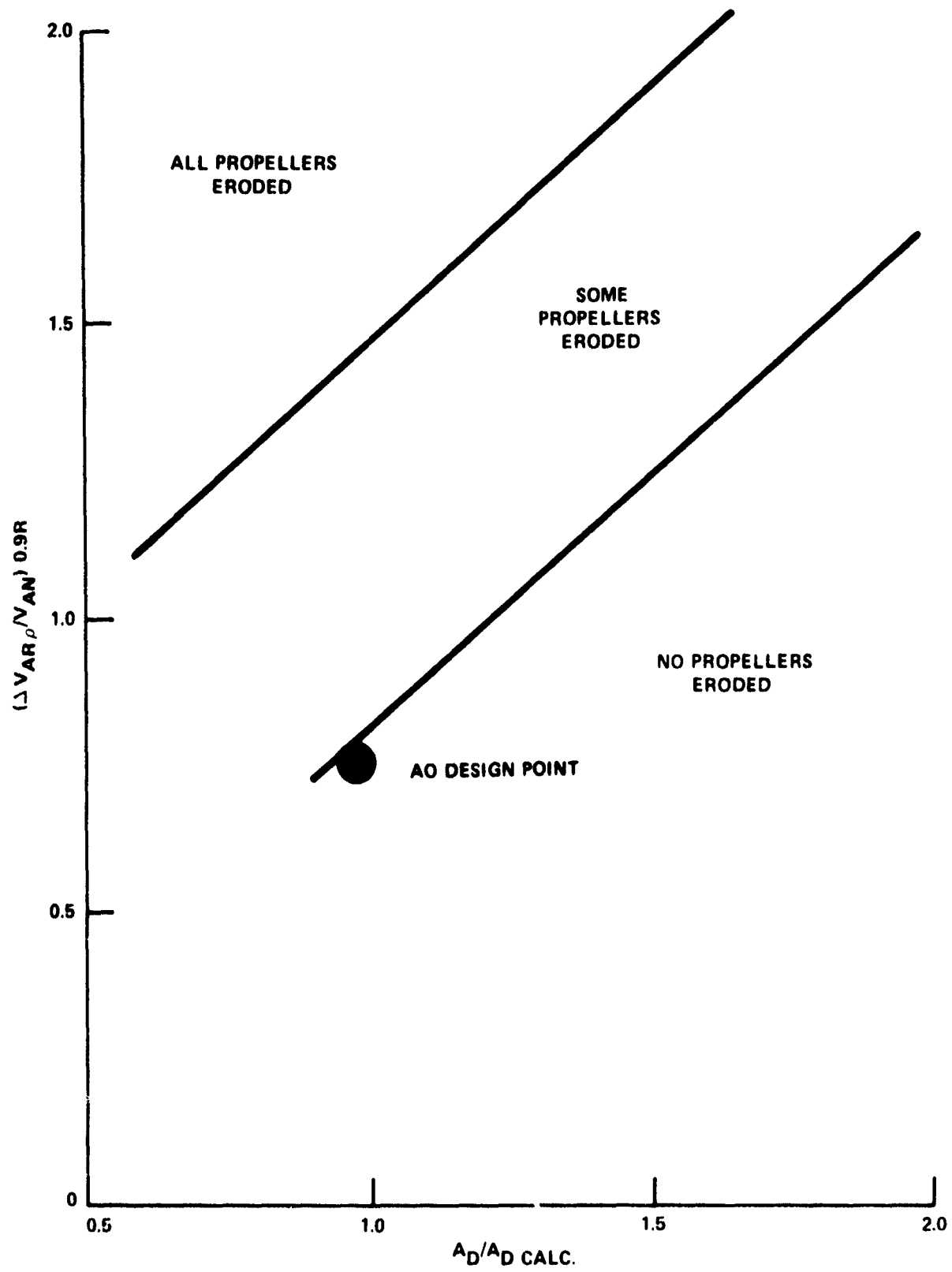


Figure 4 - Influence of Blade Area and Wake Variations on Cavitation Erosion on Merchant Ship Propellers  
 (From Reference 15)

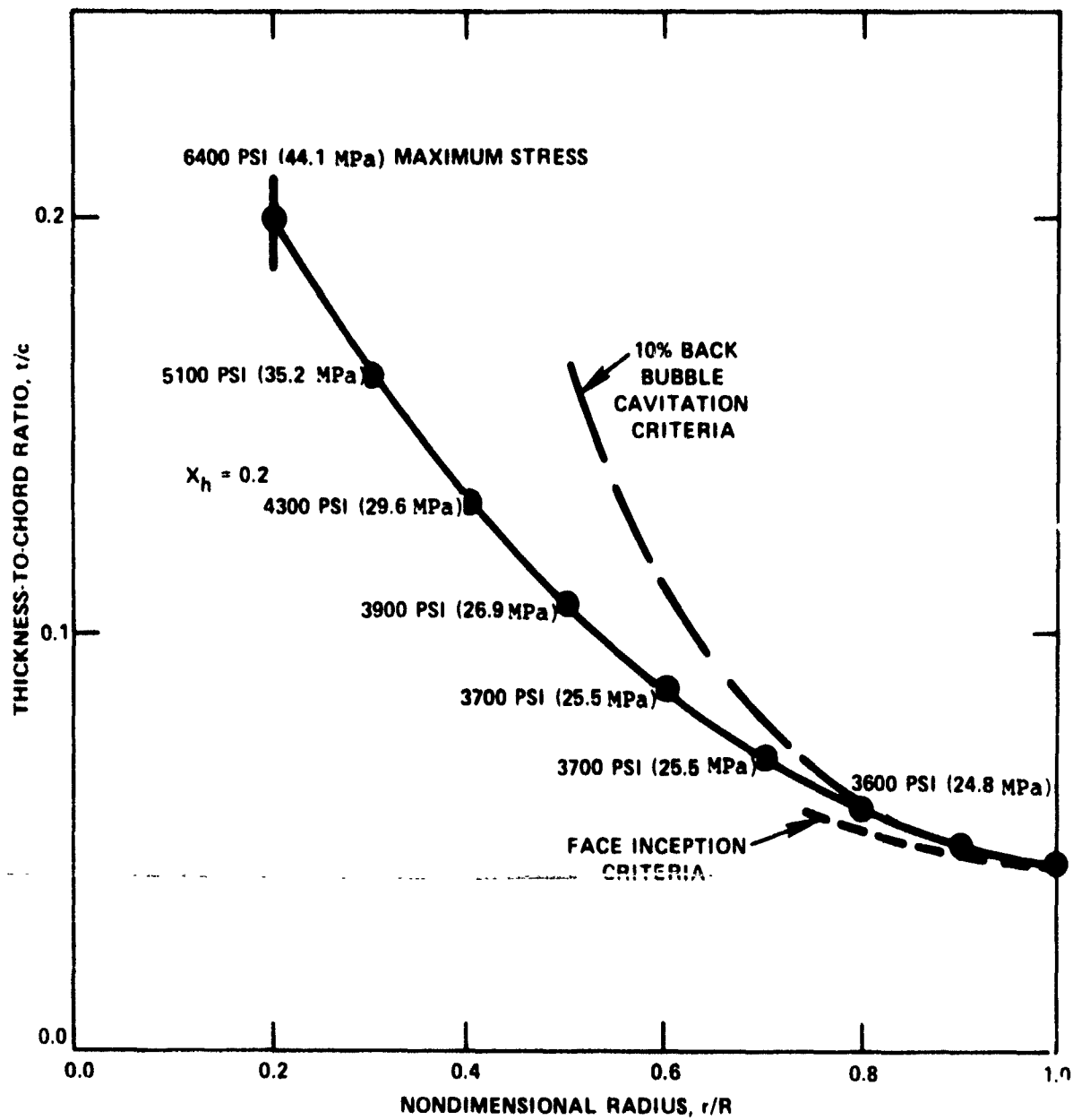


Figure 5 - Radial Distribution of Thickness-to-Chord Ratio Based on Strength and Cavitation Criteria for the Final AO Propeller Design

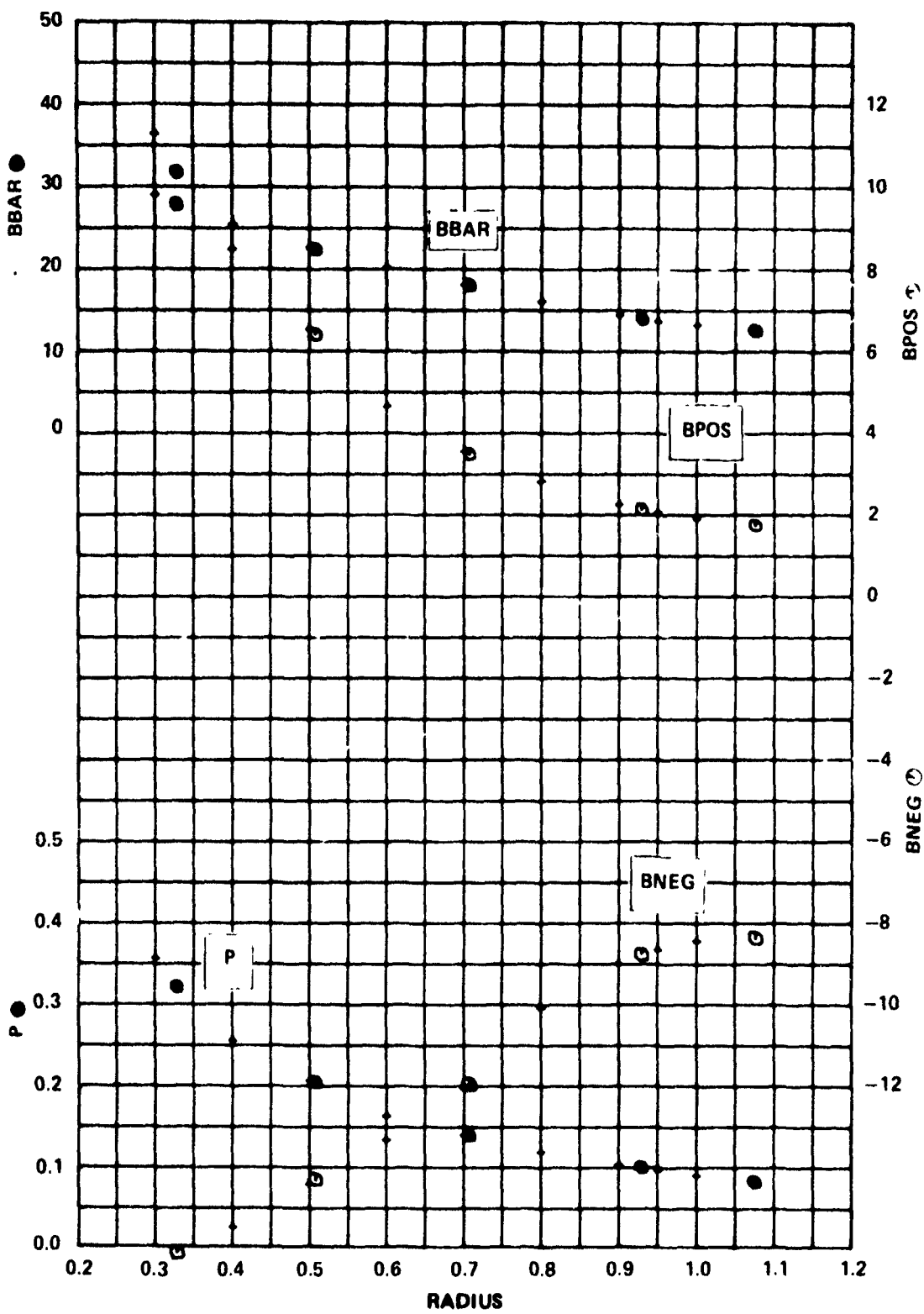


Figure 6 -- Radial Distribution of the Mean Advance Angle, the Maximum Variations of the Advance Angle, and the Pressure Factor

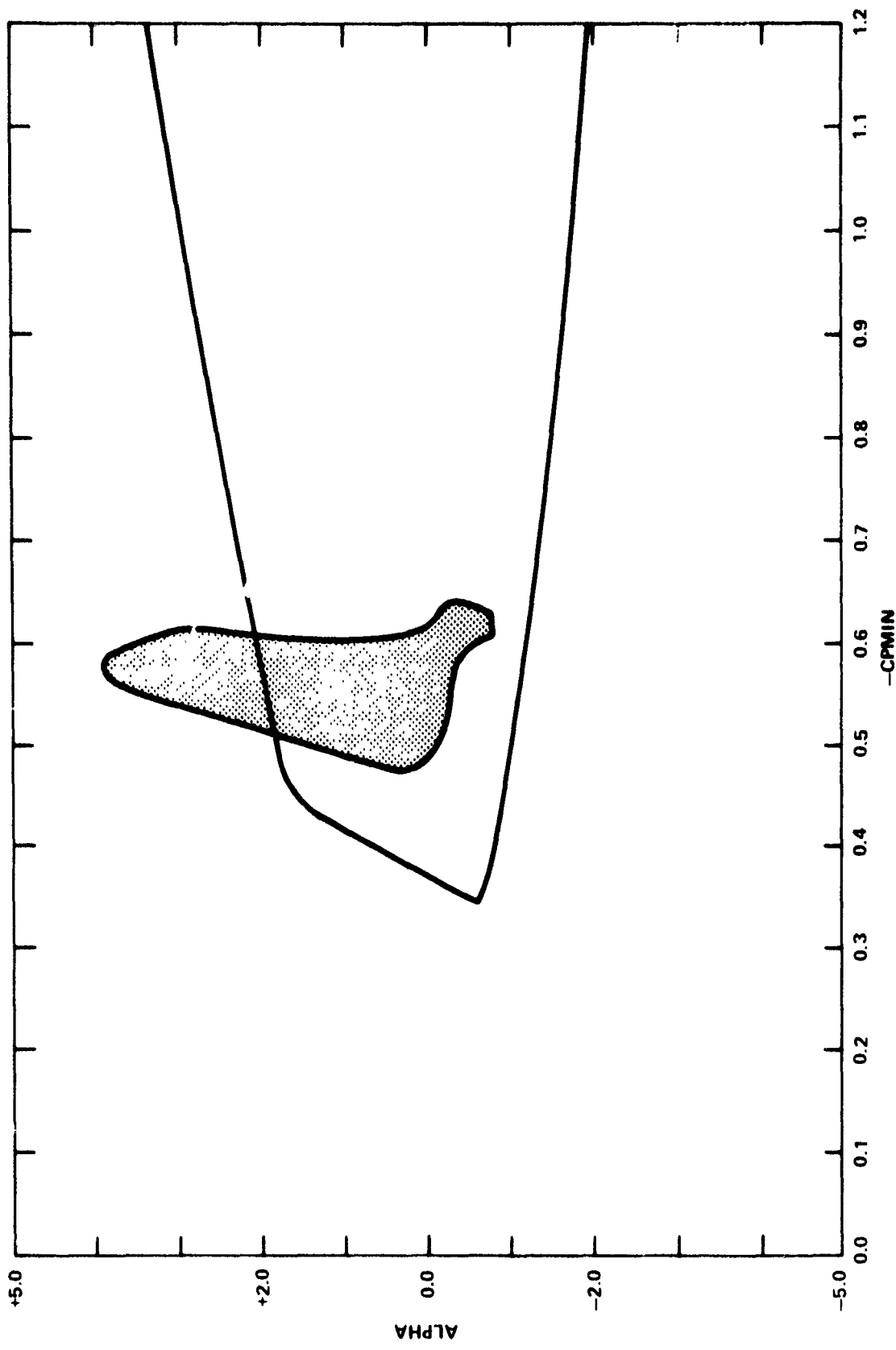


Figure 7 - Cavitation Inception Diagram for the 0.6 Radius of  
the AO Propeller

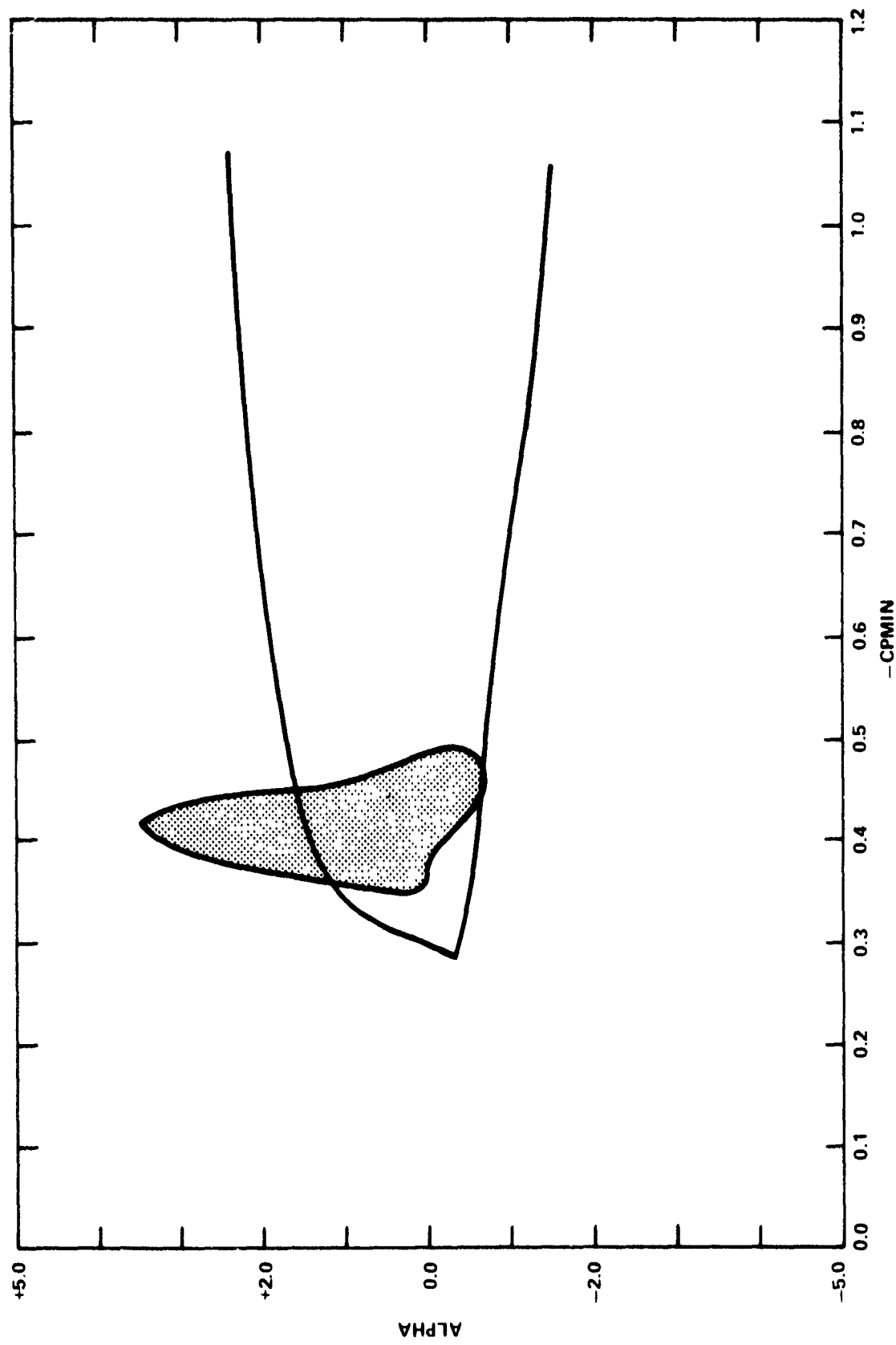


Figure 8 - Cavitation Inception Diagram for the 0.7 Radius of the AO Propeller

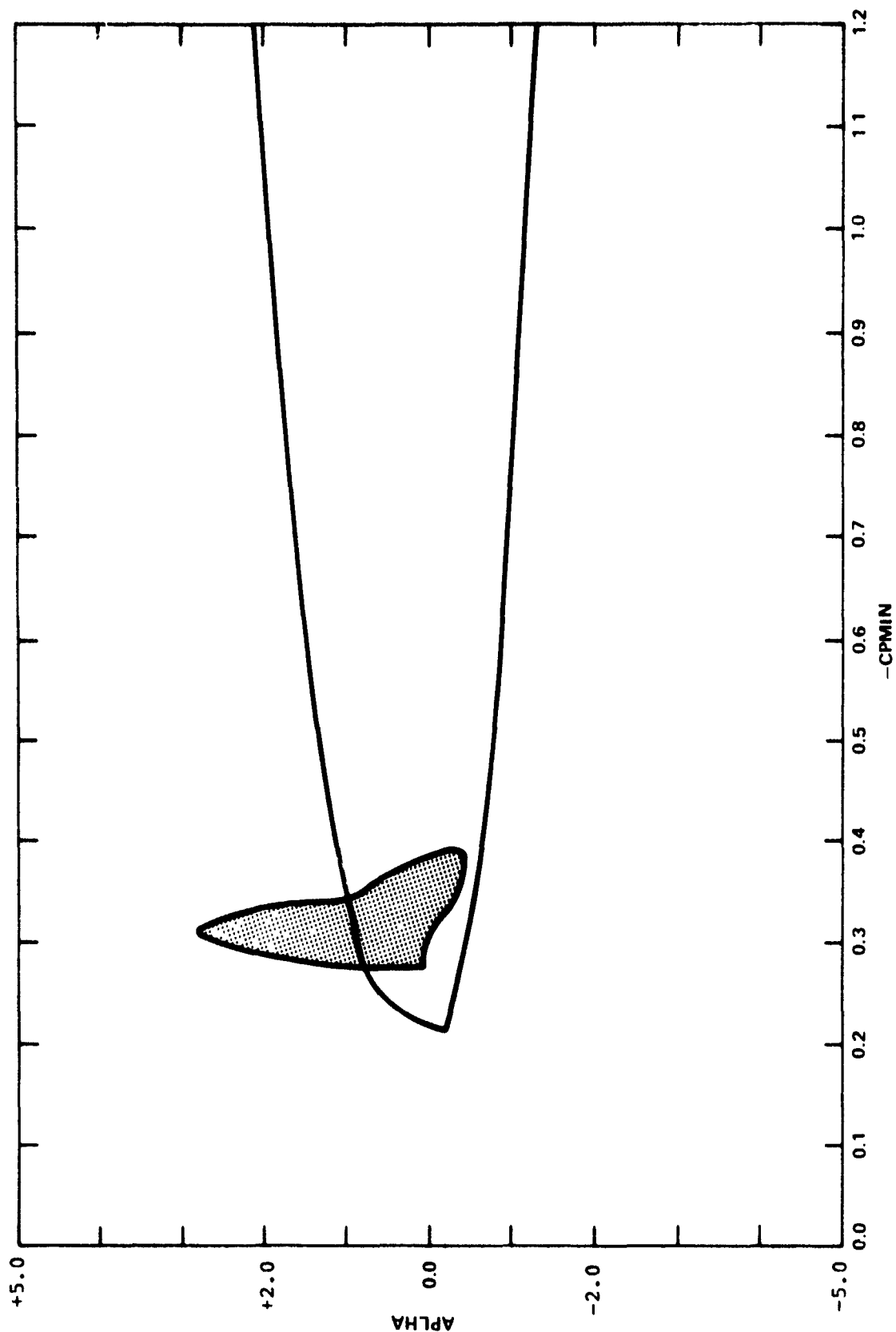


Figure 9 - Cavitation Inception Diagram for the 0.8 Radius of the  
AO Propeller

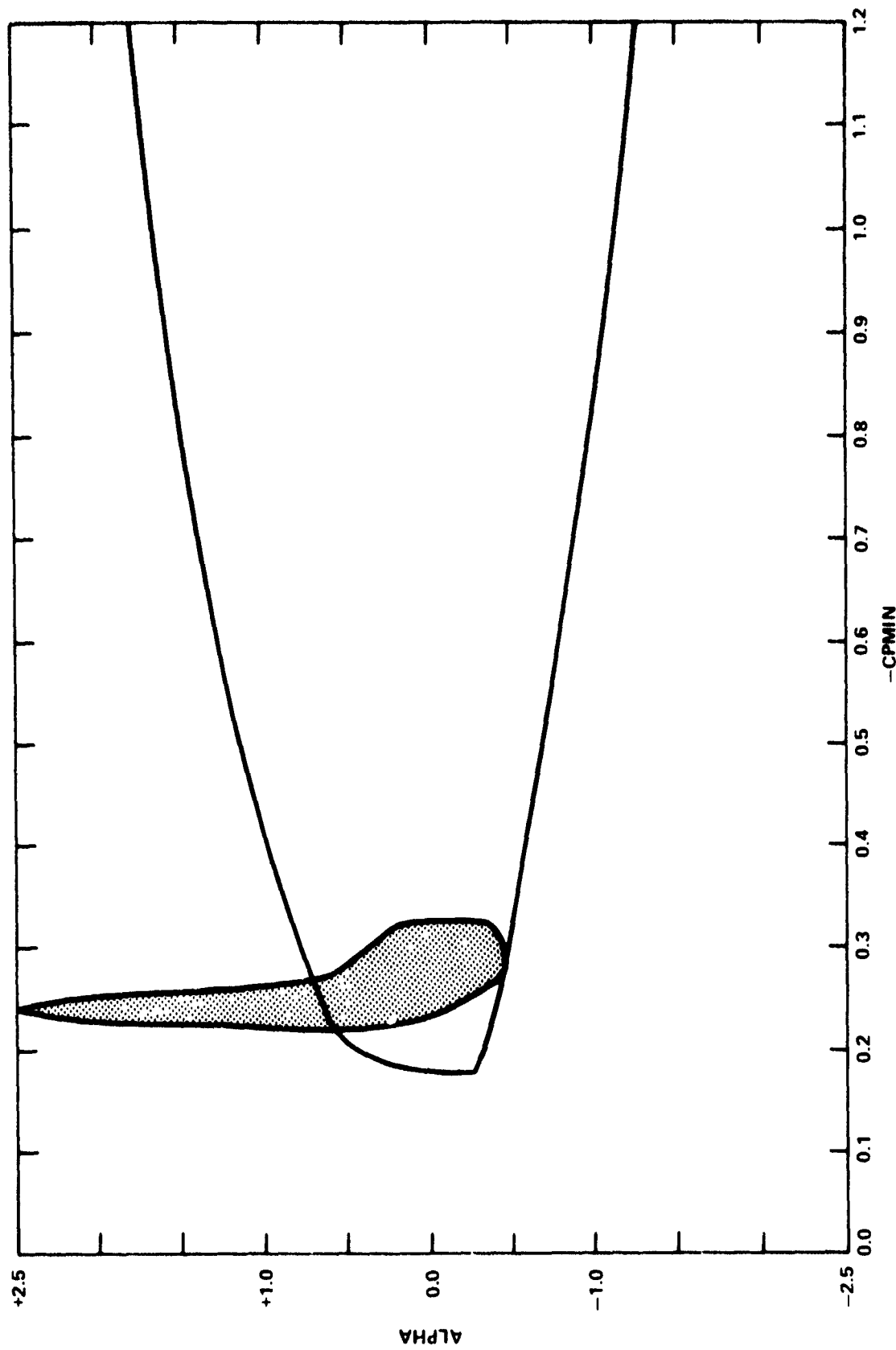


Figure 10 - Cavitation Inception Diagram for the 0.9 Radius of the  
AO Propeller

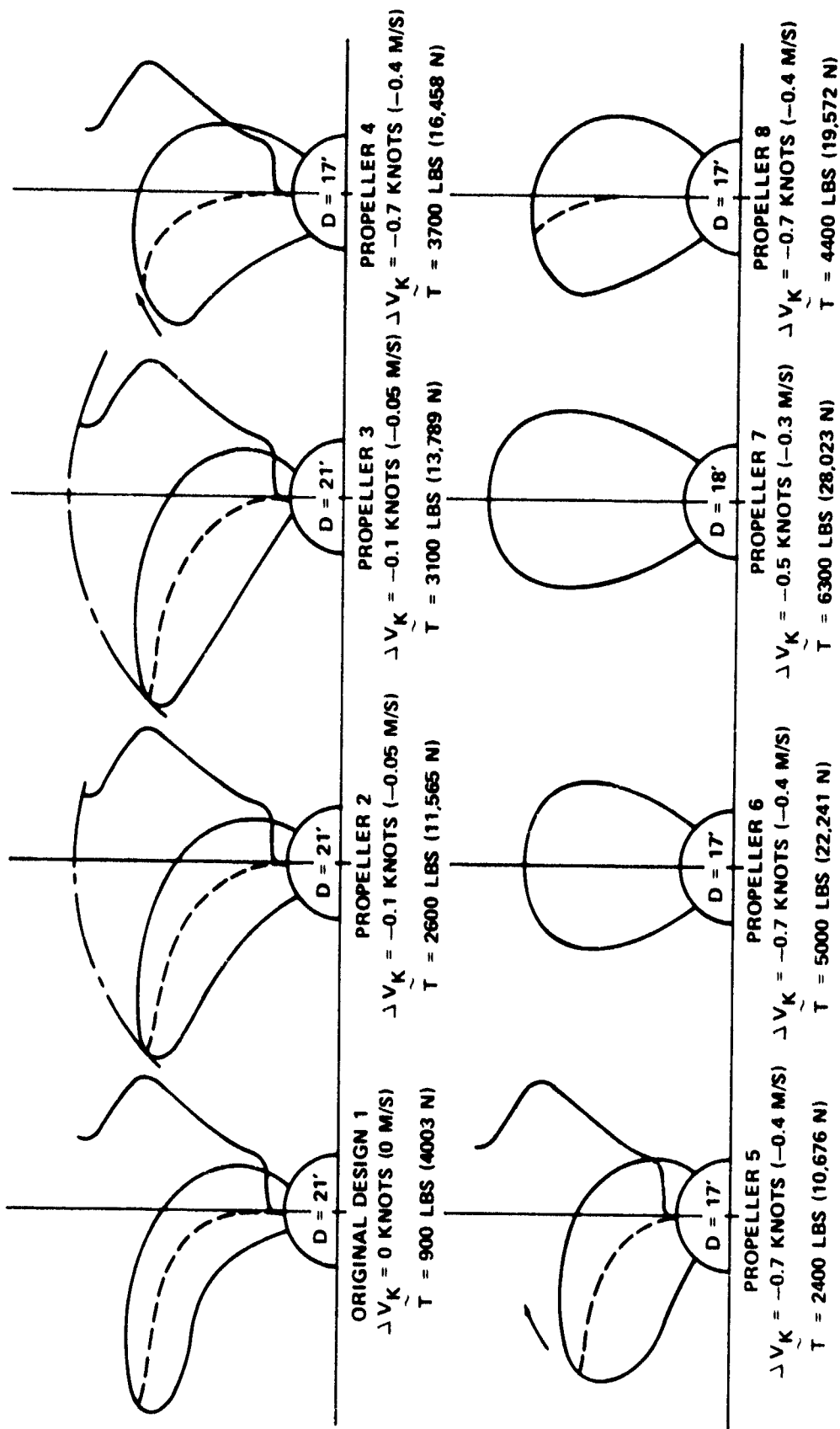


Figure 11 – Several Samples of Geometry Changes Evaluated in the AO Design from the Viewpoint of Minimizing Unsteady Forces

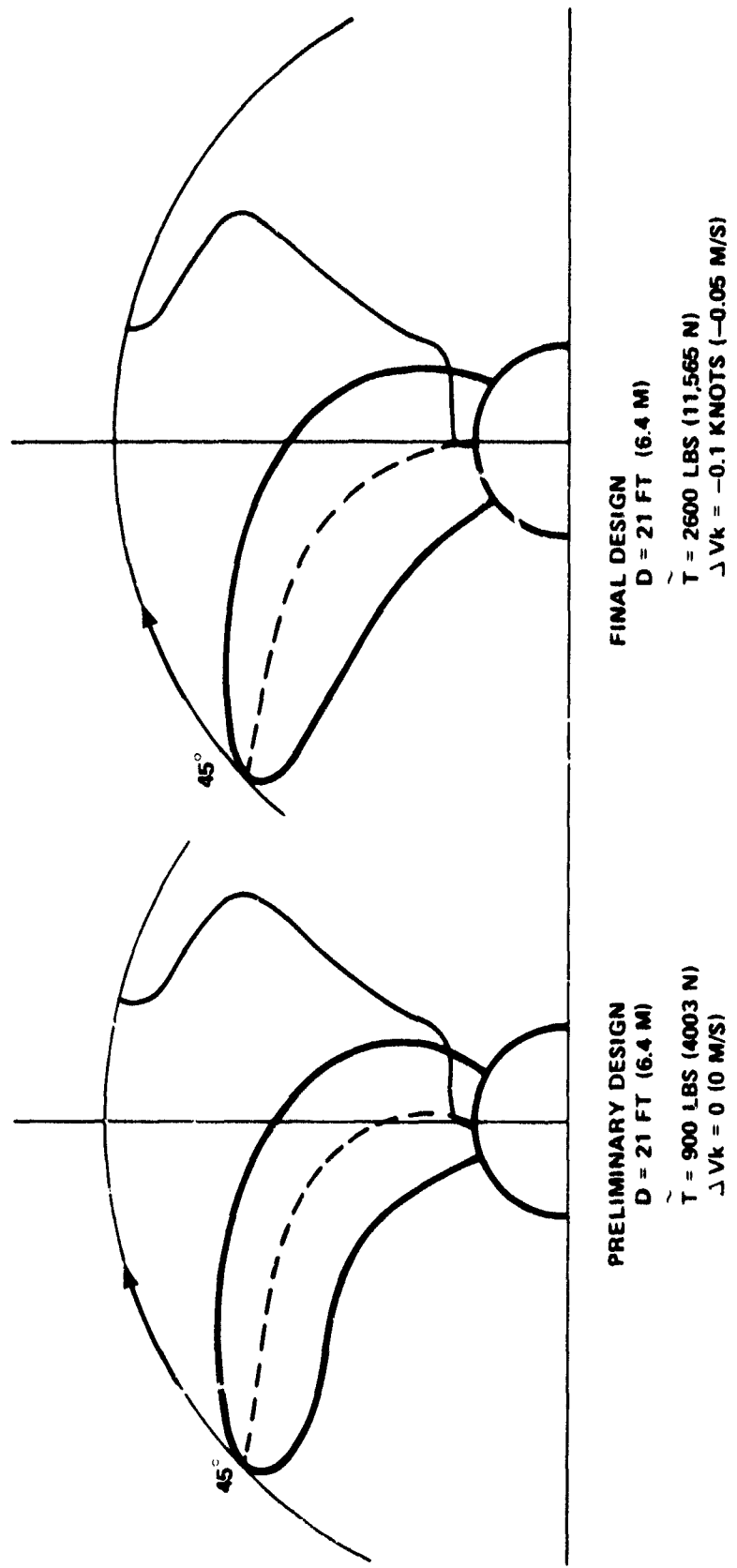


Figure 12 – Comparison of Predictions of Unsteady Thrust, and of Blade Shape  
for Preliminary and Final Designs for AO

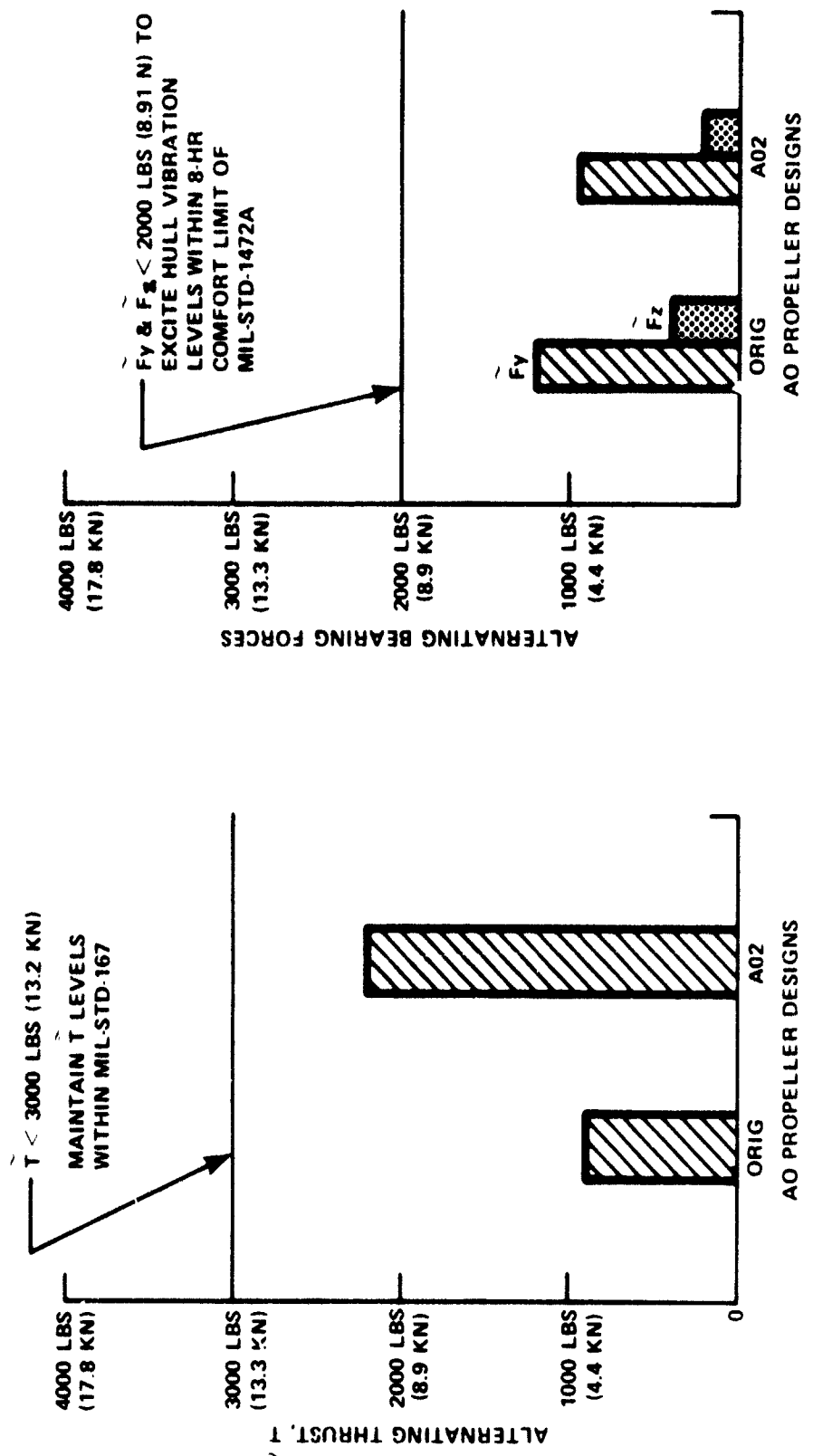


Figure 13 Comparison of Alternating Forces with MIL-STDS

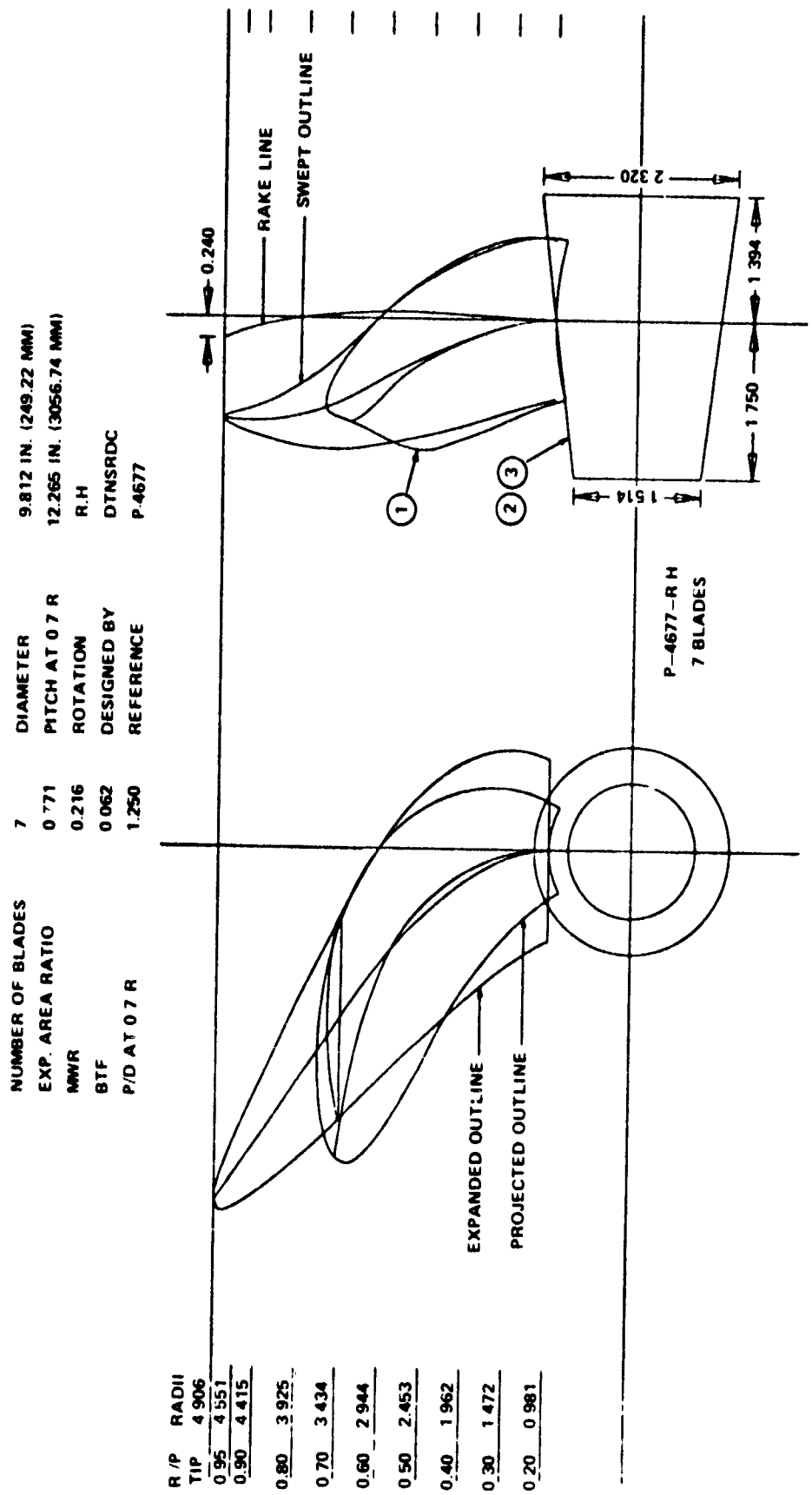


Figure 14 – Drawing of Propeller 4677 (Forward AO Propeller Design)

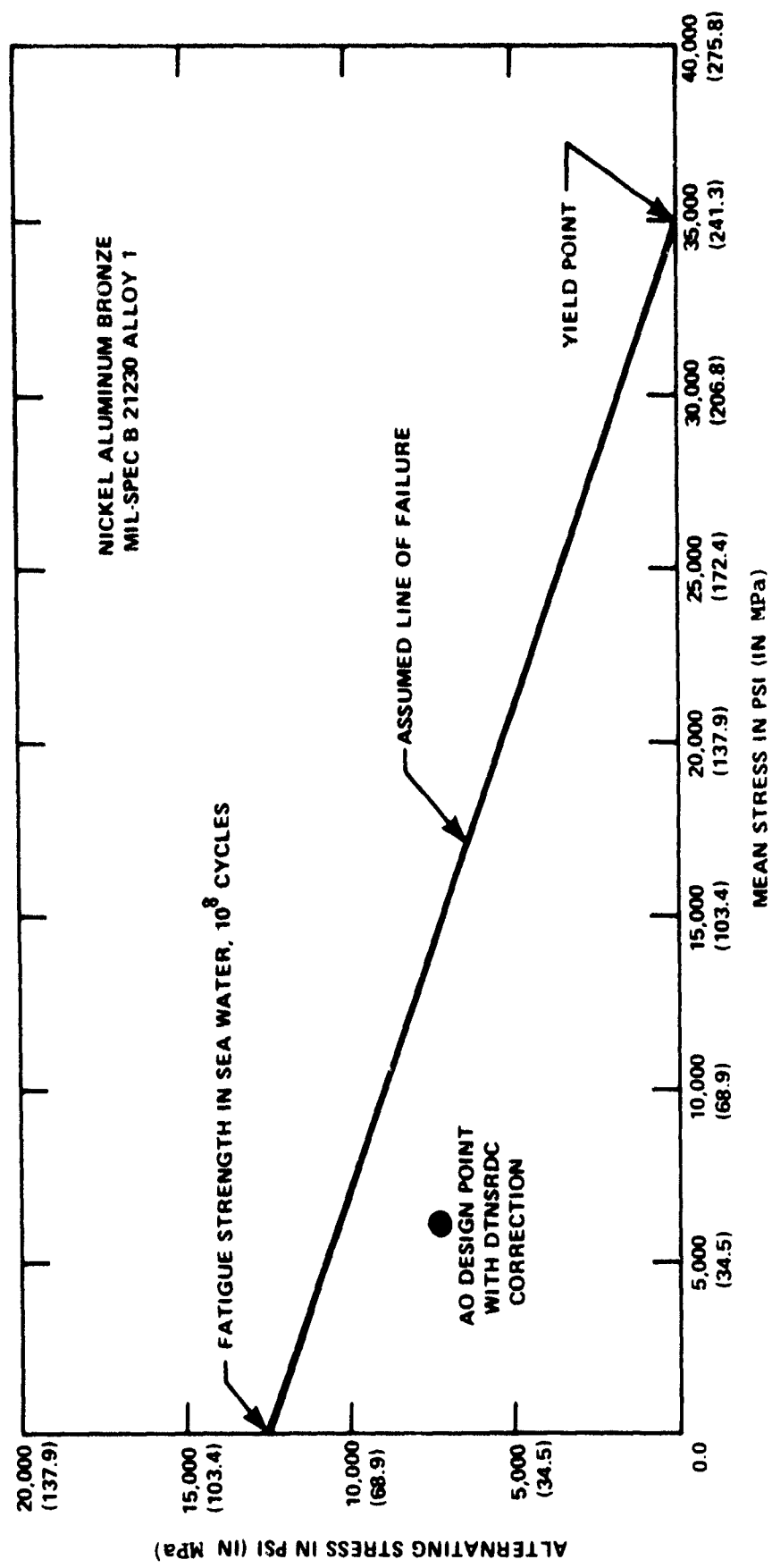


Figure 15 – Modified Goodman, Working Stress Diagram

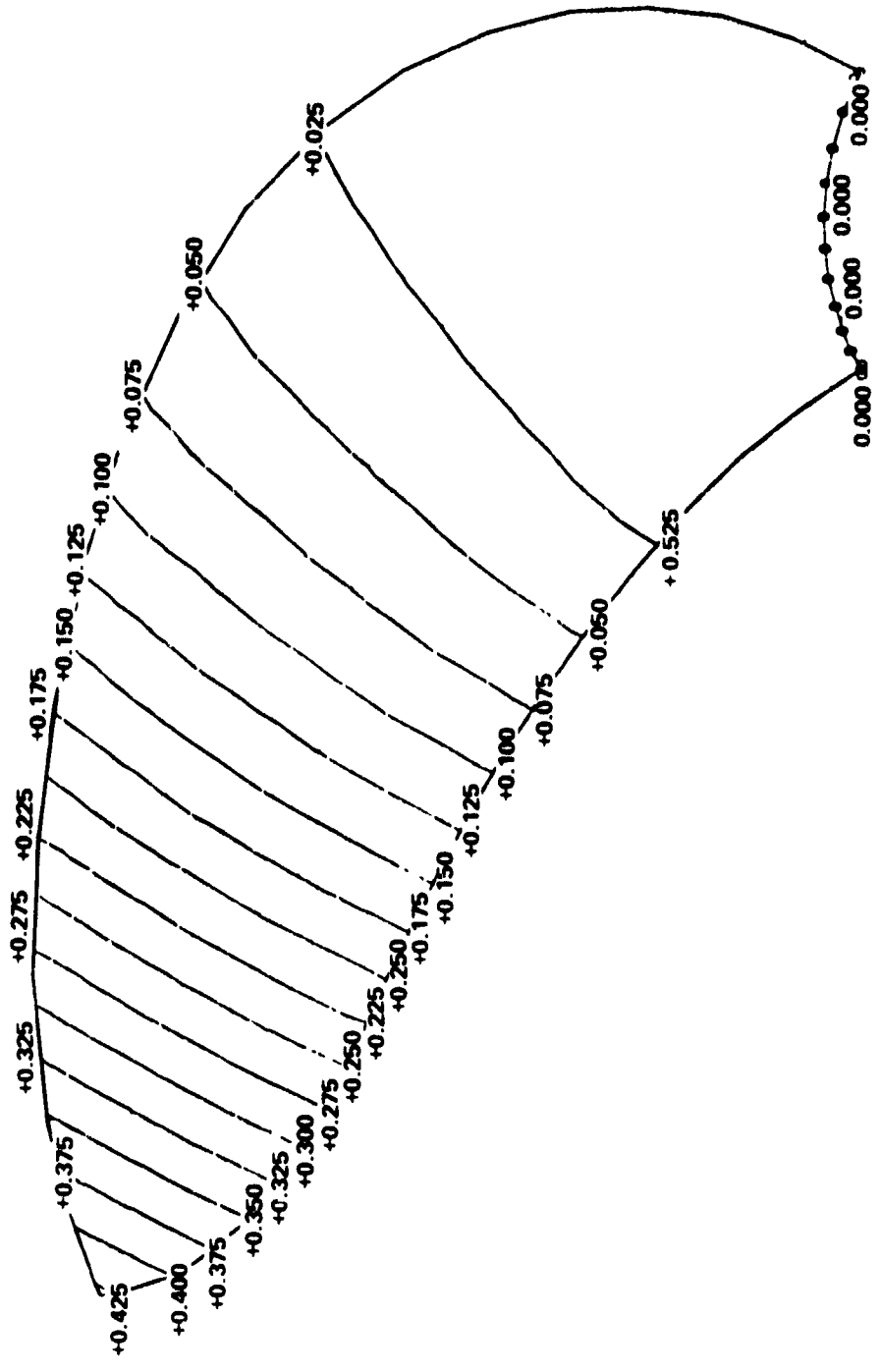
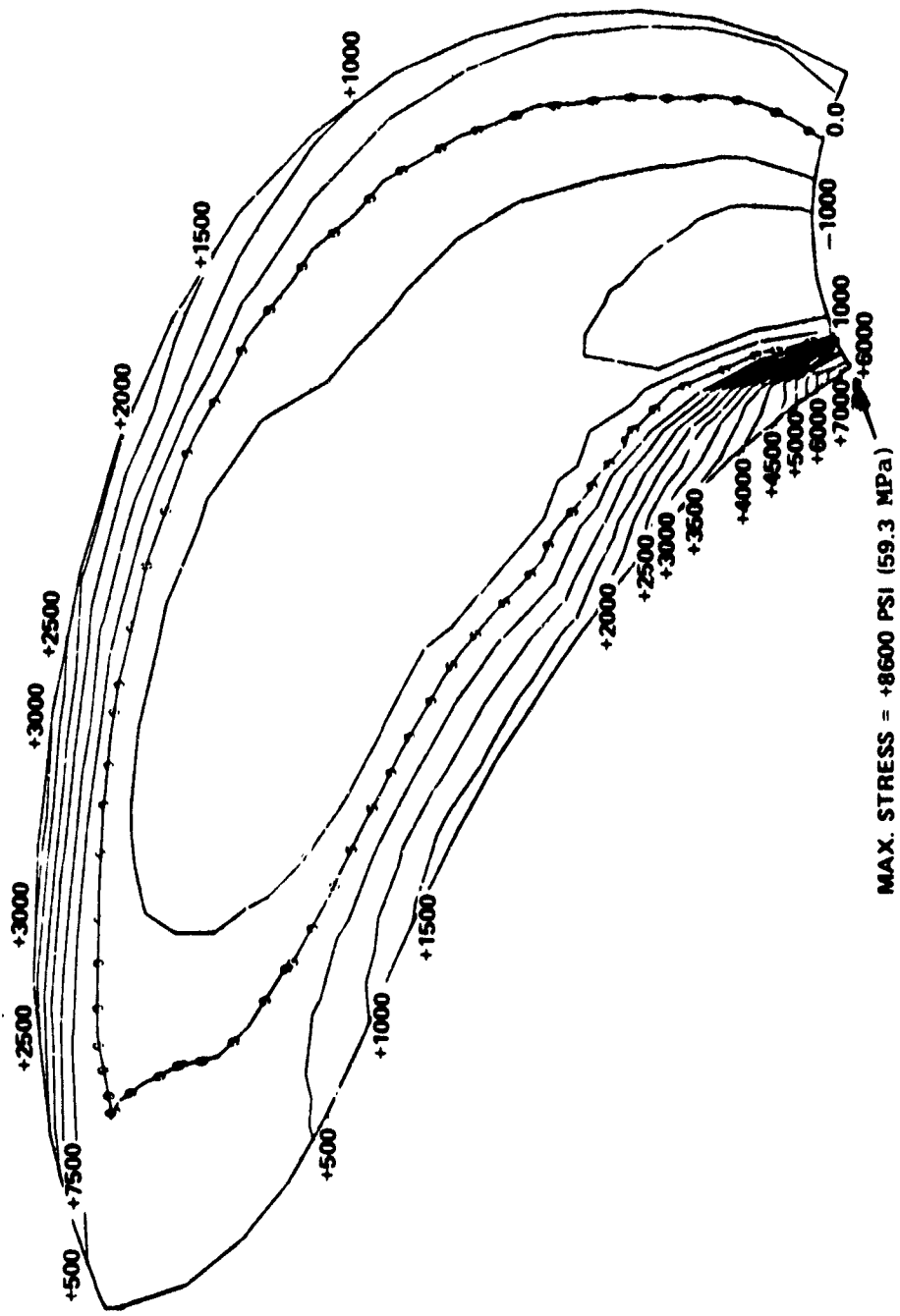


Figure 16 – Blade Deflections Calculated Using a Finite Element Method



**Figure 17 – Maximum Principal Stresses Calculated on the Suction Side of the AO Propeller Blade Finite Element Method**

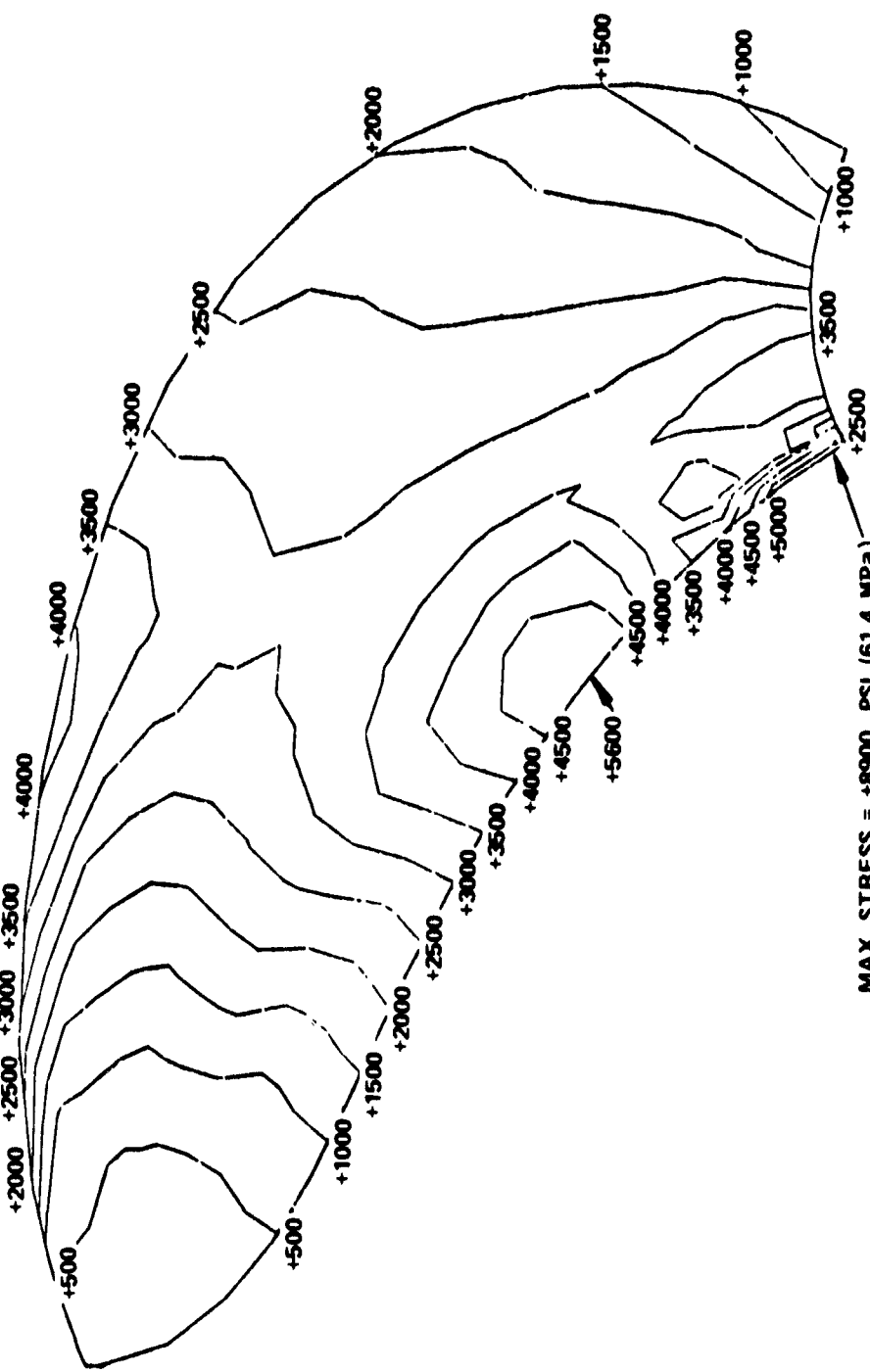


Figure 18 – Maximum Principal Stresses on the Pressure Side of the AO Propeller  
Blade Calculated by a Finite Element Method

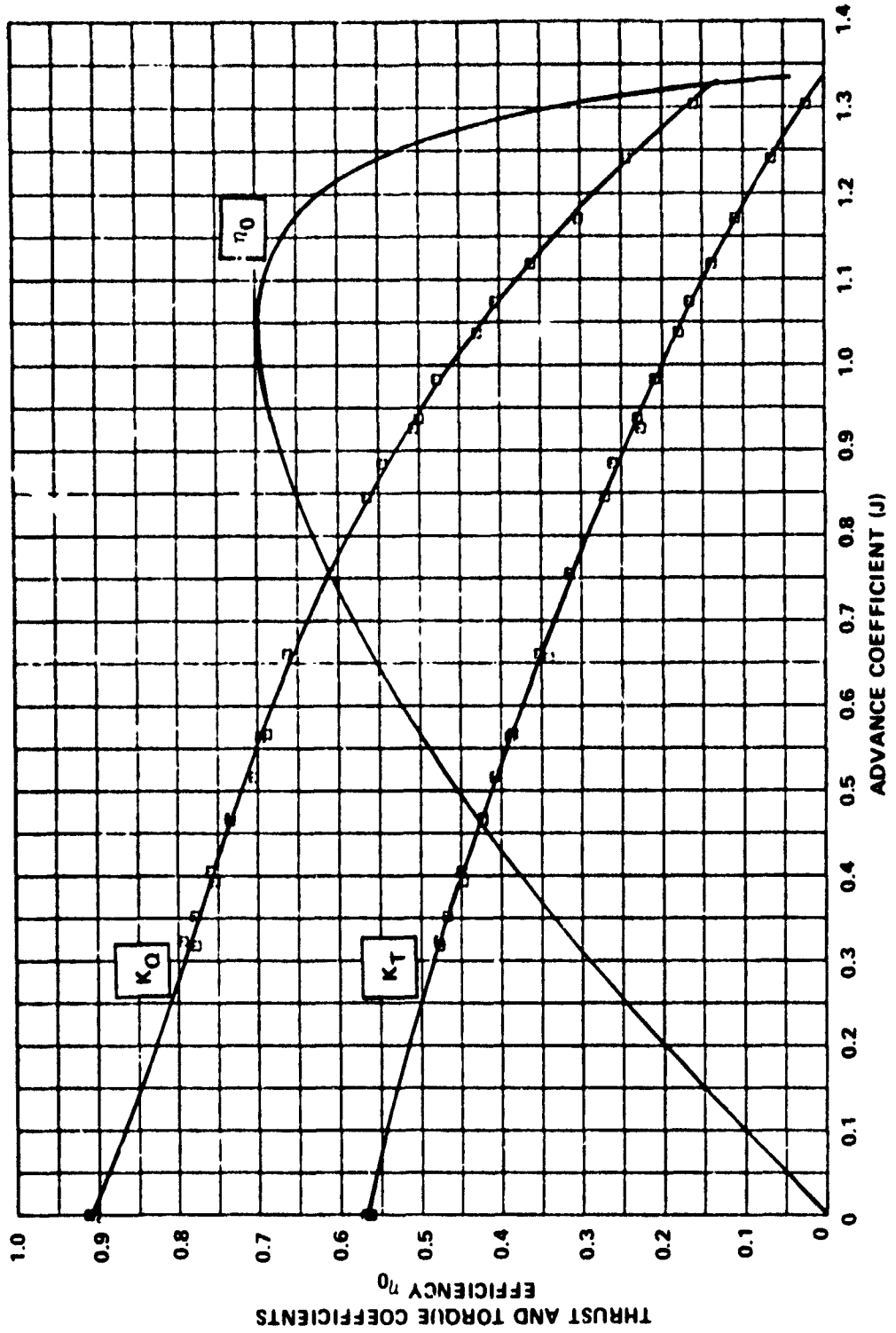


Figure 19 – Open-Water Characteristics of Final AO Propeller (4677)

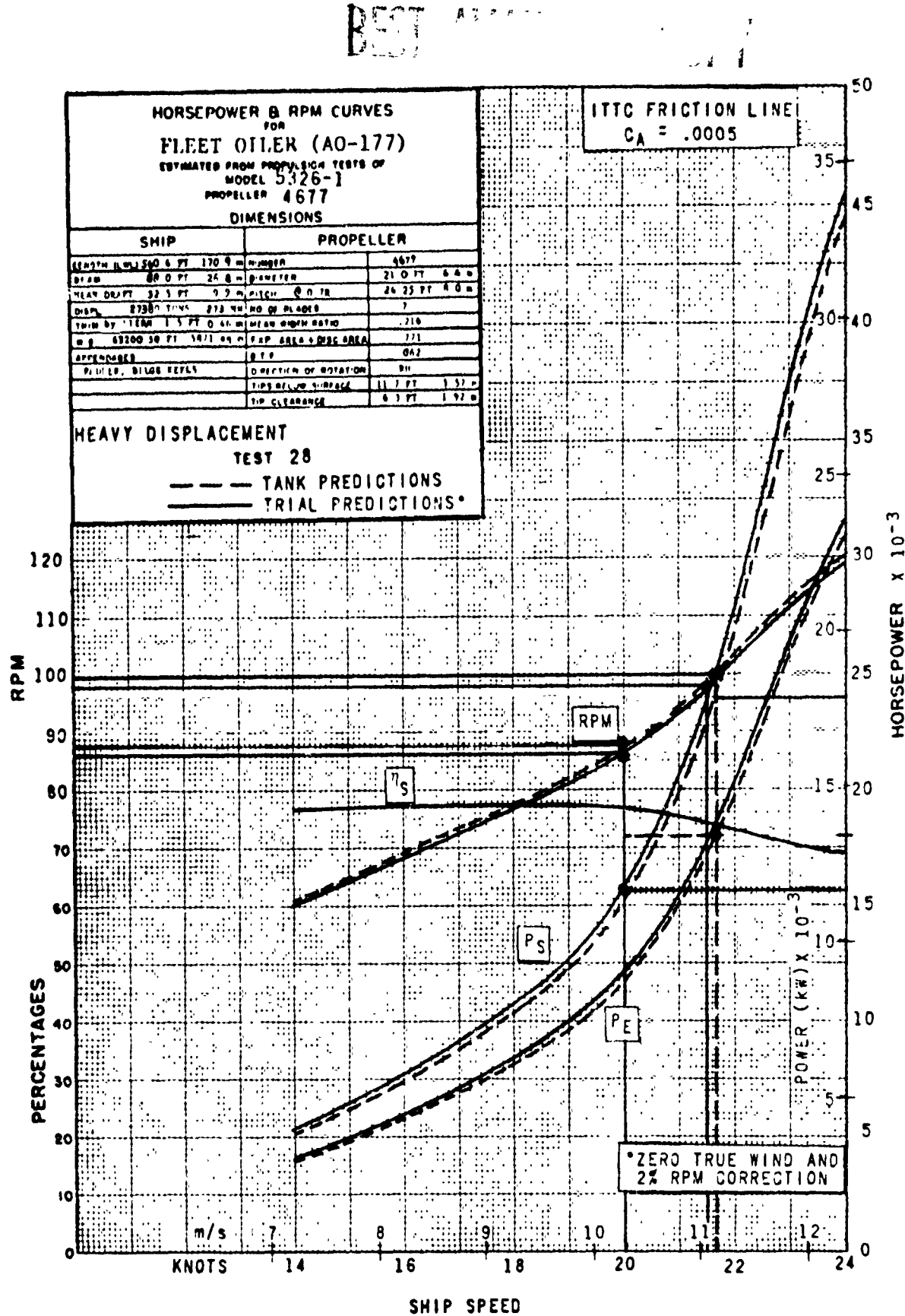


Figure 20 – Towing Tank and Trial Powering Predictions for AO,  $C_A = 0.0005$

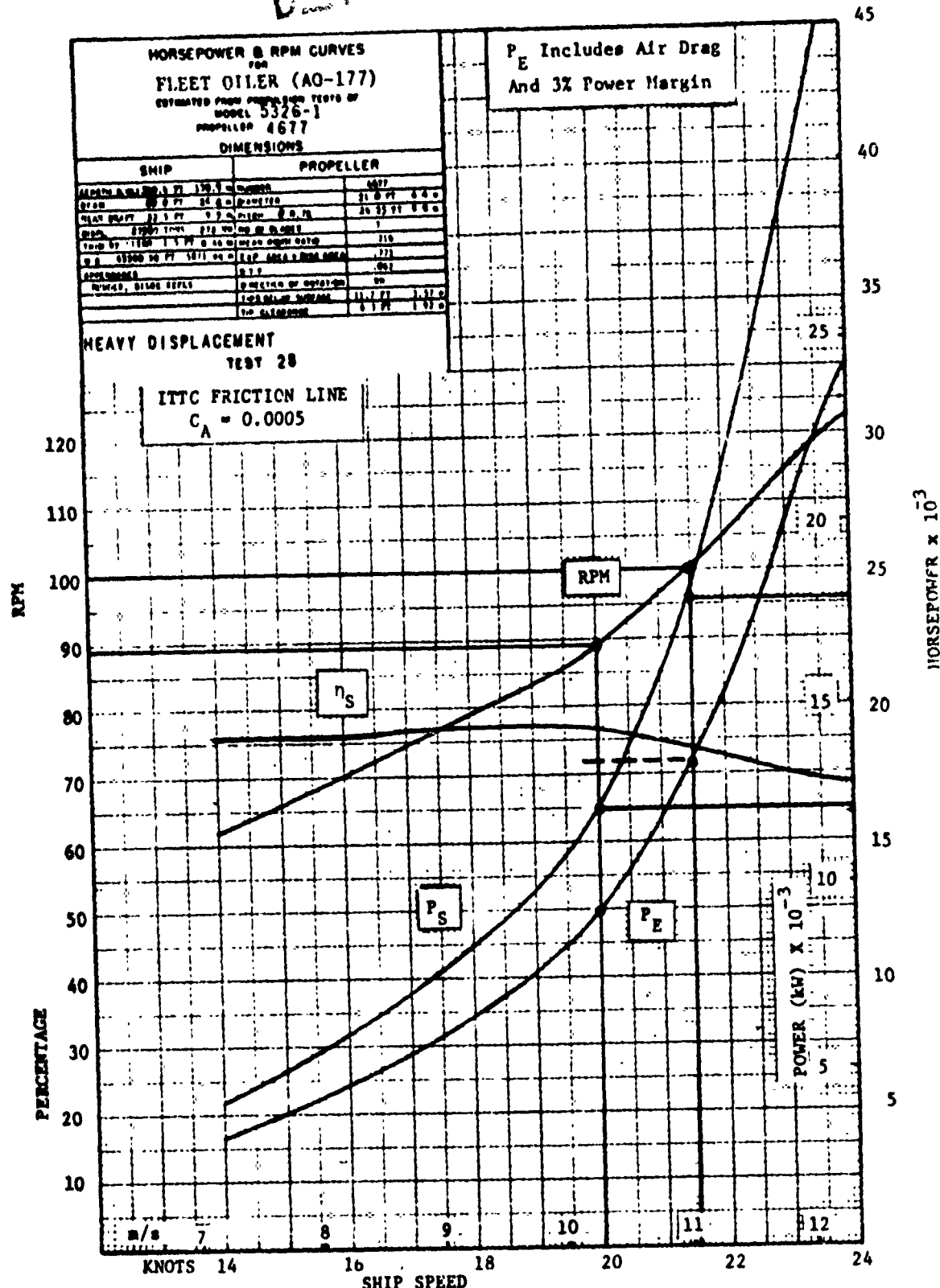


Figure 21 – Powering Predictions with Power Margin for AO,  $C_A = 0.0005$

TABLE 1 - DESIGN CONDITIONS

Diameter: 21 feet (6.4 meters)

RPS: 1.66 at the design point

Delivered Power at the Propeller: 24,000 SHP (17,897 kw) at full power

Design Point: Full power at full load displacement (displacement = 27,380 tons (273 mn), Draft = 32.5 feet (9.9 m), Trim = 1.5 feet by stern (0.46 m),  $C_A = 0.0005$ , still air drag added to  $P_E$ )

Endurance: 20 knots (10.3 m/s) at 80 percent of full power at same ship conditions as design point

Margin: Three percent on  $P_S$  to ensure endurance conditions are met

Cavitation Criteria: Ten percent speed margin on the inception of back bubble at the design point. Other forms of cavitation to be minimized to the extent practicable.

Type: Fixed pitch

Blade Numbers to be Considered: 5, 6, and 7

Hub Diameter: 0.2 x propeller diameter

Blade Skew: Use the amount practicable in order to minimize vibration excitation forces imparted to the hull and propulsion machinery

Rake: Use as necessary to maintain proper clearance

Material: Nickel-Aluminum-Bronze, MIL-B-21230, Alloy 1

Fatigue Strength: Alternating stress, 12,500 psi (86.2 MP<sub>a</sub>) for  $10^8$  cycles in sea water

Static Stress: Not to exceed 12,500 psi (86.2 MP<sub>a</sub>) when calculated using beam theory

Other: To facilitate handling, no portion of the blades shall extend closer than 4 inches (10.2 cm) to the forward and aft faces of the hub.

TABLE 2

a. Resistance and Propulsion DAta for AO-177 Class Fleet Oiler for Full-Load  
Clean Hull, Calm Seas, and Zero True Wind

$C_F = 0.0005$

Displacement = 27,380 tons (273 MN)

Length = 561 feet (171 meters)

Beam = 88 feet (26.8 meters)

Mean Draft = 32.5 feet (9.9 meters)

Trim = 1.5 feet (0.46 meters) by stern

$V_K$	$P_S$	$1-w_T$	$1-t$
20 knots (10.3 m/s)	12,120 hp (9,038 kw)	0.78	0.86
21 knots (10.8 m/s)	15,480 hp (11,543 kw)	0.78	0.86
21.5 knots (11.1 m/s)	17,720 hp (13,214 kw)	0.78	0.86
22 knots (11.3 m/s)	20,140 hp (15,018 kw)	0.78	0.86
23 knots (11.8 m/s)	26,280 hp (19,597 kw)	0.78	0.86

b. Design Point

$V_K = 21.4$  knots (11.0 m/s)

$P_E = 17,406$  hp (12,979 kw)

$P_S = 24,000$  hp (17,897 kw)

$N = 100$  rpm (10.5 rad/s)

TABLE 3  
MODEL 5326 (AO) RADIAL DISTRIBUTION OF AMPLITUDE OF  
HARMONIC LONGITUDINAL AND TANGENTIAL VELOCITY COMPONENTS  
RADIAL RATIO

	0.359	0.556	0.774	1.017	1.178
Harmonic Number	$v_x/v$	$v_t/v$	$v_z/v$	$v_t/v$	$v_z/v$
0	0.615	0.000	0.741	0.000	0.814
1	-0.243	-0.074	-0.214	-0.122	-0.192
2	-0.173	-0.012	-0.221	-0.028	-0.175
3	0.050	-0.020	0.015	-0.015	-0.041
4	-0.017	-0.006	-0.056	0.002	-0.078
5	0.023	0.021	0.042	0.018	-0.005
6	-0.011	-0.010	-0.025	-0.010	-0.021
7	0.003	0.008	0.026	0.011	0.021
8	0.004	-0.004	-0.024	-0.010	-0.014

$A_N$  is used as amplitude for harmonics of  $v_x/v$ .

$B_N$  is used as amplitude of harmonics of  $v_t/v$ .

TABLE 3 (CONTINUED)

MODEL 5326 (AO) RADIAL DISTRIBUTION OF AMPLITUDE OF  
HARMONIC LONGITUDINAL AND TANGENTIAL VELOCITY COMPONENTS

Harmonic Number	RADIUS RATIO					
	0.300	0.400	0.500	0.600	0.700	
	$v_x/v$	$v_t/v$	$v_x/v$	$v_t/v$	$v_x/v$	$v_t/v$
0	0.590	0.000	0.673	0.000	0.737	0.000
1	-0.249	-0.063	-0.230	-0.097	-0.215	-0.120
2	-0.158	-0.009	-0.202	-0.019	-0.220	-0.027
3	0.062	0.057	0.021	0.035	-0.017	0.016
4	-0.010	-0.009	-0.035	-0.002	-0.055	0.002
5	0.014	0.021	0.038	0.021	0.043	0.019
6	-0.008	-0.009	-0.019	-0.011	-0.025	-0.010
7	-0.003	0.006	0.015	0.010	0.025	-0.011
8	0.001	-0.002	-0.015	-0.008	-0.024	-0.010

$A_N$  is used as amplitude for harmonics of  $v_x/v$ .

$B_N$  is used as amplitude for harmonics of  $v_t/v$ .

TABLE 3 (CONTINUED)  
 MODEL 5326 (AO) RADIAL DISTRIBUTION OF AMPLITUDE OF  
 HARMONIC LONGITUDINAL AND TANGENTIAL VELOCITY COMPONENTS

Harmonic Number	RADIAL RATIO				$v_x/v^{1.000}v_t/v$	$v_x/v^{1.000}v_t/v$
	$v_x/v^{0.800}v_t/v$	$v_x/v^{0.900}v_t/v$	$v_x/v^{0.950}v_t/v$	$v_t/v^{0.950}$		
0	0.811	0.000	0.815	0.000	0.820	0.000
1	-0.181	-0.135	-0.176	-0.134	-0.176	-0.133
2	-0.153	-0.046	-0.137	-0.050	-0.132	-0.052
3	-0.092	-0.018	-0.094	-0.022	-0.093	-0.023
4	-0.066	-0.003	-0.058	-0.005	-0.056	-0.006
5	-0.016	0.001	-0.024	-0.003	-0.026	-0.004
6	-0.016	0.002	-0.015	0.002	-0.015	0.001
7	0.058	0.003	-0.003	0.001	-0.007	-0.001
8	-0.008	0.000	-0.005	0.002	-0.005	0.001

$A_N$  is used as amplitude for harmonics of  $v_x/v$ .

$B_N$  is used as amplitude for harmonics of  $v_t/v$ .

TABLE 4  
CIRCUMFERENTIAL AVERAGE AXIAL  
VELOCITY DISTRIBUTION OF WAKE

R = 10.5 feet (3.2 meters)

r/R	(V <sub>x</sub> /V) <sub>nominal</sub>	(V <sub>x</sub> /V) <sub>corrected</sub>
0.2	0.470	0.485
0.3	0.565	0.582
0.4	0.645	0.665
0.5	0.710	0.732
0.6	0.760	0.783
0.7	0.795	0.819
0.8	0.811	0.836
0.9	0.810	0.835
1.0	0.815	0.840

Table 5a - English Units

AO 177 CLASS FLEET OILER PROPELLER DESIGN

 $PS(IMP) = 2.4888E+04$ , DENSITY OF PROPULSION(FT3) = 483.0400

W(KNOTS) = 2.1888E+01 2.1888E+01 2.1588E+01 2.2888E+01 2.3388E+01

PE(IMP) = 1.2128E+04 1.5488E+04 1.7722E+04 2.0314E+04 2.3888E+04

D(FT) = 21.8888 , I-MTTS=7880 , I-FMD=-8668 , RHO(SLUG/FT3)= 1.9985

X	Y	Z	1-MX	C/D	T/C	TAN	TAN	RAKE/D	P/D	CD
INPUT:	LINEAR	INPUT:	CALCULATED							
2.8888E-01	6.8598E-01	2.8788E-01	2.0888E-01	9.0888E-01	7.8888E-01	8.	8.	0.	1.1258E+00	1.1688E-02
2.5888E-01	5.3788E-01	2.2788E-01	1.6788E-01	9.2988E-01	6.9988E-01	6.	6.	0.	1.1788E+00	1.0588E-02
3.8888E-01	5.6888E-01	2.4568E-01	1.6258E-01	8.6888E-01	6.2798E-01	2.2888E+00	0.	0.	1.2238E+00	1.0322E-02
4.8888E-01	6.6588E-01	2.7222E-01	1.3258E-01	5.3378E-01	5.3798E-01	7.1888E+00	D	0.	1.2688E+00	9.6332E-03
5.8888E-01	7.3222E-01	2.9122E-01	1.6838E-01	6.2138E-01	4.7168E-01	1.3188E+01	0.	0.	1.3188E+00	9.2168E-03
6.8888E-01	7.6368E-01	2.6648E-01	6.6038E-02	5.3798E-01	4.2223E-01	2.9888E+01	0.	0.	1.3898E+00	8.9888E-03
7.8888E-01	8.1988E-01	2.3288E-01	7.1508E-02	5.9038E-02	3.9218E-02	3.7558E-01	0.	0.	1.2598E+00	8.7711E-03
8.8888E-01	8.3688E-01	1.8158E-01	5.0068E-02	5.1968E-02	5.1968E-02	3.8918E-01	0.	0.	1.1498E+00	8.4621E-03
9.8888E-01	8.7588E-01	1.1988E-01	6.1038E-02	6.7808E-02	2.6588E-01	4.8938E-01	0.	0.	9.7888E+01	8.5863E-03
1.0888E+00	8.9988E-01	8.1038E-02	4.5888E-02	2.5338E-01	2.7178E-01	6.5888E+01	0.	0.	8.5788E-01	8.4749E-03
										7.2288E-01
X	Y	Z	1-MX	C/D	T/C	TAN	TAN	RAKE/D	P/D	CD
INPUT:	LINEAR	INPUT:	CALCULATED							
2.0888E-01	1.0437E+00	7.9375E-01	0.	9.6388E-02	6.2145E-02	0.	0.	0.	3.2798E+01	3.3802E+00
2.5888E-01	1.3275E+00	6.9258E-01	1.4363E-02	1.5662E-01	1.2935E-01	1.7952E-01	1.4948E-01	1.	3.2795E+01	3.8464E+00
3.8888E-01	1.3030E+00	1.3030E+00	4.9313E-02	1.7913E-01	1.7913E-01	3.1174E-01	2.9255E-01	2.	3.2394E+01	4.2239E+00
4.8888E-01	8.4658E-01	5.3589E-01	2.3639E-02	1.8439E-01	2.2903E-01	6.0537E-01	6.3622E-01	5.0037E+01	1.3237E+00	1.3237E+00
5.8888E-01	7.1620E-01	6.7115E-01	2.3430E-02	1.6982E-01	2.5647E-01	9.0575E-01	1.0108E+00	6.1644E+01	6.6338E-01	6.6338E-01
6.8888E-01	6.2435E-01	3.3803E-01	2.6282E-02	1.5627E-01	2.7677E-01	1.3177E+00	1.3778E+00	7.2633E+01	6.0495E-01	6.0495E-01
7.8888E-01	5.3803E-01	3.7717E-01	2.4022E-02	1.3229E-01	2.7959E-01	1.3749E+00	1.6805E+00	8.3746E+01	4.4497E-01	4.4497E-01
8.8888E-01	4.5227E-01	3.4599E-01	2.5149E-02	9.7166E-02	2.4235E-01	1.2552E+00	1.5699E+00	9.4619E+01	3.3521E-01	3.3521E-01
9.8888E-01	3.6667E-01	3.1313E-01	2.5056E-02	1.3193E-01	1.7310E-01	1.0153E+00	1.0348E+00	1.0327E+00	2.6610E-01	2.3770E-01
1.0888E+00	2.9239E-01	2.2563E-01	6.3202E-02	3.5510E-02	1.9971E-01	6.7026E-01	6.5930E-01	1.0082E+00	1.0082E+00	2.1308E-01
										1.1623E+00
X	Y	Z	1-MX	C/D	T/C	TAN	TAN	RAKE/D	P/D	CD
INPUT:	LINEAR	INPUT:	CALCULATED							
2.0888E-01	1.0437E+00	7.9375E-01	0.	9.6388E-02	6.2145E-02	0.	0.	0.	3.2798E+01	3.3802E+00
2.5888E-01	1.3275E+00	6.9258E-01	1.4363E-02	1.5662E-01	1.2935E-01	1.7952E-01	1.4948E-01	1.	3.2795E+01	3.8464E+00
3.8888E-01	1.3030E+00	1.3030E+00	4.9313E-02	1.7913E-01	1.7913E-01	3.1174E-01	2.9255E-01	2.	3.2394E+01	4.2239E+00
4.8888E-01	8.4658E-01	5.3589E-01	2.3639E-02	1.8439E-01	2.2903E-01	6.0537E-01	6.3622E-01	5.0037E+01	1.3237E+00	1.3237E+00
5.8888E-01	7.1620E-01	6.7115E-01	2.3430E-02	1.6982E-01	2.5647E-01	9.0575E-01	1.0108E+00	6.1644E+01	6.6338E-01	6.6338E-01
6.8888E-01	6.2435E-01	3.3803E-01	2.6282E-02	1.5627E-01	2.7677E-01	1.3177E+00	1.3778E+00	7.2633E+01	6.0495E-01	6.0495E-01
7.8888E-01	5.3803E-01	3.7717E-01	2.4022E-02	1.3229E-01	2.7959E-01	1.3749E+00	1.6805E+00	8.3746E+01	4.4497E-01	4.4497E-01
8.8888E-01	4.5227E-01	3.4599E-01	2.5149E-02	9.7166E-02	2.4235E-01	1.2552E+00	1.5699E+00	9.4619E+01	3.3521E-01	3.3521E-01
9.8888E-01	3.6667E-01	3.1313E-01	2.5056E-02	1.3193E-01	1.7310E-01	1.0153E+00	1.0348E+00	1.0327E+00	2.6610E-01	2.3770E-01
1.0888E+00	2.9239E-01	2.2563E-01	6.3202E-02	3.5510E-02	1.9971E-01	6.7026E-01	6.5930E-01	1.0082E+00	1.0082E+00	2.1308E-01
X	Y	Z	1-MX	C/D	T/C	TAN	TAN	RAKE/D	P/D	CD
INPUT:	LINEAR	INPUT:	CALCULATED							
2.0888E-01	0.	0.	0.	0.	0.	0.	0.	0.	-2.870E-01	2.070E-01
2.5888E-01	3.163E-01	4.871E-01	2.144E-02	3.430E-02	1.979E-02	1.727E-02	1.613E-02	-1.10E-02	2.239E-01	8.112E-02
3.8888E-01	3.5866E-01	5.5225E-01	2.4352E-02	2.079E-02	1.979E-02	2.079E-02	2.086E+00	2.2676E-01	2.645E+00	7.981E-02
4.8888E-01	3.-166E-01	5.261E-01	2.4325E-02	2.080E-02	2.010E-02	4.866E+00	7.100E+00	-2.012E-01	3.432E-01	7.733E-02
5.8888E-01	3.080E-01	4.745E-01	2.5149E-02	2.5149E-02	2.5149E-02	6.932E+00	6.310E+00	-1.359E-01	6.059E-01	6.059E-02
6.8888E-01	2.691E-01	4.4525E-01	1.963E-02	3.032E-02	2.250F-01	6.570E+00	2.300E+00	-1.343E-01	5.236E-02	5.773E-02
7.8888E-01	2.016E-01	4.336E-01	1.912E-02	3.114E-02	2.508E-02	9.575E-03	2.770E-01	1.573E-01	0.213E-01	3.310E-02
8.8888E-01	2.665E-01	4.104E-01	1.013E-02	3.228E-02	2.975E-02	9.051E-03	3.450E+01	3.474E-01	7.102E-01	2.122E-02
9.8888E-01	2.379E-01	3.664E-01	1.615E-02	3.576E-02	3.766E-02	6.567E+00	4.03DE+01	5.502E+01	7.082E+01	1.193E+01
9.500E-01	2.106E-01	3.2435E-01	1.430E-02	4.625E-02	4.512E-02	4.376E-03	4.20DE+01	6.573E+01	6.193E+01	7.644E-03
1.0888E+00	0.	0.	0.	0.	0.	0.	0.	0.	0.059E+01	0.059E+01

ETAO=7.2310E-01 PS(<sup>(imp)</sup>) = 2.4001E+04 1-TMD=9.6800E-01 1-WTTS=7.0000E-01 V(KNOTS) = 2.1442E+01 DESIGN TH(LB)<sup>(1)</sup>=3.8791E+05  
<sup>(2)</sup> = 7. MFR(MIN)=1.620E+04 1-FMD=0.6668 , RHO(SLUG/FT3)= 1.9985 CALCULATED TH(LB)<sup>(2)</sup>=3.6155E+01

TABLE 5 - Lifting Line Design of AO-177 Class Fleet Oiler Propeller

X	AREA (IN <sup>2</sup> )	XBAR (IN)	YBAR (IN)	INC	IY0	MY0	M1B (IN-LBF)	M2B (IN-LBF)	MAXRESS
2.00E-01	3.924E+02	2.067E+02	2.927E+01	1.326E+01	2.510E+03	6.146E+04	2.503E+06	2.572E+06	1.630E+06
3.00E-01	6.406E+02	2.067E+02	2.927E+01	1.326E+01	2.668E+03	9.723E+04	2.393E+06	2.026E+06	5.962E+03
4.00E-01	4.495E+02	3.264E+02	1.166E+01	2.165E+03	1.197E+05	1.605E+05	3.577E+06	1.501E+06	4.095E+03
5.00E-01	3.924E+02	3.264E+02	1.166E+01	2.165E+03	1.197E+05	1.119E+05	2.923E+06	1.826E+06	7.788E+03
6.00E-01	2.903E+02	3.193E+02	6.692E+01	6.354E+02	6.412E+02	6.803E+04	6.803E+05	5.068E+06	3.792E+03
7.00E-01	1.762E+02	2.165E+01	1.816E+02	1.816E+02	3.439E+04	3.411E+05	9.736E+05	3.143E+05	6.258E+03
8.00E-01	0.699E+01	2.165E+01	3.898E+01	3.898E+01	1.054E+04	1.259E+05	2.666E+05	1.167E+05	3.653E+03
X	R A KG/C/D	P1 H TAN31	P1 TAMP						
2.00E-01	0.	6.550E-01	4.912E-01						
2.500E-01	0.	8.416E-01	5.488E-01						
3.000E-01	0.	9.649E-01	6.694E-01						
4.000E-01	0.	1.063E+00	6.355E-01						
5.000E-01	0.	1.126E+00	7.613E-01						
6.000E-01	0.	1.178E+00	7.930E-01						
7.000E-01	0.	1.185E+00	8.794E-01						
8.000E-01	0.	1.137E+00	9.667E-01						
9.000E-01	0.	1.042E+00	1.1556E-01						
9.500E-01	0.	9.624E-01	4.997E-01						
1.000E+00	0.	9.174E-01	9.507E-01						

WEIGHT OF BLADES(LBF) = 51363.0091  
 WEIGHT OF PROP (BLADES + CYLINDRICAL HUB(LBF) = 79536.3713  
 CENTER OF GRAVITY OF PROOF REFERENCED FROM MACHORD OF ROOT SECTION (- FWD, + AFT)/Dz = -0.21636  
 CENTER OF GRAVITY OF BLADES REFERENCED FROM MACHORD OF ROOT SECTION (- FWD, + AFT)/Dz = -0.33587  
 HUB DIMENSIONS/D  
 HUB DIAM = .2000  
 HUB LENGTH = .2000  
 MACHORD OF ROOT SECTION TO AFT END OF HUB = .1000  
 KELLEFS MINIMUM LAR = .0266E+00  
 SPEED CFF W/IND1 JS= .1013E+01  
 ADVANCE Q\_CFF V11-W77) / (IND1 JA= .7899E+00  
 DESIGN THRUST C\_JEFF KT= .2764E+00  
 TORQUE CJeffF Q= .5260E-01  
 PROPELLIVE EFFICIENCY ETAD= .7232E+00  
 BURRII THUST COEFF TC= .2065E+00  
 BURRII JAVITATION COEFF SIGMA(0.7) = .5496E+00  
 CLEARANCE AT HUB BETWEEN BLADES/C = .2140E-02  
 CLEARANCE AT HUB BETWEEN FILLETS/D = -3.3691E-01

Table 5a (Continued)

MASS POLAR MOMENT OF INERTIA OF BLADES (LBIN-IN<sup>2</sup>) = .157764E+89  
 TOTAL MASS POLAR MOMENT OF INERTIA (LBIN-IN<sup>2</sup>) = .157764E+89  
 RADIUS OF GYRATION OF BLADE/D= .2199  
 RADIUS OF GYRATION OF MUS/D= 6.0000  
 TOTAL RADIUS OF GYRATION/D= .1767

ABS COEFFICIENTS (CALCULATED AT THE .25 RADIUS)

ABS MINIMUM THICKNESS IN INCHES (USING P/D INPUT)-  
 USING ABS RAKE = CONVENTIONAL RAKE, T/D=.2954E-81  
 USING ABS RAKE = CONVENTIONAL + SKEW-INDUCED RAKE, T/D= -.3173E-81  
 VALUES USED IN DETERMINING THICKNESS-  
 A= -100654E-02  
 B= -153771E+03  
 C= .138286E+15  
 SECTION AREA COEFFICIENT CS= .7842E+00  
 SECTION MODULUS COEFFICIENT CM= .0550E-01  
 AREA OF EXPANDED CYLINDRICAL SECTION IN SQ.INCHES AS= -4148E+03

FOR CN=.1  
 ABS MINIMUM THICKNESS IN INCHES (USING P/D INPUT)-  
 USING ABS RAKE = CONVENTIONAL RAKE, T/D=.2731E-81  
 USING ABS RAKE = CONVENTIONAL + SKEW-INDUCED RAKE, T/D= -.2919E-81

Table 5a (Continued)

Table 5b - SI Units

## AO 177 CLASS FLEET OILER PROPELLER DESIGN

PSI(M)= 2.4688E+04, DENSITY OF PROPER GAS= 7750, RT=17

V(FT/SEC) 1.013E+01 1.013E+01 1.1061E+01 1.1310E+01 1.1632E+01  
 PE(FT) 9.8374E+03 1.1453E+04 1.3214E+04 1.5016E+04 1.7591E+04  
 D(M)= 6.0030 1-MTT=.76800 .1-T=0=.66000 ,MINI = 16.0250 ,MEMO(M)= 1025.8615

7 7

AE/A0 7.6979E-01

W(ME)V/MIN 1.9288E+02

X	1-MX	C/D	T/C	TAB1	TAB2	TET1DEG	RNG/D	P/D
INPUT	INPUT	INPUT	INPUT	INPUT	INPUT	ONLINEAR	LINEAR	IN=UT
2.0000E-01	4.9500E-01	2.8780E-01	2.0000E-01	9.8459E-01	7.8461E-01	8.	1.1250E+00	1.1400E+02
2.5000E-01	5.1790E-01	2.2700E-01	1.0000E-01	9.2900E-01	6.9499E-01	6.	1.1700E+00	1.0050E+02
3.0000E-01	5.4250E-01	2.4550E-01	1.6250E-01	8.6690E-01	6.2759E-01	2.2000E	1.2230E+00	1.0322E+02
3.5000E-01	5.6500E-01	2.7220E-01	7.3250E-01	7.3370E-01	5.3790E-01	7.1000E+00	1.2600E+00	9.6332E+01
4.0000E-01	7.1200E-01	2.0170E-01	1.0000E-01	6.2100E-01	4.7300E-01	1.1000E+01	1.2160E+00	9.2160E+01
4.5000E-01	7.0190E-01	2.6040E-01	8.0000E-02	5.3700E-01	4.2223E-01	2.0000E	1.3890E+00	8.9460E+01
5.0000E-01	6.9900E-01	3.3280E-01	7.1500E-01	6.6770E-01	3.7655E-01	2.7700E	1.2520E+00	8.7411E+01
5.5000E-01	6.9600E-01	1.0150E-01	5.9000E-02	3.9210E-01	3.3015E-01	3.6500E	1.1600E+00	8.6021E+01
6.0000E-01	8.3500E-01	1.1900E-01	5.0000E-02	3.1930E-01	3.0019E-01	4.3000E	1.0800E+00	8.5030E+01
6.5000E-01	8.9500E-01	1.1300E-02	4.7000E-02	2.0590E-01	2.0570E-01	4.2000E	1.0200E+00	8.4700E+01
7.0000E-01	8.4600E-01	0.	4.5000E-02	2.5310E-01	2.1710E-01	4.3000E	1.0000E+00	8.4500E+01
X	TAB1	TAB2	G	UT/2V	UA/2V	DC1ST	DCPST	CADV
2.0000E-01	1.8637E+00	7.8175E-01	C.	9.6500E-02	5.2105E-02	0.	0.	8.3800E+00
2.5000E-01	1.8975E+00	1.0563E-01	1.	2.0595E-01	2.0595E-01	1.4948E-01	1.4948E-01	3.8600E+00
3.0000E-01	1.8822E+00	6.2500E-01	1.4691E-02	1.7913E-01	1.7913E-01	3.1374E-01	3.9255E-01	2.2340E+00
4.0000E-01	8.4620E-01	5.3500E-01	2.0643E-02	1.8639E-01	2.0530E-01	6.0557E-01	6.3622E-01	1.3237E+00
5.0000E-01	7.1670E-01	2.3600E-02	1.6902E-02	2.5602E-01	2.5602E-01	1.8737E-01	1.8737E-01	6.6338E-01
6.0000E-01	6.2055E-01	6.2055E-01	2.4631E-02	1.5020E-01	2.7712E-01	1.1077E+00	2.2557E+01	6.8059E-01
7.0000E-01	5.3476E-01	3.7777E-01	2.4022E-02	1.3229E-01	2.7959E-01	1.3798E+00	2.5559E+01	6.4497E-01
8.0000E-01	4.5227E-01	3.3660E-01	9.7146E-02	2.4230E-02	2.4230E-02	1.3632E+00	3.3932E+01	5.8600E+00
9.0000E-01	5.6837E-01	2.9939E-01	1.3131E-02	5.7039E-02	1.7319E-01	1.0032E+00	3.2158E+01	5.6618E+01
9.5000E-01	3.2929E-01	2.4574E-01	8.3202E-03	3.5539E-02	1.1971E-01	6.7636E-01	3.3779E+01	2.3738E+01
1.0000E+00	2.9201E-01	2.7974E-01	0.	1.6101E-02	6.1135E-02	0.	0.	3.5428E+01
CPI=1.5.4264E-01	CPSI=7.6379E-01	FTAI=7.1893E-01	CTSI=9.3494E-01	CTSY=9.04847E-01	CTSY=9.0490E-01	CTSY=9.0490E-01	CTSY=9.0490E-01	CTSY=9.0490E-01
CP5=5.3293E-01	CP5=6.1321E-01	ETA=6.55777E-01	CTSI=6.6111E-01	CTSI=6.6111E-01	CTSI=6.6111E-01	CTSI=6.6111E-01	CTSI=6.6111E-01	CTSI=6.6111E-01
X	CL	ALI(TDFG)	FMC	CO/C	F(X)	L1(W/H)	T/TDFG	T/RO
2.0000E-01	0.	0.	0.	0.	0.	0.	0.000E-01	2.070E-01
2.5000E-01	3.163E-01	6.571E-01	2.1460E-02	3.430E-02	1.8790E-01	2.3540E+00	4.0000E-01	2.78E-01
3.0000E-01	3.586E-01	5.5222E-01	2.035E-02	2.0790E-02	1.9710E-01	3.9740E+00	2.0000E-01	2.2399E-01
4.0000E-01	3.416E-01	5.2615E-01	2.3200E-02	2.0200E-02	2.0320E-01	7.1020E+00	2.2000E-01	2.2676E-01
5.0000E-01	3.0500E-01	6.743E-01	2.8910E-02	2.9900E-02	2.1140E-01	1.0000E+00	1.3100E-01	1.3295E-01
6.0000E-01	2.8910E-01	6.4522E-01	1.9930E-02	3.8920E-02	2.2500E-01	1.2510E+00	1.3640E-01	5.2340E-01
7.0000E-01	2.016E-01	6.336E-01	1.9120E-02	3.1000E-02	2.5000E-01	1.3970E+00	1.5730E-01	6.2130E-01
8.0000E-01	2.669E-01	6.040E-01	1.6120E-02	3.2200E-02	2.9500E-01	1.3210E+00	3.4760E-01	2.3620E-01
9.0000E-01	2.3779E-01	3.6640E-01	1.0150E-02	3.5700E-02	3.7000E-01	9.5870E+00	4.0380E-01	5.5002E-01
9.5000E-01	2.206E-01	3.2430E-01	1.4300E-02	4.0200E-02	4.5210E-01	6.3300E+00	4.2800E-01	6.9370E-01
1.0000E+00	0.	0.	0.	0.	0.	0.	0.5800E+01	0.6540E+01
EYD=7.2710E-01	PSIKW=1.7097E+06	1-TMD=0.6000E-01	1-MTT=7.6000E-01	1-MTT=7.6000E-01	VIMNTSI	9.14222E+01	DESIGN TM(M)	9.13650E+01
2=7	W(ME)V/MIN	W(ME)V/MIN	W(ME)V/MIN	W(ME)V/MIN	W(M/SEC)	-1.1020E+01	CALCULATED TM(M)	-1.3050E+01

$R$	AREA(m <sup>2</sup> )	BLADE(m)	YAW(deg)	PRO1(m)	PRO1(m)	PRO1(m)	PRO1(m)
2.000E-01	2.531E-01	6.267E-01	0.	1.465E-03	2.515E-02	2.828E+02	6.375E+02
3.000E-01	2.099E-01	7.435E-01	3.366E-03	1.111E-03	4.958E-02	2.372E+02	6.597E+02
4.000E-01	2.086E-01	6.245E-01	2.618E-03	9.818E-03	5.922E-02	1.814E+02	3.232E+02
5.000E-01	2.032E-01	6.528E-01	1.752E-03	5.643E-03	6.658E-02	1.258E+02	3.303E+02
6.000E-01	1.973E-01	6.125E-01	6.177E-04	3.216E-04	7.694E-02	7.694E+01	3.386E+01
7.000E-01	1.437E-01	7.823E-01	0.	7.532E-05	1.419E-02	3.858E+01	7.671E+01
8.000E-01	5.761E-02	5.495E-01	0.	1.955E-05	4.958E-03	3.897E+01	3.525E+01
X	RADE/0	PT. X(YAW)	PT. Y(YAW)	PRO1(m)	PRO1(m)	PRO1(m)	PRO1(m)
2.000E-01	0.	6.550E-01	6.912E-01	0.912E-01	0.912E-01	0.912E-01	0.912E-01
3.000E-01	0.	6.426E-01	5.438E-01	0.438E-01	0.438E-01	0.438E-01	0.438E-01
4.000E-01	0.	6.043E-01	5.079E-01	0.079E-01	0.079E-01	0.079E-01	0.079E-01
5.000E-01	0.	5.205E-01	4.125E-01	-1.25E-01	-1.25E-01	-1.25E-01	-1.25E-01
6.000E-01	0.	4.176E-01	7.938E-01	7.938E-01	7.938E-01	7.938E-01	7.938E-01
7.000E-01	0.	3.075E-01	0.295E-01	0.295E-01	0.295E-01	0.295E-01	0.295E-01
8.000E-01	0.	1.337E-01	0.4657E-01	0.4657E-01	0.4657E-01	0.4657E-01	0.4657E-01
9.000E-01	0.	0.422E-01	0.456E-01	0.456E-01	0.456E-01	0.456E-01	0.456E-01
1.000E-01	0.	9.020E-02	0.497E-01	0.497E-01	0.497E-01	0.497E-01	0.497E-01
9.179E-02	0.	9.179E-01	0.9307E-01	0.9307E-01	0.9307E-01	0.9307E-01	0.9307E-01

WEIGHT OF BLADE - m1 = 220963.0345

WEIGHT OF PROP (BLADE + CYLINDRICAL HUB) (m1) = 353770.1853

CENTER OF GRAVITY OF PROP REFERENCED FROM MIDCHORD OF ROOT SECTION 1 - FWD. + AFT1/0° - 0.21698

CENTER OF GRAVITY OF BLADES REFERENCED FROM MIDCHORD OF ROOT SECTION 1 - FWD. + AFT1/0° - 0.33587

HUB DIMENSIONS/0

HUB DIAM = 2000  
HUB LENGTH = 2000  
MIDCHORD OF ROOT SECTION TO AFT END OF HUB = .1988

KELLERS MINIMUM EAR = .8268E+00

SPEED COEFF V/1000 JS+ .1812E+01

ADVANCE COEFF U11-WT1/(100) JS+ .7099E+00

BEST THRUST COEFF K7+ .2744E+00

TORQUE COEFF K8+ .9268E+01

PROPELLER EFFICIENCY ETAB= .7222E+00

SUPERILL THRUST COEFF TCF+ .2062E+00

SUPERILL CAVITATION COEFF SIGMA10.71+ .5845E+00

CLEARANCE AT HUB BETWEEN BLADES/0 4.2368E-02

CLEARANCE AT HUB BETWEEN FILLETS/0 -3.3693E-02

Table 5b (Continued)

MASS POLAR MOMENT OF INERTIA OF BLADES (KG-M <sup>2</sup> )	<b>-461689E+05</b>
TOTAL MASS POLAR MOMENT OF INERTIA (KG-M <sup>2</sup> )	<b>-461689E+05</b>
RADIUS OF CYRATION OF BLADE/0°	<b>-2199</b>
RADIUS OF CYRATION OF HUB/0°	<b>8.4888</b>
TOTAL RADIUS OF CYRATION/0°	<b>-1767</b>

ABS COEFFICIENTS (CALCULATED AT THE .25 RADIUS)

ABS MINIMUM THICKNESS IN INCHES (USING P/D INPUT)-	USING ABS RATE = CONVENTIONAL RATE, T/0 = <b>.2958E-01</b>
USING ABS RATE = CONVENTIONAL + SKIN-INDUCED RATE, T/0 = <b>.3173E-01</b>	
VALUES USED IN DETERMINING THICKNESS-	
A=	<b>.188895E+02</b>
B=	<b>.153771E+03</b>
C=	<b>.138216E+05</b>
SECTION AREA COEFFICIENT	<b>CS= .7842E+00</b>
SECTION MODULUS COEFFICIENT	<b>CM= .0558E-01</b>
AREA OF EXPANDED CYLINDRICAL SECTION IN SQ. METERS	<b>AS= .2670E+00</b>

FOR CM=.1  
 ABS MINIMUM THICKNESS IN INCHES (USING P/D INPUT)-  
 USING ABS RATE = CONVENTIONAL RATE, T/0 = **.2731E-01**  
 USING ABS RATE = CONVENTIONAL + SKIN-INDUCED RATE, T/0 = **.2919E-01**

Table 5b (Cont'dued)

**TABLE 6**  
**GEOMETRIC CHARACTERISTICS OF FINAL AO-177 CLASS FLEET OILER HIGHLY SKewed PROPELLER DESIGN**

<b>r/R</b>	<b>C/C</b>	<b>P/D</b>	<b><math>\theta_s</math> (degrees)</b>	<b><math>\theta_s</math> (rad)</b>	<b>t/c</b>	<b><math>f_N/c</math></b>	<b><math>z_R/D</math></b>
0.2	0.2070	1.125	0.0	0.0	0.20	0.0490	0.0
0.3	0.2456	1.223	2.2	0.0384	0.1625	0.0444	-0.0017
0.4	0.2722	1.288	7.1	0.1239	0.1325	0.0367	-0.0044
0.5	0.2817	1.318	13.1	0.2296	0.1080	0.0314	-0.0070
0.6	0.2684	1.309	20.0	0.3491	0.0880	0.030	-0.0077
0.7	0.2320	1.250	27.7	0.4835	0.0175	0.0295	-0.0049
0.8	0.1815	1.140	34.5	0.6021	0.0590	0.0281	-0.0003
0.9	0.1180	0.970	40.3	0.7034	0.0500	0.0263	0.0082
1.0	0.0	0.722	45.0	0.7854	0.045	0.0240	0.0245

TABLE 7 - SUMMARY OF AO-177 CLASS FLEET OILER  
DESIGN POINT ANALYTICAL PREDICTIONS

**Powering**

$P_N$	Shaft power	24,000 hp (17,897 kw)
$N$	Shaft speed	100 rpm (10.5 rad/s.)
$V_K$	Ship speed	21.4 knots (11.6 m/s)
$\eta_D$	Propulsive coefficient	0.69

**Strength**

Stress at 0.7 radius	3,794 psi (26.2 MPa)
Stress at root	6,400 psi (44.1 MPa)

**Estimate of Weight**

79,200 lbs (352.3 KN)

**Unsteady Loading**

$\tilde{T}$	Unsteady thrust	2,600 lbs (11,565 N)
$\tilde{Q}$	Unsteady torque	9,800 ft-lbs (13,287 N·M)
$\tilde{F}_y$	Horizontal bearing force	960 lbs (4,270 N)
$\tilde{F}_z$	Vertical bearing force	230 lbs (1,023 N)
$\tilde{M}_H$	Horizontal bending moment	11,900 ft-lbs (16,134 N·M)
$\tilde{M}_V$	Vertical bending moment	5,770 ft-lbs (7,823 N·M)
$\tilde{T}/\bar{T} \times 100$	Percent of mean thrust	0.84

TABLE 8 - LIFTING SURFACE CORRECTION FACTORS FOR AO-177  
 CLASS FLEET OILER HIGHLY SKEWED PROPELLER

x	$k_t$	$k_c$	$k_\alpha$
0.3	1.142	1.734	6.358
0.4	0.785	1.444	5.946
0.5	0.508	1.411	5.777
0.6	0.310	1.579	4.746
0.7	0.188	1.691	0.835
0.8	0.140	1.644	-2.040
0.9	0.166	1.561	-7.276

$$k_c = \frac{f_M \text{ due to loading}}{f_{M_{2-D}}}$$

$$k_\alpha = \frac{\alpha_i \text{ due to loading}}{\alpha_{i_{1.0}} \cdot C_L}$$

$$k_t = \frac{\alpha_t \text{ due to thickness (in radians)}}{BTF}$$

TABLE 9 - PERFORMANCE VALUES AT ENDURANCE CONDITION

Values used for calculations (from Reference 3)

Displacement	27,380 tons (273 MN)
Draft	32.5 ft (9.9 m)
Trim (by stern)	1.5 ft (0.46 m)
$C_A$ (full load, clean hull, calm seas)	0.0005
Speed	20 knots (10.3 m/s)
$P_E$ (excluding air drag)	11,760 hp (8,769 kw)
$P_E$ (including air drag)	12,335 hp (9,198 kw)
$l-t$	0.815

Calculated values

Thrust	242,530 lbs (1,079 KN)
$P_S$	17,100 ph (12,751 kw)
P.C.	0.72
N	90 rpm (9.4 rad/s)

Specified Values

Maximum allowable $P_S$ with no margin	19,200 hp (14,317 kw)
Maximum allowable $P_S$ with 6 percent power margin	18,048 hp (13,458 kw)

Conclusions

Endurance power specification (including margin) was met with an additional 5 percent margin.

TABLE 10 - PERFORMANCE VALUES AT FULL POWER BALLAST CONDITION

Values used for calculations (from Reference 3)

Displacement	17,580 tons (175 MN)
Draft	22.2 ft (6.8 m)
Trim (by stern)	1.0 ft (0.305 m)
$C_A$ (ballast, clean hull, calm seas)	0.0005
Speed	Range considered
$P_E$	Range considered
1-t	0.835
$P_S$ no margin	24,000 hp (17,897 kw)
$P_S$ 6 percent power margin	22,560 hp (16,823 kw)

Calculated values, no margin

Thrust	no margin	304,000 lbs (1,352 KN)
$P_E$	no margin	17,700 hp (13,199 kw)
P.C.	no margin	0.74
Shaft speed, N	no margin	101 rpm (10.6 rad/s)
Speed	no margin	22.7 knots (11.7 m/s)
Speed	6 percent power margin	22.3 knots (11.5 m/s)

## **APPENDIX**

**Final propeller geometry as presented in the ship specifications submitted for bids by NAVSEC (The dimensions are as given in the specifications without metric equivalents.).**

PRECEDING PAGE BLANK NOT FILMED

TABLE A1

Definitions of terms used in Tables A2, A3, and Figures A1 and A2.

1. B - The distance, normal to the chord line, from chord line to the back (suction side) surface of the blade.
2. C/C - Ratio of the distance of a point on the chord line to the total chord length, measured from the leading edge (i.e., leading edge = 0.0, trailing edge = 1.0).
3. Chord length - The length of the straight line connecting the extremities of the mean line. It passes through, or nearly through, the fore and aft extremities of the section. Synonymous with nose-tail line, pitch line.
4. Epsilon - TMB thickness modifications to the basic NACA 66 thickness distribution.
5. F - The distance, normal to the chord line, from chord line to the face (pressure side) surface of the blade. Positive values indicate chord line is outside of blade section. Total thickness is the difference (not sum) of B and F values.
6. Generator line - The line formed by the intersection of the pitch helices and the plane containing the shaft axis and the propeller reference line.
7. LER - Leading edge radius.
8. Pitch - Distance of advance of a point on the propeller in one revolution.
9. Propeller plane - The plane normal to the shaft axis and passing through the intersection of the generator line (extended) and the shaft axis.
10. Radii - Distances from shaft axis (axis of rotation of propeller) to points on propeller.
11. Rake - The distance from the propeller plane to the generator line in the direction of the shaft axis. Aft displacement is considered positive rake.
12. Reference line - The straight line, normal to the shaft axis, which passes through the mid-chord of the root section. It lies in the plane containing the shaft axis and the generator line.
13. RL - LE - The distance from generator line to the leading edge. Negative values indicate that generator line is outside of blade section.

TABLE A1 (CONTINUED)

14. RL - TE - The distance from generator line to the trailing edge.
15. R/R, R - Nondimensional propeller radius. The ratio of radius of point on propeller to outside radius of propeller.
16. Skew - The displacement of any blade section along the pitch helix, measured from the generator line to the mid-chord of the section. Positive skew is opposite to the direction of ahead motion of the blade section.
17. TER - Trailing edge radius(see Figure A1).

TABLE A.2 - PROPELLER GEOMETRY

R/R	RADIUS (INCHES)	PITCH (INCHES)	RAE (INCHES)	LER (INCHES)	PITCH TER (INCHES)	EPYLON TER (INCHES)
*20000	25.200	283.500	0.000	.935	.347	0
*22500	28.350	290.423	-.066	.885	.346	0
*25000	31.500	296.853	-.163	.834	.344	0
*27500	34.650	302.780	-.285	.783	.340	0
*30000	37.800	309.196	-.428	.732	.335	0
*32500	40.950	313.092	-.587	.682	.328	0
*35000	44.100	317.460	-.758	.633	.321	0
*37500	47.250	321.291	-.935	.586	.312	0
*40000	50.400	324.575	-1.113	.546	.303	0
*42500	53.550	327.308	-1.289	.495	.278	0
*45000	56.700	329.481	-1.457	.452	.150	0
*47500	59.850	331.092	-1.613	.410	.033	0
*50000	63.000	332.116	-1.752	.371	.016	0
*52500	66.150	332.598	-1.867	.334	.016	0
*55000	69.300	332.421	-1.947	.299	.016	0
*57500	72.450	331.534	-1.978	.266	.016	0
*60000	75.600	329.468	-1.946	.235	.016	0
*62500	78.750	327.370	-1.843	.206	.016	.0134
*65000	81.900	324.045	-1.680	.179	.016	.0269
*67500	85.050	319.914	-1.474	.195	.016	.0403
*70000	88.200	315.000	-1.241	.134	.016	.0538
*72500	91.350	309.313	-0.973	.115	.016	.0672
*75000	94.500	302.823	-0.723	.099	.016	.0807
*77500	97.650	295.492	-0.420	.084	.016	.0941
*80000	100.800	287.280	-0.073	.071	.016	.1076
*82500	103.950	279.142	.333	.060	.016	.1210
*85000	107.100	269.906	.812	.050	.014	.1066
*87500	110.250	256.798	1.382	.041	.012	.0921
*90000	113.400	246.440	2.059	.033	.010	.0777
*92500	116.550	230.855	2.862	.026	.008	.0633
*95000	119.700	215.964	3.805	.020	.006	.0469
*96000	120.960	209.624	4.225	.018	.006	.0431
*97000	122.220	203.057	4.671	.015	.005	.0374
*98000	123.480	196.258	5.144	.012	.004	.0316
*99000	124.740	189.222	5.645	.009	.003	.0258
1.00000	126.000	181.944	6.174	0.07	0.000	.0200

21.0 FT. DIAMETER, 7 BLADES

\* Epsilon values for information. Epsilon modifications  
are included in table of offsets.

TABLE A.2 (Continued)

R/R	CHORD LENGTH (inches)	HALF CHORD LENGTH (inches)	SKEW (inches)	RL-LE (inches)	RL-TE (inches)	MAX. CAMBER (inches)	MAX. THICK. (inches)
.20000	52.164	26.082	0.000	26.082	26.082	2.596	10.433
.22500	56.825	27.413	.179	27.234	27.591	2.698	10.405
.25000	57.342	28.671	.636	28.035	29.307	2.722	10.331
.27500	59.702	29.851	1.372	28.479	31.223	2.791	10.214
.30000	61.891	30.946	2.378	28.568	33.323	2.748	10.057
.32500	63.893	31.947	3.657	28.289	35.604	2.717	9.864
.35000	65.691	32.846	5.191	27.654	38.037	2.664	9.637
.37500	67.265	33.633	6.963	26.670	40.595	2.595	9.378
.40000	68.594	34.297	8.942	25.355	43.239	2.517	9.089
.42500	69.655	34.826	11.117	23.711	45.944	2.439	8.770
.45000	70.425	35.213	13.476	21.736	48.689	2.362	8.425
.47500	70.879	35.440	16.044	19.396	51.483	2.292	8.056
.50000	70.988	35.494	18.800	16.694	54.294	2.229	7.667
.52500	70.727	35.364	21.773	13.590	57.137	2.176	7.259
.55000	70.065	35.043	24.978	10.864	60.021	2.128	6.835
.57500	69.057	34.529	28.420	6.109	62.948	2.081	6.398
.60000	67.637	33.819	32.131	1.687	65.950	2.029	5.952
.62500	65.827	32.914	36.108	-3.194	69.021	1.969	5.499
.65000	63.660	31.030	40.301	-8.471	72.131	1.898	5.047
.67500	61.184	30.592	44.635	-14.043	75.227	1.816	4.685
.70000	58.464	29.732	49.052	-19.820	78.284	1.725	4.180
.72500	55.561	27.781	53.451	-25.671	81.232	1.624	3.779
.75000	52.480	26.240	57.844	-31.604	84.084	1.516	3.399
.77500	49.211	24.606	62.244	-37.639	86.850	1.403	3.040
.80000	45.738	22.869	66.643	-43.774	89.512	1.285	2.699
.82500	42.049	21.025	71.065	-50.041	92.090	1.164	2.372
.85000	38.143	19.072	75.497	-56.925	94.568	1.039	2.062
.87500	34.031	17.016	79.919	-62.934	96.935	.912	1.766
.90000	29.736	14.868	84.328	-69.450	99.196	.782	1.487
.92500	25.264	12.632	88.694	-76.062	101.326	.651	1.222
.95000	20.412	10.206	93.015	-82.809	103.221	.515	.959
.96000	18.253	9.127	94.733	-85.606	103.859	.456	.869
.97000	15.861	7.931	96.442	-88.512	104.373	.393	.730
.98000	13.067	6.534	98.149	-91.615	104.682	.320	.597
.99000	9.422	4.711	99.847	-95.136	104.558	.229	.427
1.00000	0.000	0.000	101.538	-101.538	101.538	0.000	0.000

**TABLE A.3 – PROPELLER OFFSETS**  
 (Values in inches)

C/C	.200R.	.225R.	.250R.	.275R.	.300R.	.325R.	.350R.
0.0000 R	0.000	0.000	0.000	0.000	0.000	0.000	0.000
F	-0.000	-0.000	-0.000	-0.000	-0.000	-0.000	-0.000
.0125 R	1.321	1.327	1.325	1.316	1.299	1.276	1.248
F	-.857	-.845	-.832	-.817	-.801	-.783	-.764
.0250 R	1.935	1.947	1.946	1.934	1.910	1.877	1.835
F	-1.124	-1.104	-1.083	-1.061	-1.039	-1.015	-.990
.0500 R	2.849	2.871	2.873	2.856	2.823	2.775	2.713
F	-1.462	-1.429	-1.396	-1.364	-1.333	-1.301	-1.269
.0750 R	3.569	3.599	3.604	3.585	3.544	3.484	3.408
F	-1.700	-1.655	-1.613	-1.573	-1.534	-1.497	-1.459
.1000 R	4.178	4.216	4.223	4.202	4.155	4.085	3.995
F	-1.887	-1.833	-1.783	-1.736	-1.692	-1.650	-1.607
.1500 R	5.174	5.224	5.235	5.211	5.154	5.068	4.957
F	-2.173	-2.104	-2.040	-1.982	-1.928	-1.879	-1.830
.2000 R	5.961	6.021	6.036	6.009	5.944	5.846	5.718
F	-2.386	-2.303	-2.229	-2.162	-2.101	-2.046	-1.992
.3000 R	7.045	7.120	7.141	7.112	7.036	6.920	6.769
F	-2.631	-2.530	-2.440	-2.361	-2.291	-2.228	-2.168
.4000 R	7.624	7.708	7.733	7.703	7.622	7.497	7.334
F	-2.709	-2.597	-2.499	-2.413	-2.338	-2.272	-2.211
.5000 R	7.733	7.821	7.848	7.819	7.738	7.612	7.446
F	-2.621	-2.505	-2.404	-2.317	-2.242	-2.178	-2.118
.6000 R	7.356	7.443	7.471	7.445	7.369	7.249	7.091
F	-2.353	-2.240	-2.143	-2.060	-1.990	-1.931	-1.877
.7000 R	6.483	6.562	6.589	6.568	6.502	6.396	6.257
F	-1.937	-1.835	-1.748	-1.675	-1.614	-1.564	-1.520
.8000 R	5.041	5.104	5.126	5.110	5.059	4.977	4.869
F	-1.449	-1.368	-1.300	-1.243	-1.197	-1.158	-1.125
.9000 R	2.875	2.906	2.915	2.904	2.873	2.826	2.764
F	-1.042	-1.000	-.963	-.931	-.902	-.877	-.854
.9500 R	1.630	1.645	1.647	1.639	1.520	1.593	1.558
F	-.755	-.734	-.715	-.696	-.679	-.662	-.645
1.0000 R	.347	.346	.344	.340	.335	.328	.321
F	-.347	-.346	-.344	-.340	-.335	-.328	-.321

Camber distribution: NACA  $\alpha = 0.8$

Thickness distribution: NACA 66, TMB Modified (epsilon).

Epsilon values for information. Epsilon modifications are included in table of offsets.

TABLE A.3 (Continued)

C/C	.375R.	.400R.	.425R.	.450R.	.475R.	.500R.	.525R.
0.0000 R	0.000	0.000	0.000	0.000	0.000	0.000	0.000
F	-0.000	-0.000	-0.000	-0.000	-0.000	-0.000	-0.000
.0125 R	1.214	1.177	1.137	1.094	1.049	1.003	.955
F	-.744	-.721	-.694	-.665	-.633	-.598	-.560
.0250 R	1.786	1.732	1.673	1.610	1.545	1.478	1.409
F	-.963	-.933	-.899	-.860	-.817	-.770	-.719
.0500 R	2.641	2.560	2.473	2.381	2.286	2.189	2.090
F	-1.234	-1.195	-1.150	-1.100	-1.043	-.979	-.910
.0750 R	3.317	3.215	3.06	2.991	2.872	2.751	2.629
F	-1.419	-1.375	-1.22	-1.264	-1.196	-1.121	-1.037
.1000 R	3.889	3.770	3.643	3.508	3.369	3.228	3.085
F	-1.563	-1.514	-1.456	-1.390	-1.315	-1.230	-1.135
.1500 R	4.825	4.677	4.519	4.353	4.182	4.008	3.833
F	-1.779	-1.723	-1.56	-1.580	-1.491	-1.391	-1.279
.2000 R	5.566	5.396	5.14	5.022	4.825	4.626	4.425
F	-1.937	-1.875	-1.802	-1.718	-1.620	-1.508	-1.382
.3000 R	6.589	6.388	6.173	5.946	5.715	5.480	5.245
F	-2.108	-2.041	-1.961	-1.867	-1.756	-1.630	-1.487
.4000 R	7.139	6.921	6.688	6.443	6.193	5.940	5.687
F	-2.149	-2.081	-1.998	-1.901	-1.786	-1.654	-1.502
.5000 R	7.248	7.027	6.791	6.542	6.289	6.033	5.778
F	-2.058	-1.993	-1.913	-1.818	-1.705	-1.575	-1.426
.6000 R	6.903	6.692	6.467	6.232	5.991	5.749	5.507
F	-1.824	-1.766	-1.694	-1.609	-1.506	-1.386	-1.248
.7000 R	6.091	5.906	5.707	5.500	5.289	5.076	4.864
F	-1.477	-1.429	-1.370	-1.299	-1.213	-1.112	-.994
.8000 R	4.740	4.595	4.441	4.280	4.116	3.951	3.787
F	-1.093	-1.058	-1.014	-.960	-.895	-.818	-.728
.9000 R	2.691	2.609	2.521	2.428	2.334	2.238	2.143
F	-.830	-.803	-.772	-.734	-.690	-.540	-.582
.9500 R	1.516	1.470	1.420	1.368	1.313	1.258	1.202
F	-.627	-.608	-.585	-.558	-.528	-.495	-.457
1.0000 R	.312	.303	.292	.281	.268	.255	.242
F	-.312	-.303	-.292	-.281	-.268	-.255	-.242

TABLE A.3 (Continued)

C/C	.550R.	.575R.	.600R.	.625R.	.650R.	.675R.	.700R.
0.0000 R	0.000	0.000	0.000	0.000	0.000	0.000	0.000
F	-0.000	-0.000	-0.000	-0.000	-0.000	-0.000	-0.000
.0125 R	.907	.857	.805	.753	.699	.645	.593
F	-.521	-.479	-.437	-.396	-.355	-.316	-.280
.0250 R	1.340	1.268	1.194	1.118	1.041	.963	.886
F	-.665	-.608	-.551	-.494	-.439	-.387	-.339
.0500 R	1.989	1.886	1.780	1.670	1.557	1.444	1.331
F	-.835	-.757	-.679	-.602	-.528	-.459	-.396
.0750 R	2.504	2.377	2.245	2.109	1.968	1.827	1.686
F	-.948	-.854	-.761	-.668	-.580	-.499	-.425
.1000 R	2.941	2.793	2.640	2.481	2.318	2.153	1.988
F	-1.033	-.927	-.821	-.716	-.616	-.525	-.442
.1500 R	3.656	3.474	3.287	3.092	2.891	2.687	2.484
F	-1.158	-1.031	-.905	-.781	-.663	-.556	-.459
.2000 R	4.222	4.014	3.800	3.577	3.346	3.112	2.878
F	-1.246	-1.104	-.962	-.823	-.692	-.572	-.466
.3000 R	5.007	4.764	4.512	4.250	3.979	3.703	3.428
F	-1.332	-1.170	-1.008	-.850	-.701	-.567	-.449
.4000 R	5.431	5.169	4.898	4.616	4.324	4.026	3.729
F	-1.339	-1.167	-.997	-.830	-.674	-.534	-.411
.5000 R	5.520	5.256	4.982	4.698	4.403	4.101	3.800
F	-1.264	-1.094	-.924	-.760	-.607	-.469	-.350
.6000 R	5.263	5.013	4.755	4.487	4.208	3.923	3.637
F	-1.098	-.941	-.784	-.633	-.493	-.369	-.261
.7000 R	4.650	4.432	4.206	3.972	3.730	3.481	3.232
F	-.866	-.731	-.597	-.471	-.354	-.252	-.164
.8000 R	3.621	3.452	3.277	3.099	2.914	2.725	2.534
F	-.630	-.527	-.425	-.332	-.247	-.172	-.110
.9000 R	2.046	1.947	1.845	1.747	1.646	1.543	1.439
F	-.520	-.455	-.390	-.335	-.285	-.240	-.202
.9500 R	1.146	1.088	1.028	.977	.924	.871	.818
F	-.417	-.375	-.333	-.302	-.274	-.249	-.227
1.0000 R	.228	.213	.198	.197	.195	.194	.193
F	-.228	-.213	-.198	-.197	-.195	-.194	-.193

TABLE A.3 (Continued)

C/C	.725R.	.750R.	.775R.	.800R.	.825R.	.850R.	.875R.
0.0000 R	0.000	0.000	0.000	0.000	0.000	0.000	0.000
F	-0.000	-0.000	-0.000	-0.000	-0.000	-0.000	-0.000
.0125 R	.542	.492	.445	.398	.353	.310	.267
F	-.247	-.217	-.190	-.165	-.142	-.121	-.102
.0250 R	.812	.739	.668	.599	.532	.467	.404
F	-.296	-.258	-.223	-.192	-.163	-.138	-.114
.0500 R	1.221	1.113	1.009	.906	.806	.708	.612
F	-.340	-.291	-.248	-.209	-.174	-.144	-.118
.0750 R	1.548	1.413	1.281	1.151	1.025	.901	.779
F	-.360	-.304	-.255	-.12	-.173	-.141	-.112
.1000 R	1.826	1.668	1.513	1.361	1.211	1.065	.922
F	-.371	-.309	-.255	-.209	-.168	-.134	-.105
.1500 R	2.284	2.087	1.894	1.704	1.518	1.336	1.157
F	-.377	-.307	-.247	-.196	-.152	-.116	-.087
.2000 R	2.647	2.420	2.197	1.978	1.763	1.551	1.344
F	-.376	-.299	-.235	-.181	-.135	-.098	-.069
.3000 R	3.155	2.885	2.621	2.361	2.105	1.853	1.606
F	-.350	-.267	-.198	-.142	-.095	-.059	-.031
.4000 R	3.433	3.141	2.854	2.572	2.294	2.020	1.751
F	-.310	-.226	-.156	-.01	-.055	-.022	.002
.5000 R	3.500	3.203	2.912	2.625	2.342	2.063	1.789
F	-.252	-.171	-.106	-.055	-.014	.015	.035
.6000 R	3.353	3.071	2.794	2.521	2.250	1.983	1.720
F	-.174	-.104	-.049	-.006	.028	.051	.065
.7000 R	2.983	2.736	2.494	2.254	2.012	1.773	1.539
F	-.095	-.040	.001	.031	.058	.074	.083
.8000 R	2.344	2.155	1.969	1.786	1.595	1.406	1.220
F	-.061	-.024	.002	.020	.041	.054	.062
.9000 R	1.337	1.236	1.137	1.039	.927	.816	.708
F	-.172	-.148	-.130	-.118	-.092	-.071	-.054
.9500 R	.766	.715	.665	.617	.550	.484	.419
F	-.209	-.195	-.185	-.177	-.151	-.128	-.107
1.0000 R	.193	.194	.195	.197	.175	.154	.133
F	-.193	-.194	-.195	-.197	-.175	-.154	-.133

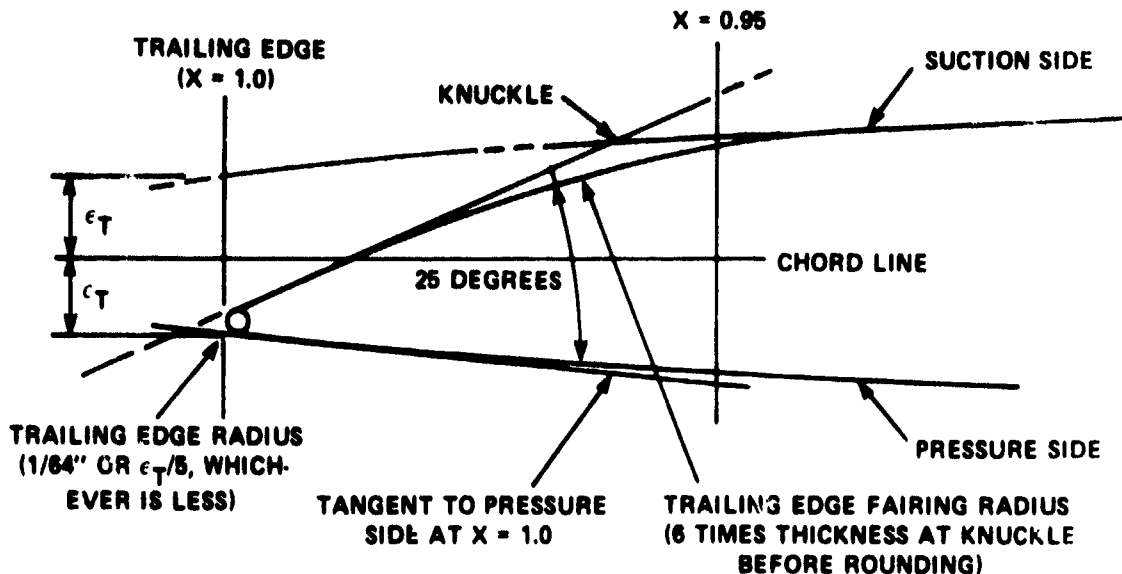
TABLE A.3 (Continued)

C/C	.900R.	.925R.	.950R.	.960R.	.970R.	.980R.	.990R.
0.0000 R	0.000	0.000	0.000	0.000	0.000	0.000	0.000
F	-0.000	-0.000	-0.000	-0.000	-0.000	-0.000	-0.000
.0125 R	.226	.187	.147	.130	.112	.091	.065
F	-.084	-.069	-.053	-.047	-.041	-.033	-.024
.0250 B	.342	.282	.222	.197	.169	.138	.099
F	-.094	-.076	-.059	-.052	-.045	-.037	-.026
.0500 B	.519	.429	.338	.299	.257	.210	.150
F	-.095	-.076	-.058	-.052	-.044	-.037	-.026
.0750 B	.661	.547	.430	.381	.328	.268	.192
F	-.089	-.070	-.054	-.048	-.041	-.034	-.024
.1000 R	.783	.647	.510	.451	.388	.317	.227
F	-.082	-.063	-.048	-.042	-.036	-.030	-.021
.1500 B	.983	.812	.640	.567	.488	.398	.285
F	-.065	-.048	-.035	-.031	-.026	-.022	-.016
.2000 B	1.142	.944	.744	.658	.567	.463	.331
F	-.048	-.034	-.023	-.021	-.017	-.015	-.011
.3000 B	1.365	1.129	.889	.787	.678	.553	.396
F	-.014	-.005	.000	.000	.001	-.001	-.000
.4000 R	1.488	1.231	.970	.859	.739	.603	.432
F	.016	.021	.020	.018	.016	.012	.009
.5000 B	1.520	1.258	.991	.878	.755	.616	.441
F	.044	.044	.039	.034	.031	.024	.017
.6000 B	1.462	1.210	.953	.844	.727	.593	.425
F	.069	.065	.055	.048	.043	.033	.024
.7000 R	1.308	1.083	.853	.756	.651	.531	.381
F	.082	.075	.062	.055	.048	.038	.027
.8000 B	1.038	.959	.677	.599	.516	.422	.303
F	.061	.056	.047	.042	.036	.028	.019
.9000 B	.602	.498	.392	.347	.299	.246	.178
F	-.041	-.031	-.023	-.020	-.017	-.016	-.014
.9500 R	.356	.294	.232	.205	.177	.145	.107
F	-.088	-.071	-.055	-.049	-.042	-.037	-.029
1.0000 B	.113	.093	.073	.065	.056	.048	.038
F	-.113	-.093	-.073	-.065	-.056	-.048	-.038

Figure A.1 – Trailing Edge Geometry for Propellers

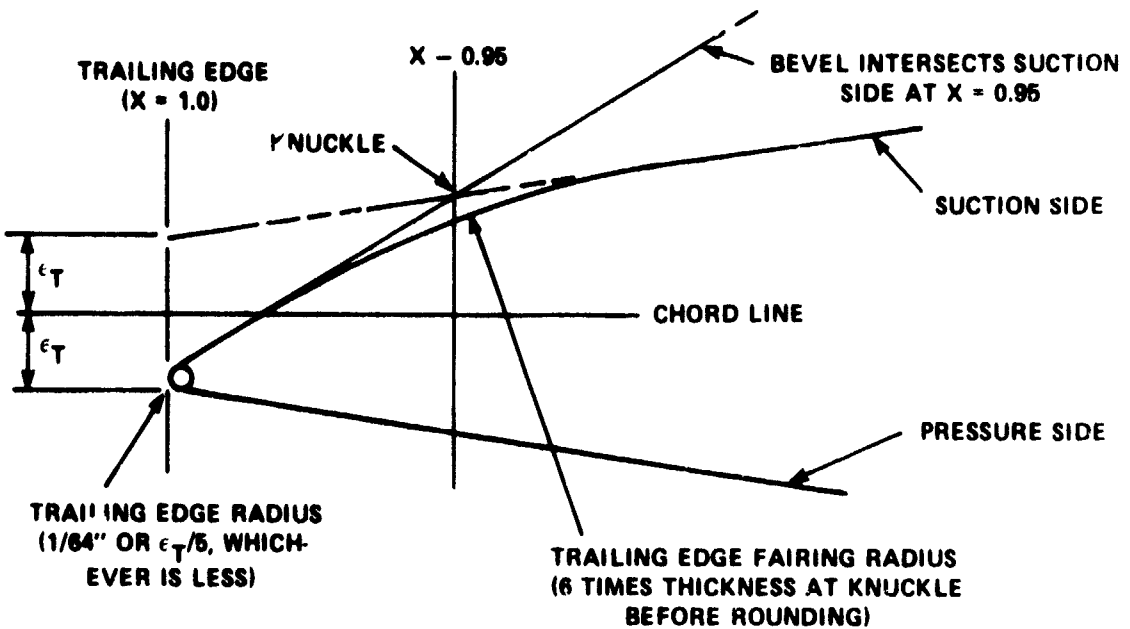
TRAILING EDGE DETAIL A

(TO BE USED WHEN 25 DEGREE BEVEL INTERSECTS SUCTION SIDE AT  $X < 0.95$ )  
 $X = (\text{DISTANCE FROM LEADING EDGE ALONG CHORD})/(\text{CHORD LENGTH})$



TRAILING EDGE DETAIL B

(TO BE USED WHEN 25 DEGREE BEVEL INTERSECTS SUCTION SIDE AT  $X < 0.95$ )  
 $X = (\text{DISTANCE FROM LEADING EDGE ALONG CHORD LINE})/(\text{CHORD LENGTH})$



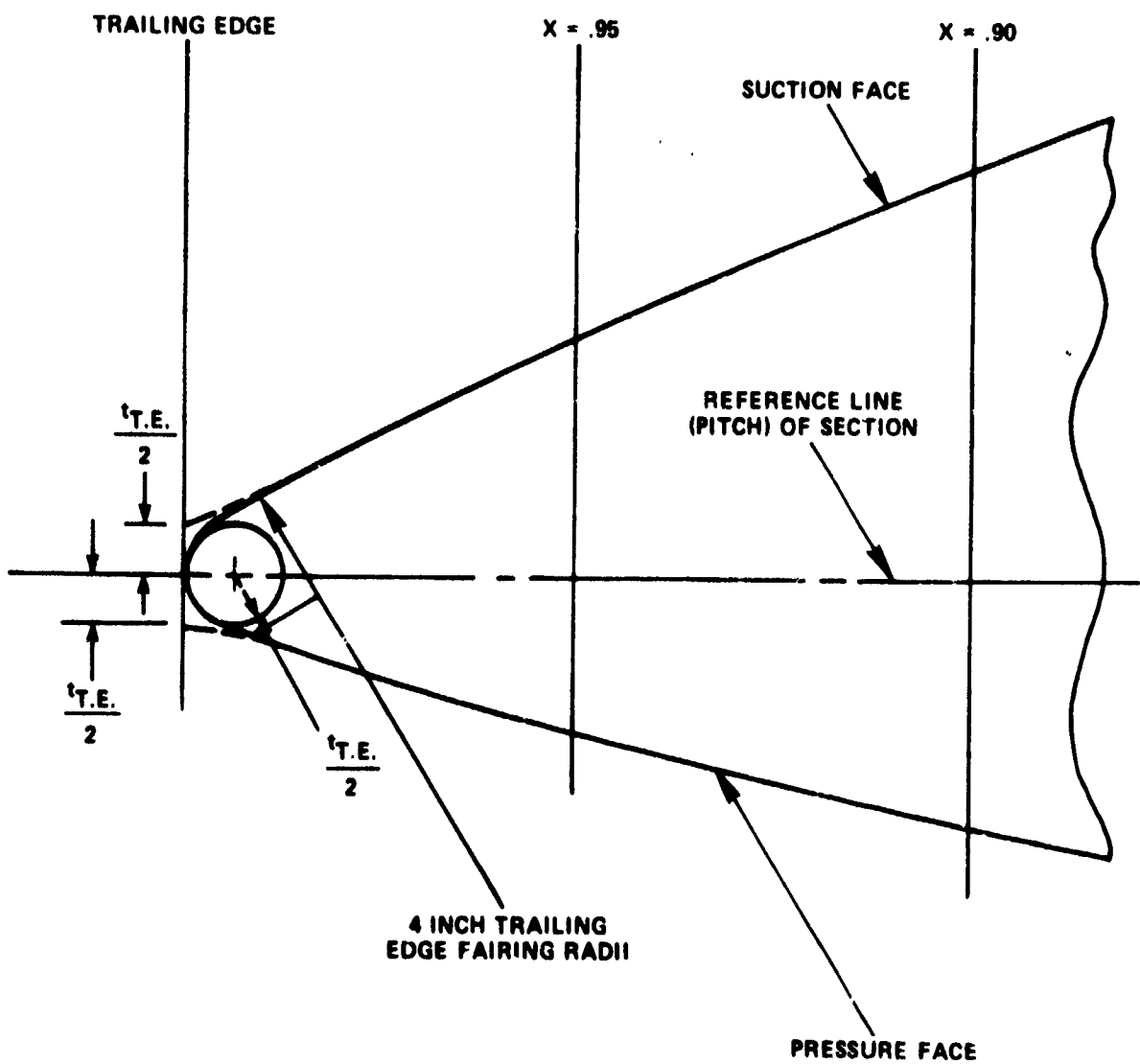


Figure A.1 (Continued)

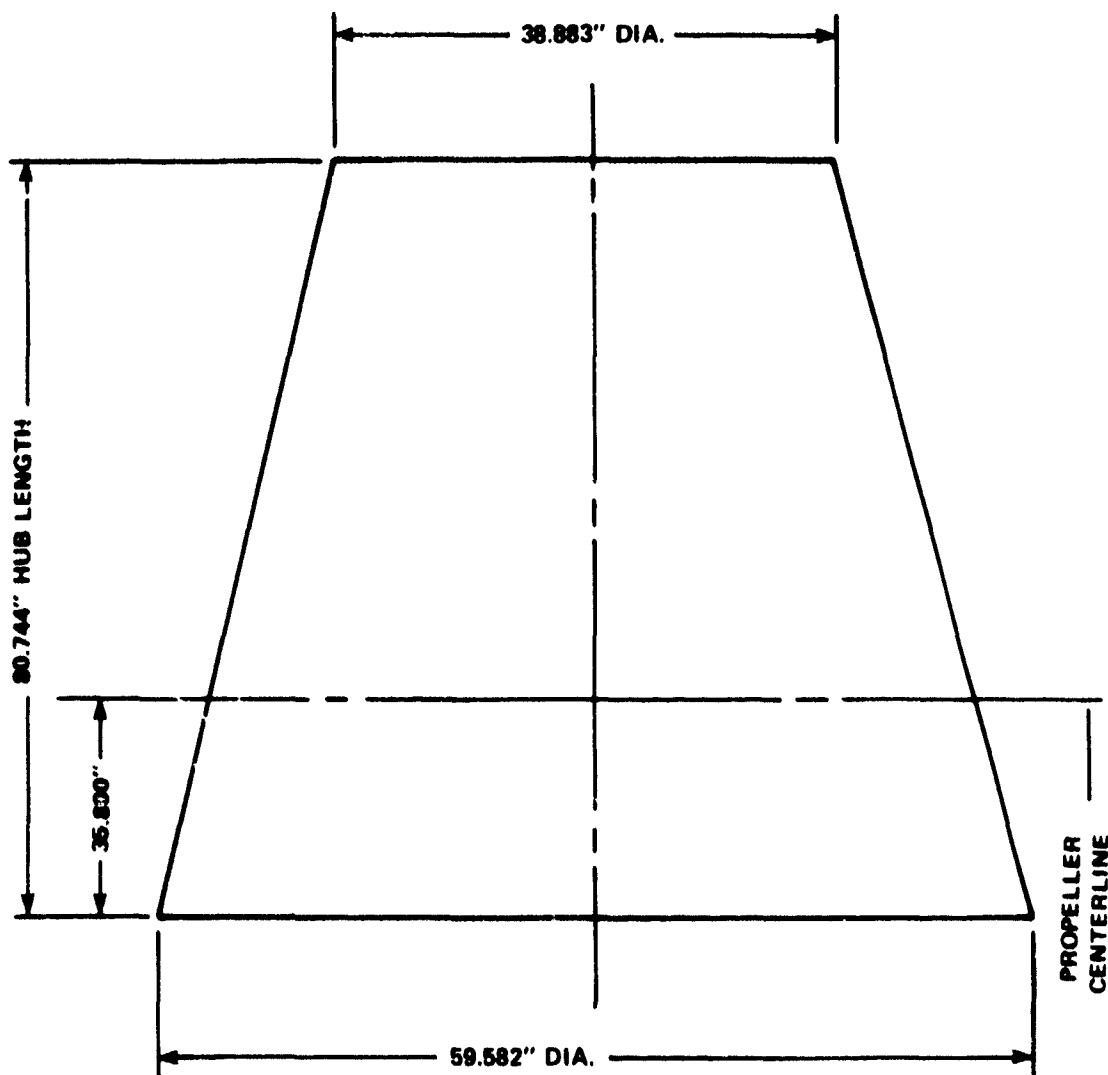


Figure A.2 – Hub Configuration

**DTNSRDC ISSUES THREE TYPES OF REPORTS**

- (1) DTNSRDC REPORTS, A FORMAL SERIES PUBLISHING INFORMATION OF PERMANENT TECHNICAL VALUE, DESIGNATED BY A SERIAL REPORT NUMBER.**
- (2) DEPARTMENTAL REPORTS, A SEMIFORMAL SERIES, RECORDING INFORMATION OF A PRELIMINARY OR TEMPORARY NATURE, OR OF LIMITED INTEREST OR SIGNIFICANCE, CARRYING A DEPARTMENTAL ALPHANUMERIC IDENTIFICATION.**
- (3) TECHNICAL MEMORANDA, AN INFORMAL SERIES, USUALLY INTERNAL WORKING PAPERS OR DIRECT REPORTS TO SPONSORS, NUMBERED AS TM SERIES REPORTS; NOT FOR GENERAL DISTRIBUTION.**